SEMMELWEIS EGYETEM

DOKTORI ISKOLA

Ph.D. értekezések

2684.

KŐVÁRI DÓRA

Neuroendokrinológia
című program

Programvezető: Dr. Fekete Csaba, tudományos tanácsadó

Témavezető: Dr. Fekete Csaba, tudományos tanácsadó

Central regulation of the HPT axis

PhD thesis

Dóra Kővári

Semmelweis University
János Szentágothai Ph.D. School of Neuroscience

Supervisor:	Csaba Fekete, M.D., D.Sc
Official reviewers:	Dániel Tóth, Ph.D. Endre Nagy, M.D., D.Sc.
Head of the Final Examination Committee:	András Csillag, M.D., D.Sc.
Members of the Final Examination Committee:	Attila Patócs, M.D., Ph.D. Balázs Gaszner, M.D., Ph.D.

Budapest

2022

Table of contents

Abbreviations

α-MSH	alpha-melanocyte stimulating hormone
2-AG	2-arachydonoylglicerol
Actb	actin beta
AGRP	agouti-related peptide
AMPA	α-amino-3-hydroxy-5-methyl-4-isoxazolepropionic acid
ARC	arcuate nucleus
BAT	brown adipose tissue
BBB	blood-brain barrier
CART	cocaine- and amphetamine-regulated transcript
CB1	type 1 endocannabinoid receptor
cDNA	complementer DNA
CNS	central nervous system
CpG	cytosine-phosphate-guanine
cpm	counts per million
CSF	cerebrospinal fluid
D1	type 1 deiodinase
D2	type 2 deiodinase
D3	type 3 deiodinase
Dagla	diacylglycerol lipase alpha
DAGLα	diacylglycerol lipase α
Dio1	type 1 deiodinase gene

Dio2	type 2 deiodinase gene
DMN	dorsomedial nucleus
DNMT	DNA-methyltransferase
Dnmt1	DNA-methyltransferase 1
Dnmt3a	DNA-methyltransferase 3A
Dnmt3b	DNA-methyltransferase 3B
E	embrionic day
FASN	fatty acid synthase
fT3	free triiodothyronine
fT4	free thyroxine
G6PC	glucose-6-phosphatase
GABA	gamma-aminobutyric acid
Gapdh	glyceraldehyde-3-phosphate dehydrogenase
GRIA1	glutamate receptor, ionotropic, AMPA1 (alpha 1)
GRIA2	glutamate receptor, ionotropic, AMPA2 (alpha 2)
GRIA3	glutamate receptor, ionotropic, AMPA3 (alpha 3)
GRIA4	glutamate receptor, ionotropic, AMPA4 (alpha 4)
GRIK1	glutamate receptor, ionotropic, kainate 1
GRIK2	glutamate receptor, ionotropic, kainate 2 (beta 2)
GRIK3	glutamate receptor, ionotropic, kainate 3
GRIK4	glutamate receptor, ionotropic, kainate 4
GRIK5	glutamate receptor, ionotropic, kainate 5 (gamma 2)
GRIN1	glutamate receptor, ionotropic, NMDA1 (zeta 1)

GRIN2A	glutamate receptor, ionotropic, NMDA2A (epsilon 1)
GRIN2B	glutamate receptor, ionotropic, NMDA2B (epsilon 2)
GRIN2C	glutamate receptor, ionotropic, NMDA2C (epsilon 3)
GRIN2D	glutamate receptor, ionotropic, NMDA2D (epsilon 4)
GRIN3A	glutamate receptor ionotropic, NMDA3A
GRIN3B	glutamate receptor, ionotropic, NMDA3B
GRM1	glutamate receptor, metabotropic 1
GRM2	glutamate receptor, metabotropic 2
GRM3	glutamate receptor, metabotropic 3
GRM4	glutamate receptor, metabotropic 4
GRM5	glutamate receptor, metabotropic 5
GRM6	glutamate receptor, metabotropic 6
GRM7	glutamate receptor, metabotropic 7
GRM8	glutamate receptor, metabotropic 8
GW	gestational day
Hprt	hypoxanthine-guanine phosphoribosyltransferase
HPT axis	hypothalamic-pituitary-thyroid axis
i.p.	intraperitoneal
ISH	*in situ* hybridization
KO	knock out
LBM	lean body mass
LCM	laser capture microdissection
luc	luciferase

MBH	mediobasal hypothalamus
MCT 8	monocarboxylate transporter 8
ME	median eminence
ME1	malic enzyme 1
mTRH	mouse proTRH
NHS	normal horse serum
NMDA	*N*-methyl-D-aspartate
NPY	neuropeptide Y
OATP1C1	organic anion-transporting polypeptide1 C1
P	postnatal day
PB	phosphate buffer
PBS	phosphate-buffered saline
PD	postnatal day
PFA	paraformaldehyde
PPII	pyroglutyamyl-peptidase II
PVN	hypothalamic paraventricular nucleus
qPCR	quantitative polymerase chain reaction
RER	respiratory exchange ratio
RIN	RNA integrity number
rT3	reverse triiodothyronine
SLC1A1	solute carrier family 1, member 1
SLC1A2	solute carrier family 1, member 2
SLC1A3	solute carrier family 1, member 3

SLC1A6	solute carrier family 1, member 6
SLC1A7	solute carrier family 1, member 7
Spot14	thyroid hormone responsive gene
SSC	standard sodium citrate
T2	diiodothyronine
T3	triiodothyronine
T4	thyroxine
TBW	total body weight
T-DAGLα KO	tanycyte-specific deletion of DAGLα
TH	thyroid hormone
THAI	thyroid hormone action indicator mouse
THRA	thyroid hormone receptor alpha
THRB	thyroid hormone receptor beta
TR	thyroid hormone receptor
TRH	thyrotropin-releasing hormone
Trhde	pyroglutamyl-peptidase II
TRHR1	thyrotropin-releasing hormone receptor 1
TRHR2	thyrotropin-releasing hormone receptor 2
TRα	thyroid hormone receptor alpha
TRβ	thyroid hormone receptor beta
TSH	thyroid-stimulating hormone
TSHβ	thyroid stimulating hormone beta subunit
VMN	ventromedial nucleus

1. Introduction

1.1. Thyroid hormones

1.1.1. Role of thyroid hormones and thyroid hormone receptors

Thyroid hormones (TH) produced by the thyroid gland are involved in the regulation of most of our organs and physiological processes and responsible for the maintenance of normal function and development of most tissues, including the bone, liver, cardiovascular system and brain (1, 2). Furthermore, THs play critical role in the regulation of a number of physiological functions, including food intake and energy expenditure (3). The effects of THs are exerted via TH receptors. These nuclear receptors are encoded by two genes, the TH receptor α (TRα) and TH receptor β (TRβ) genes (4). Distribution of these receptors show tissue specificity, TRα isoforms have very widespread distribution including the brain, heart, skeletal muscle, while the distribution of TRβ isoforms is more restricted. These receptors are expressed predominantly in some brain regions, the retina, hypophysis, kidney, liver and lung (5, 6). The TH binding modifies the configuration of TH receptors that results in release of co-repressors and binding co-activators that induces the transcriptional control of TH-dependent genes influencing the TH action in certain tissues (4, 7, 8).

1.1.2. Thyroid hormones and deiodinases

The two major forms of TH are the thyroxine (T4) and triiodothyronine (T3). T4, the major product of thyroid gland is considered a prohormone (9). It has long half-life, but cannot bind efficiently to the nuclear TH receptors (9). T4 has to be converted to T3 by removal of one iodine residue from the outer ring (9, 10). This activation is catalyzed by deiodinase enzymes (10).There are three deiodinase enzymes: type 1 deiodinase (D1), type 2 deiodinase (D2) and type 3 deiodinase (D3) enzymes. D1 can catalyze the removal of iodine residue from both rings of TH (9). Thus, it can convert T4 to T3 or T4 to reverse T3 (rT3) and can also catalyze the conversion of rT3 to diiodothyronine (T2). The rT3 has two iodine on the outer ring and one on the inner ring (11) and it is an inactive hormone as it cannot bind to the nuclear TH receptors (12). T2 is also an inactive TH

metabolite (12). As rT3 is much better substrate of D1 than T4, this enzyme preferentially catalyzes the degradation of rT3 under euthyroid conditions (12). D1 can, however, play important role in the T4 to T3 conversion, when the T4 level is increased in the circulation (11). D2 catalyzes the outer ring deiodination of TH and it converts T4 to T3 and rT3 to T2 (12). The activation of TH is catalyzed primarily by D2 under euthyroid conditions (9). As D1 is not expressed in the human brain, D2 is the only deiodinase enzyme that can catalyze the TH activation in the central nervous system (CNS) (12). D3 can only catalyze inner ring deiodination, therefore, this enzyme inactivates TH by conversion of T4 to rT3 or T3 to T2 (12). The deiodinase enzymes show different abundance in tissues and the activity of these enzymes is regulated very rapidly and cell type specifically (10, 11). Thus, the activity of these enzymes allows very rapid and cell type-specific regulation of TH action despite of the relatively stable circulating TH levels (11). In the liver and kidney, the most active deiodinase is D1, while in the CNS, pituitary, brown adipose tissue (BAT) and placenta, the D2 is the primary TH activating enzyme (11). The highest D3 activity is observed in the placenta and CNS, but D3 can also be found in many other organs (11).

Thus, the local TH activation or inactivation catalyzed by the deiodinases ensure that TH signaling in different tissues can change independently from the serum TH levels (11, 13). In most tissues, the TH induced transcriptional regulation of these enzymes and the very rapid posttranslational regulation of D2 activity help to optimize the local TH action in tissues when the circulating TH level is altered. For example, during hypothyroidism or iodine deficiency when the T4 level is low in the blood, the D2 activity is up-regulated while the D3 expression is down-regulated to increase the production of T3 from T4 and decrease the T3 degradation (14). Contrarily, during hyperthyroidism, the TH activation is markedly reduced as a result of down-regulation of D2 synthesis and the ubiquitination mediated inactivation of this enzyme, while the TH degradation is increased due to the increase of D3 synthesis (10).

Furthermore, tissue-specific regulation of deiodinase enzymes can highly increase the local TH action in certain tissues to meet the demand of tissues even if the circulating TH level is unchanged or decreased (9). For example, the increased activity of the sympathetic innervation induces increased D2 activity that results in markedly increased TH action in the BAT after cold exposure (15). This increase of TH action in the BAT is

critical to increase uncoupling protein 1 expression in this tissue that helps to increase the thermogenesis and thus helps to maintain the body temperature (16).
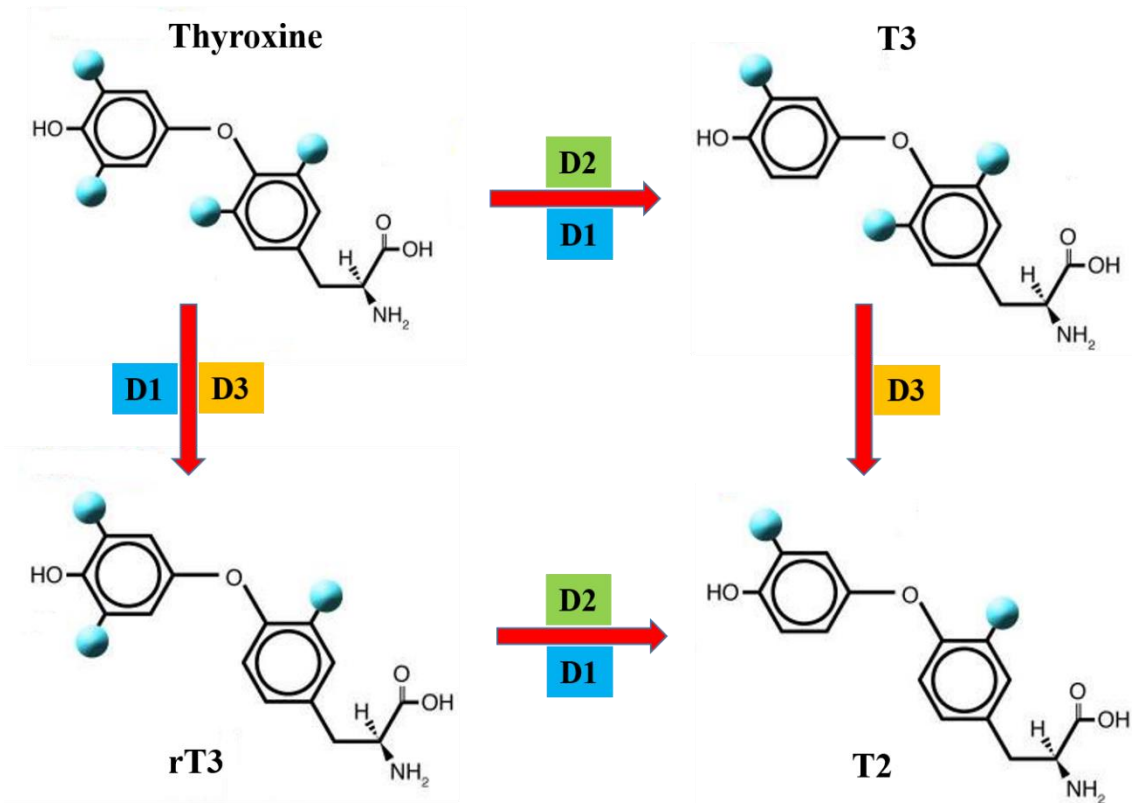
Figure 1: Role of deiodinase enzymes in the metabolism of TH

The D1 or D2 mediated outer ring deiodination of the prohormone thyroxine (T4) generates the active form of TH, the T3, while the D1 or D3 catalyzed inner ring deiodination of T4 results in the inactive reverse T3 (rT3). T2 is an inactive form of THs which can be produced by the D3 catalyzed inner ring deiodination of T3 or by the D1 or D2 catalyzed inner ring deiodination of rT3.

Abbreviations: T3 - triiodothyronine, T2 - diiodothyronine, rT3 - reverse triiodothyronine, D1 - Type 1 deiodinase, D2 - Type 2 deiodinase, D3 - Type 3 deiodinase.

Modified from Bianco and Kim, 2006 (11).

1.1.3. Hyperthyroidism

TH regulates the metabolism which is essential to maintain tissue function and for normal development, its level correlates with energy expenditure and body weight (6, 17). The effects of TH on metabolism occurs primarily through actions in the brain, white- and brown adipose tissues, skeletal muscle and liver (18). In hyperthyroid state, the excess of TH manifesting in hypermetabolism characterized by weight loss, increased resting energy expenditure and resting tachycardia, increased gluconeogenesis and lipolysis (19, 20). The cardiovascular system is one of the most important targets of TH, therefore the risks of functional cardiovascular abnormalities and diseases are high in hyperthyroid patients (21). Furthermore, hyperthyroidism increases the possibility of diabetes mellitus by increasing blood glucose level and inducing insulin resistance (22) and by increasing appetite, food intake, glucose absorption and plasma insulin level (22). Hyperthyroidism also influences the development and neuropsychological state, the TH excess results in growth acceleration, delayed pubertal onset, muscle weakness, sleep disturbances and emotional lability (23).

1.1.4. Hypothyroidism

As TH regulates the metabolism, in contrast with hyperthyroidism, hypothyroidism results in lower TH levels in association with hypometabolism, characterized by weight gain, reduced resting energy expenditure, reduced lipolysis and gluconeogenesis (18), decreases the absorption of glucose, hepatic glucose uptake and insulin responsiveness of tissues (22). Furthermore, hypothyroidism induces cardiovascular abnormalities (24) and influences the regulation of cold-induced thermogenesis by BAT, supporting that hypothyroidism increases cold sensitivity (25).

During development, TH is essential for growth and neural differentiation, therefore TH deficiency manifesting in neurologic discrepancies and growth retardation (6, 26). Decreased TH levels during the fetal and neonatal period results in intrauterine growth restriction and lower birth weight (27), furthermore impaired brain development, characterized by irreversible cretinism (28). There is growing evidence that during ontogeny maternal thyroid status is critical and even moderate forms of maternal thyroid dysfunction may have long-lasting effects of the cognitive and neuronal development of

the fetus, which alterations are largely irreversible (29). These changes are more reversible when the hypothyroid state occurs in adults (30).

1.2. The regulation of HPT axis

1.2.1. Organization of HPT axis

The relatively steady circulating levels of TH that is necessary for the preservation of normal function of the brain and peripheral organs is maintained by the hypothalamic-pituitary-thyroid (HPT) axis (31). The central regulator of this neuroendocrine system is a group of thyrotropin-releasing hormone (TRH)-synthetizing neurons in the hypothalamic paraventricular nucleus (PVN) (32). These so called hypophysiotropic TRH neurons integrate the humoral and neuronal signals and serve as a final common pathway in the regulation of the HPT axis (32, 33). These hypophysiotropic TRH neurons release TRH into the portal circulation of the pituitary in the external zone of median eminence (ME) where their axons terminate (31). The released TRH then reach the thyrotrophs of the anterior pituitary (31, 34) and stimulates the thyroid-stimulating hormone (TSH) synthesis, glycosylation and secretion and thus stimulates the TH production of the thyroid gland (32, 35).

In the PVN, not all TRH neurons are involved in the negative feedback regulation of HPT axis. Only the hypophysiotropic TRH neurons that project to the external zone of ME are involved in the control of thyroid gland (36). These TRH cells are located in the periventricular and medial parvocellular subdivision at the mid and caudal levels of the PVN in rats (37) and only at the mid-level in mice (38). The remaining TRH neurons of the PVN are called non-hypophysiotropic TRH neurons (31). These neurons do not project to the ME and are not involved in the regulation of the HPT axis (31, 39).
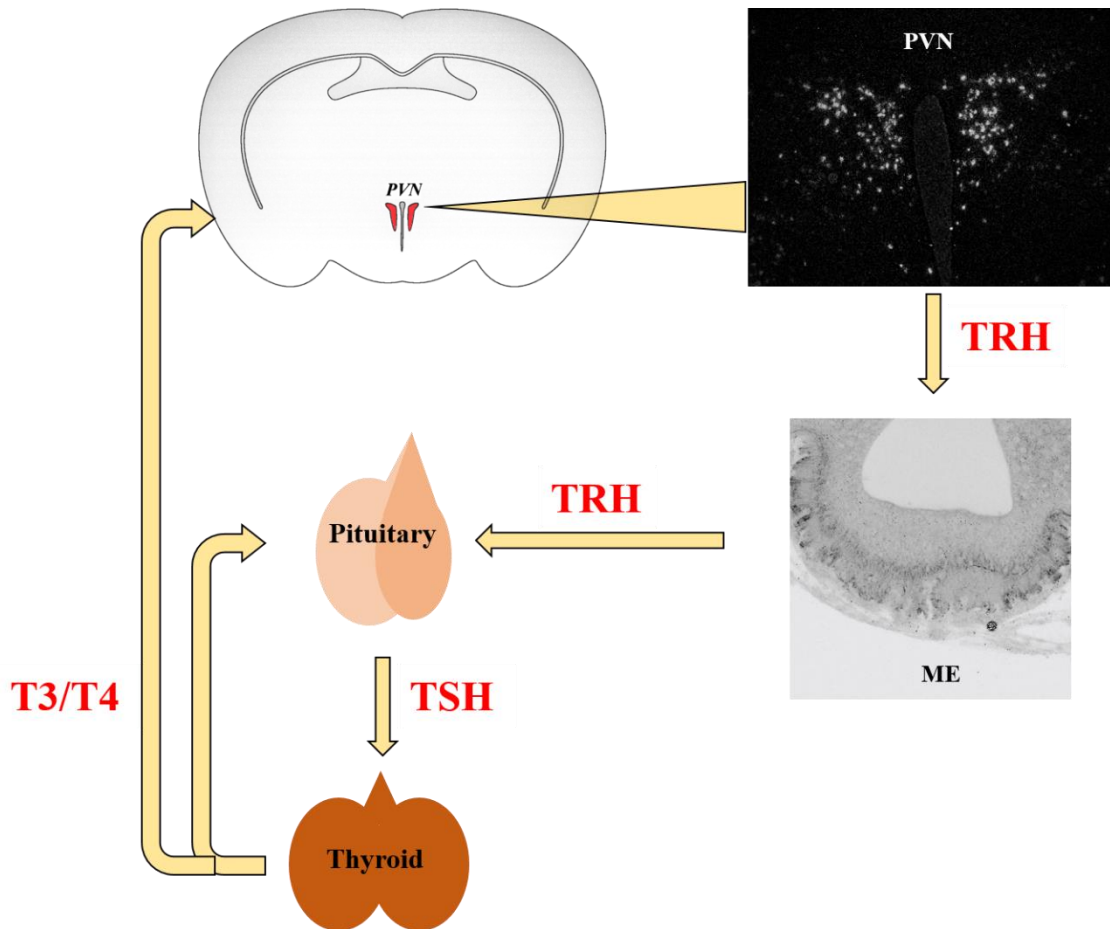
Figure 2: Organization of the hypothalamic-pituitary-thyroid axis

In the hypothalamus, the hypophysiotropic TRH neurons of the PVN project to the external zone of ME and release the TRH into the portal circulation of pituitary. The released TRH induces the TSH production of thyrotrophs in the pituitary and increases the release of TSH into the circulation. In the thyroid gland, TSH increases the T4 and T3 production which hormones exert negative feedback regulation in pituitary and hypothalamus to reduce the TSH and TRH production, respectively.

Abbreviations: PVN – hypothalamic paraventricular nucleus, ME – median eminence, TRH – thyrotropin-releasing hormone, TSH – thyroid-stimulating hormone, T3 – triiodothyronine, T4 – thyroxine

1.2.2. The negative feedback regulation of HPT axis

The negative feedback regulation of HPT axis is responsible for the stable circulating TH level (31). When the TH concentration is increased in the blood, the TRH and TSH synthesis and release are inhibited by TH and contrarily, when the TH level is decreased, the production of TRH and TSH are increased to help to normalize the circulating TH level (40).

TH inhibits both the gene expression and posttranslational modification of proTRH in the hypophysiotropic neurons but has no effect on the TRH production of the non-hypophysiotropic TRH populations (41). The negative feedback effect of TH is exerted directly on the hypophysiotropic TRH neurons, as these neurons express TH receptors (TR) (42) and implantation of T3 in the vicinity of PVN inhibits the TRH synthesis in the PVN, but only on the side of implantation (43). TRα1, TRβ1 and TRβ2 receptors are expressed in these neurons (42). However, absence of TRβ2 in TRβ2 knockout mice completely prevents the TH induced regulation of the TRH expression in the hypophysiotropic TRH neurons indicating that the TH negative feedback regulation of hypophysiotropic TRH neurons is mediated primarily by the TRβ2 (44). The dominance of TRβ receptors in the feedback regulation is also supported by the syndromes of humans suffering from TRα or TRβ resistance syndromes. While people with TRα resistance syndrome have normal circulating TSH and TH levels, the characteristic feature of the TRβ resistance syndrome is the elevated TSH and TH levels caused by the decreased inhibitory effect of TH on the HPT axis (45).

The negative feedback mechanism in the TRH neurons is relatively rapid, as exogenous administration of TH reduces TRH expression in the PVN within 5 hours (46). However, circulating T3 concentration alone is not sufficient to maintain the feedback regulation (47). Restoration of T3 level in hypothyroid rats without T4 administration does not normalize the TRH expression in the PVN indicating that the activation of TH in the brain is necessary for the feedback regulation of hypophysiotropic TRH neurons (47). Within the hypothalamus, only tanycytes, a special glial cell type lining the ventrolateral wall and floor of the third ventricle behind the optic chiasm, produce the TH activating enzyme D2 (48), indicating that the tanycytes play critical role in the feedback regulation of TRH neurons.

Beside the hypothalamus, negative feedback regulation of TH also occurs in the thyrotroph cells of the pituitary. TH negatively regulates the synthesis of both TSH subunits, the thyroid-stimulating hormone beta (TSHβ) and the glycoprotein hormone alpha subunits (49). TSHβ mRNA level is already decreased within 4 hours after T3 administration (50). Furthermore, TH influences the release of TSH stored in the vesicles and decreases the thyrotroph response to TRH by reducing the amount of TRH receptors and by increasing the TRH degrading enzyme activity (49, 51).

1.2.3. Neuronal regulation of the hypophysiotropic TRH neurons

Beside the regulatory effect of humoral signaling, the activity of HPT axis is also controlled by the neuronal inputs of the hypophysiotropic TRH neurons (31). The regulation of the activity of the HPT axis by neuronal inputs helps to adapt the organism to the changing environment (31). The synaptic inputs of hypophysiotropic TRH neurons originate from three main areas: from the hypothalamic dorsomedial (DMN) and arcuate (ARC) nuclei and the catecholamine-producing neurons of the brainstem (32, 52). Peptidergic neurons of the ARC play critical role in the regulation of energy homeostasis partly via the mediation of the effects of peripheral, feeding-related signals - like leptin, ghrelin, insulin and glucose - to the TRH neurons (53). Two main feeding-related neuron populations of the ARC are the medially located, orexigenic, neuropeptide Y (NPY), agouti-related peptide (AGRP) and gamma-aminobutyric acid (GABA)-synthetizing neurons, and the laterally located, anorexigenic, alpha-melanocyte stimulating hormone (α-MSH) and cocaine- and amphetamine-regulated transcript (CART)-synthetizing neurons (53). Both feeding related neuronal groups of the ARC innervate the TRH neurons in the PVN (31). The orexigenic peptides inhibit (54, 55), while the anorexigenic peptides stimulate the TRH synthesis (56, 57). During fasting, the falling level of leptin increases the expression of orexigenic NPY and AGRP (58) and simultaneously inhibits the synthesis of the anorexigenic peptides (59). These changes together result in reduced TRH expression in the hypophysiotropic neurons (60). The AGRP- and α-MSH-containing innervation of TRH neurons originate exclusively from the ARC neurons (55, 56). The NPY- and CART-containing inputs of the TRH neurons, however, have multiple sources including the catecholaminerg neurons of the brainstem (61, 62).

The DMN also sends input to the TRH neurons of the PVN (63). This nucleus also plays critical role in the regulation of energy homeostasis and vegetative functions by sensing feeding-related signals like leptin directly (64) and indirectly via inputs from α-MSH neurons of the ARC (65). In addition, the DMN is involved in the regulation of circadian rhythm (32). The DMN neurons form primarily symmetric type, inhibitory synapses with the TRH neurons in the PVN (63). The inhibitory role of this input is also supported by the 24h T3 release after bilateral destruction of DMN (66).

The third major input of hypophysiotropic TRH neurons originates from the catecholaminergic neurons of the brainstem (32). These neurons have two subtypes, the adrenergic and noradrenergic neurons (31). The catecholaminergic innervation of TRH neurons has asymmetric-type synapses indicating excitatory nature of these inputs (67). Consistent with this morphological observation, noradrenaline increases the TRH expression in the PVN (68). Neurons of all three adrenergic cell groups, the medullary C1-3 adrenergic groups, innervate the PVN. In addition, three from the six noradrenergic cell groups of the brainstem also project to the subdivisions of the PVN where the TRH neurons are located (52). These catecholaminerg cell groups regulate wide variety of physiological functions, and play critical role in the mediation of the stimulatory effect of cold exposure on the HPT axis that helps to increase the thermogenesis (69).
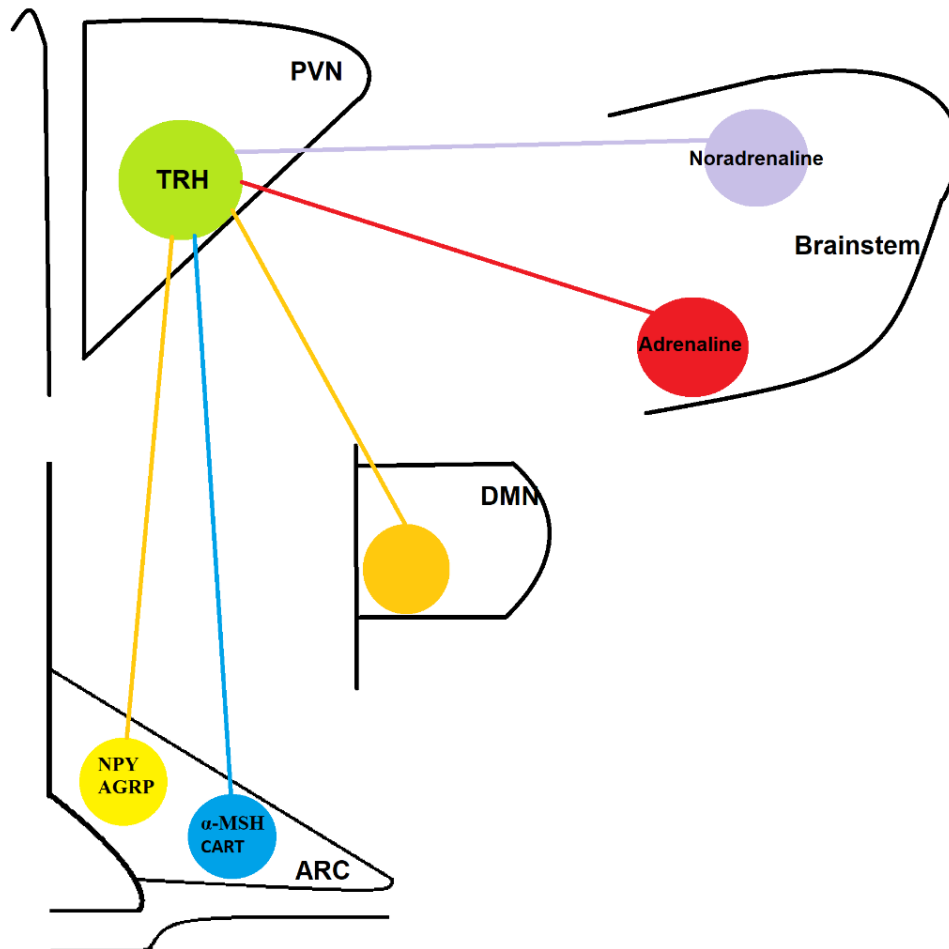
Figure 3: Illustration of the main neuronal inputs of hypophysiotropic TRH neurons

Orexigenic (NPY/AGRP) and anorexigenic (α-MSH/CART) cell populations of the ARC send projections to the hypophysiotropic TRH neurons and mediate the effect of altered energy status on the TRH neurons. The DMN sends inhibitory projections to TRH neurons likely to regulate the circadian rhythm of the hormone production. The catecholaminergic neurons of the brainstem form asymmetric-type synapses on the TRH neurons and mediate the cold induced activation of the TRH neurons.

Abbreviations: PVN – hypothalamic paraventricular nucleus, TRH - thyrotropin-releasing hormone, ARC – arcuate nucleus, NPY – neuropeptide Y, AGRP – agouti-related peptide, α-MSH - alpha-melanocyte stimulating hormone, CART - cocaine- and amphetamine-regulated transcript, DMN – hypothalamic dorsomedial nucleus.

1.3. The role of tanycytes in the regulation of HPT axis

1.3.1. Anatomy and function of tanycytes

Tanycytes are special glial cells of the hypothalamus lining the ventrolateral walls and the floor of the third ventricle behind the optic chiasm (48). The tanycytes are polarized cells. Their cell bodies are located in the ependymal layer of the third ventricle and their long basal process projects into the neuropil of the hypothalamus (70). Four subtypes of tanycytes can be classified based on their location and morphology. The α1-tanycytes line the middle third of the ventrolateral wall of the third ventricle and their basal processes project to the ventromedial nucleus (VMN) and DMN (70, 71). α2-tanycytes are located ventrally from the α1 subtype in the ventricular wall and send projections to the ARC (48, 70). The β1-tanycytes are found in the wall of the lateral extension of the infundibular recess and their processes terminate on the surface of the tuberoinfundibular sulcus, while the β2 subtype line the ventricular wall of the ME and the basal processes of these tanycytes terminate around the fenestrated capillaries of hypophyseal portal capillary system in the external zone of ME (48, 70).

Tanycytes are involved in the formation of blood-brain-barrier (BBB). In the ventricular wall of the ME, the cell bodies of the β-tanycytes are very tightly connected by tight junctions to form a barrier between the extracellular space of the ME and the cerebrospinal fluid (CSF). The cell bodies of α-tanycytes are not so tightly connected, therefore, they do not form barrier between the CSF and the extracellular fluid of neuropil, but the end feet processes of these tanycytes are involved in the BBB formation around the capillaries in the ARC, VMN and DMN (70, 72, 73).

However, tanycytes were considered as simple supporting and barrier forming cells, more and more data were published in the recent years about the importance of tanycytes in the regulation of neuroendocrine axes and the energy homeostasis (70, 74-76). Tanycytes have been shown to regulate the entry of energy homeostasis-related hormones (75) to the brain and regulate the hypothalamic-pituitary-gonadal and thyroid axes (70).

1.3.2. Role of tanycytes in the feedback regulation of the hypophysiotropic TRH neurons

The tanycytes play critical role in the negative feedback regulation of HPT axis. As described earlier, circulating T3 level alone is not sufficient for the normal negative feedback regulation of TRH expression in the hypophysiotropic neurons, the circulating T4 and local TH activation in the brain are necessary for the normal negative feedback regulation of hypophysiotropic TRH neurons (47). However, the TH activating enzyme, the D2 is not expressed in the TRH neurons (77). Only tanycytes produce D2 within the mediobasal hypothalamus (MBH), and thus only these cells can convert T4 to T3 in this brain region (78). The tanycytes express two types of TH transporters, the organic anion-transporting polypeptide (OATP1C1) which transport both T3 and T4 with similar affinity (79) and the monocarboxylate transporter 8 (MCT8) which has higher affinity for T3 (80). Thus, tanycytes are able to take up T4 from the blood or from the CSF, convert it to T3 and then release T3 to the extracellular space of the ME.

In the external zone of ME, MCT8 is present on the surface of the terminals of hypophysiotropic TRH neurons (81), therefore, T3 secreted by β2-tanycytes can be taken up and transported by retrograde axonal transport to the perikarya of TRH neurons (31). Therefore, tanycytes can modulate the feedback regulation of HPT axis by influencing the T3 availability for the hypophysiotropic TRH neurons (31).

In most brain regions, the role of D2 is to maintain stable local T3 concentration, therefore, hypothyroidism upregulates, while hyperthyroidism downregulates the activity of D2 (10). However, neither hypothyroidism (82), nor iodine deficiency induce marked changes in D2 activity of MBH (83), indicating that the main function of tanycytes is not the maintenance of stable, local T3 concentration, but rather the conversion of the changes of peripheral T4 concentration to changes of hypothalamic T3 concentration (31). Under certain conditions, however, tanycytes can increase their D2 activity independently from the changes of T4 concentration, and therefore, these cells can alter the feedback regulation of the hypophysiotropic TRH neurons and the activity of the HPT axis (31). For example, infection induces an approximately 4-fold increase of D2 activity in the MBH (84). The increased TH activating capacity of tanycytes results in local

hyperthyroidism that inhibits the hypophysiotropic TRH neurons and therefore, induces central hypothyroidism. In D2 KO mice, infection has no effect on the HPT axis (85).

Thus, the TH activating capacity of tanycytes provides an extra regulatory mechanism in the central regulation of the HPT axis.

1.3.3. Role of PPII in tanycytes

Tanycytes also synthetize the TRH degrading enzyme, the pyroglutyamyl-peptidase II (PPII) (31). PPII is a membrane-bound protein and has very high substrate specificity (86). As the axon terminals of hypophysiotropic TRH neurons are surrounded by tanycyte processes, it is likely that PPII can degrade the released TRH before it could enter into the portal capillaries (31). Peripheral administration of T4 induces significantly increased expression of PPII in tanycytes (86). Furthermore, inhibition of PPII in the ME of hyperthyroid rats markedly increases the amount of released TRH (86) supporting that the PPII production of tanycytes plays role in the feedback regulation of the HPT axis.

1.4. Role of the endocannabinoid system in the regulation of HPT axis

1.4.1. General features of the endocannabinoid system

Endocannabinoids are retrograde neurotransmitters widely spread in the brain, released from postsynaptic neurons, acting on presynaptic axon terminals (87, 88). The roles of endocannabinoids are the modulation of synaptic plasticity, motor functions, pain control, stress response, food intake, lipid and glucose metabolism, inflammatory response among others (89). Endocannabinoids are lipid-derived messengers. Their physiological role is the regulation of neurotransmitter release at synapses throughout the brain (90). Impairment of the endocannabinoid system results in behavioral, neurological and metabolic disorders (89). The two major type of endocannabinoids are anandamide and the most abundant 2-arachydonoylglicerol (2-AG) (91). This latter endocannabinoid is synthesized by the postsynaptically located diacylglycerol lipase α (DAGLα) from

22

diacylglycerol and suppresses neurotransmitter release of presynaptic terminals by activation of type 1 endocannabinoid receptor (CB1) (92, 93). In DAGLα KO mice, the 2-AG level is markedly decreased in the central nervous system, indicating that the DAGLα is the major biosynthetic enzyme of 2-AG (94).

1.4.2 The role of the endocannabinoid production of tanycytes

Recently, our group has described a novel microcircuit between the hypophysiotropic TRH axons and tanycytes which regulates the TRH release via the endocannabinoid system (95). The axons of hypophysiotropic TRH neurons in the external zone of ME contain CB1 receptor, indicating that endocannabinoids can modulate the activity of these axons (96). Since endocannabinoids can travel only short distances (97) and the external zone of ME contains only very few neuronal perikarya, it was suggested that tanycytes control the TRH release via the endocannabinoid system (95). Indeed, tanycytes express DAGLα and inhibition of endocannabinoid synthesis or administration of CB1 antagonist markedly increases the TRH release of ME explants, suggesting that tanycytes tonically inhibit the TRH release of hypophysiotropic axons (95). It raised the question, how the endocannabinoid synthesis of tanycytes is regulated. In neuronal interactions, glutamate regulates the endocannabinoid synthesis and release of postsynaptic neurons by stimulating DAGLα via metabotropic glutamate receptors and increase in intracellular Ca^{2+} level (91, 98). The hypophysiotropic TRH neurons are glutamatergic cells (99), furthermore tanycytes express glutamate receptors (100) raising the possibility that glutamate release of the hypophysiotropic TRH neurons may stimulate the endocannabinoid synthesis of tanycytes. Indeed, using combination of optogenetics and electrophysiology, our group showed that activation of the TRH axons depolarizes the tanycytes via glutamate and it was also demonstrated that the glutamate content of ME stimulates the endocannabinoid synthesis of tanycytes. These data together indicated that there is a regulatory microcircuit between tanycytes and hypophysiotropic TRH neurons in which TRH neurons stimulate the tanycytes by glutamate release, while the tanycytes inhibit the TRH release of hypophysiotropic axons via endocannabinoids. However, the relative importance of this regulatory mechanism in live animals was unknown.

1.5. Set point of the HPT axis

Under most conditions, the HPT axis maintains stable circulating TH levels (31). The TH negative feedback regulation of the HPT axis plays critical role in this process (39). During development, a set point of this feedback regulation develops as a stable characteristic of the individual for the whole life (101). The set point determines the interrelationship of TRH and free thyroxine (fT4) levels that is optimal for the individual (102). Any deviations from this TRH-fT4 relationship results in counter-regulatory action. This set point develops around birth (101).

1.5.1. The development of the HPT axis

The timing of the set point development of HPT axis is different among species (101, 103-105). The mechanism of this set point development is poorly understood. The HPT axis and its feedback regulation is already well-developed at birth in humans (29), but it develops during the first postnatal week in rats (104) and between embryonic day (E) 19 and post hatching day 2 in chickens (103).

In humans, hypothalamic nuclei start to differentiate at gestational week (GW) 15-17 and reach the adult-like anatomical structure at GW24-33 (106), while the rodent hypothalamic nuclei differentiate fully between E19 and postnatal day (PD) 10 (107).

In humans, the pituitary starts to develop at GW4 and is fully differentiated at GW16, however, the biologically active TSH production is detectable from GW17 (108). In mice, the pituitary formation occurs between E9-E17 (109).

There is a time gap between the development of HPT axis and TH-mediated negative feedback regulation of the axis both in mammals and chickens (103). For instance in chickens, TSH already stimulates the hormone secretion of the thyroid gland at E10 (110), but both the TSHβ mRNA level and the circulating TH levels continuously increases until E19 (111), indicating the lack of negative feedback regulation before E19. The TRH level in the chicken hypothalamus also increases during the ontogeny (112). In rats, TRH is expressed in the PVN from E16 (113). Increased circulating TH level has no effect on the hypophysiotropic TRH expression at E16-20, but inhibits it at PD7 (104). However, the exact timing of the set point development in rodents is currently unknown. Therefore to

examine the timing of the set point and the development of negative feedback regulation of HPT axis, in our studies we used newborn mice treated with T4 during the first postnatal week that approximately corresponds to the third trimester of the human pregnancy.

1.5.2. The effect of maternal thyroid status during the ontogeny

As described above, during the ontogeny, the HPT axis develops in different times in different species, but TH is necessary from the beginning of the pregnancy for the normal fetal development in all mammals. Therefore, at the beginning of ontogeny, the fetus is fully dependent on maternal TH status, indicating that maternal thyroid dysfunction, especially during the early gestation, can cause long-lasting changes in the offspring's development and thyroid function (29). In the human fetus, significant level of T3 and TH receptors are present in the brain before the onset of fetal TH production (114). Furthermore, TH transporters can be found in the placenta for ensuring active TH transport through the placental barrier (115) indicating the maternal origin of fetal TH at the early gestational period.

Maternal hypothyroidism during pregnancy results in decreased survival, growth retardation and impaired neuropsychological development of the offspring (116), while hyperthyroidism in this period can alter the TH status of the offspring and induce irreversible changes as well (101). Studies in humans revealed that infants born from hyperthyroid mothers show hyperthyroidism, but later this state resulting in central hypothyroidism, due to the changes in set point (117, 118). In rats, pharmacologically induced hypothyroidism in dams and pups around birth resulted in lower T4 and T3 levels, but normal TSH level at adulthood, indicating that perinatal TH status programs future set point of the HPT axis (119).

1.5.3. The role of the environment and epigenetics in the development of HPT axis set point

Beside the maternal thyroid status, environmental factors also influence the development of the offspring's HPT axis in the sensitive period.

TSH and fT4 levels have a very stable log negative relationship during the whole lifespan However, this TSH-fT4 relationship and thus the set point of the feedback regulation is highly variable among individuals (102, 120). Mathematical model published by Lowe et al. (102) revealed that the exponential curve of the fT4-TSH relationship in T4 substituted hypothyroid patients did not overlap, indicating the significant interindividual variation of the set point of the feedback regulation of HPT axis.

A study, performed by Panicker et al. (121) identified a number of genetic loci, which have impact on the HPT axis set point, but twin studies revealed (102) that heritability accounts for only 60% of the interindividual HPT axis variability. This suggests that internal and environmental factors like hormonal status, feeding status, acute or chronic inflammations (122) and endocrine disruptors (123) have also large impact on the development of set point.

The long-term effects of environmental factors or perturbations of internal milieu during the late gestational or perinatal periods can be mediated by epigenetic modifications of genes. The predominant epigenetic modification of the mammalian DNA is the methylation of cytosine, when a methyl or hydroxymethyl group binds covalently to the 5' position of cytosine in cytosine-phosphate-guanine (CpG) dinucleotids (124). These CpG dinucleotids are frequently found in the promoter region of genes. Methylation of cytosine in these regions repress gene expression by preventing the binding of specific transcription factors or attract repressors (125). Furthermore, CpG methylation also influences the initiation of transcription and the alternative splicing of transcripts (124). These changes of gene expression by methylation ensure the adaptation to the environmental changes. The transfer of the methyl group to CpG sites is catalyzed by DNA-methyltransferase (DNMT) enzymes, including DNA-methyltransferase 1 (DNMT1), DNA-methyltransferase 3A (DNMT3A) and DNA-methyltransferase 3B (DNMT3B) (124, 126).

The liver is one of the main target organs for TH, where these hormones stimulate lipogenesis, fatty acid oxidation and cholesterol metabolism (127). THRβ and various T3-responsive genes are present in high abundance in this tissue (128). In the liver, the D2 enzyme is only expressed in the neonatal mice, but it is absent at adulthood, however, the total ablation of liver D2 in transgenic mice results in changes in the methylation status of genes involved in fatty acid, triglyceride, cholesterol and bile acid synthesis (128).

These results indicate that changes in TH status at the early postnatal period when the set point of the HPT axis develops can cause epigenetic modification of TH dependent genes, but this mechanism is poorly understood yet.

2. Aims

The aim of our study was to better understand the underlying mechanisms of the development of the HPT axis set point and the central regulation of the negative feedback of HPT axis in mice, therefore our specific aims were:

1. To investigate how tanycytic endocannabinoid system regulates:
   - the TRH release of hypophysiotropic TRH neurons
   - the activity of HPT axis
   - the body composition and metabolism

2. To elucidate, that early, perinatal disturbance of the thyroid status can induce long lasting changes in
   - the activity of HPT axis
   - the body composition and metabolism
   - TH action of tissues
   - TH-dependent gene expression profile of liver

3. Materials and methods

3.1. Experimental animals and treatments

The experiments were carried out using newborn and adult mice housed under standard environmental conditions (12h light/dark cycle, temperature 22±1 °C, chow and water *ad libitum*). The mouse strains used for the experiments and the experimental design are found in **Table 1**. All experimental protocols were reviewed and approved by the Animal Welfare Committee at the Institute of Experimental Medicine and the Animal Health and Food Control Station, Budapest (PE/EA/1102-7/2020).

Table 1: *Summary of experimental design and strains used in the experiments. Abbreviations: THAI − thyroid hormone action indicator mouse, T4 − thyroxine, bwg − body weight gram.*

	Strain	Treatment	Duration of treatment	Age during treatment	Sacrifice
Experiment 1: Examination of the role of tanycytic endocannabinoid production	CD1	-	-	-	55-65
	Rax-CreERT2 Rax-CreERT2//Dagla fl/fl	175µg/bwg Tamoxifen	4 days	45-55	55-65
Experiment 2: Development of the HPT axis negative feedback regulation in mice	TRH-IRES-tdTomato	200 ng/bwg T4 or vehicle	1 day	1,2,3,4,5,6,7,10	1,2,3,4,5,6,7,10
	FVB/Ant	200 ng/bwg T4 or vehicle	1 day	1,3,4,7	1,3,4,7
Experiment 3: Effects of early disturbance in thyroid status in adult mice	TRH-IRES-tdTomato	1 µg/bwg T4 or vehicle	5 days	2-6	55-70
	THAI	1 µg/bwg T4 or vehicle	5 days	2-6	55-70

3.1.1. The role of endocannabinoid synthesis of tanycytes in the regulation of HPT axis (Experiment 1)

Rax-CreERT2 mice (129) were crossed with Dagla^{fl/fl} mice (130) to generate mice with tanycyte-specific deletion of DAGLα. In adult animals, Rax mRNA is selectively expressed in hypothalamic tanycytes (131), therefore the Rax-CreERT2 construct ensures the tanycyte-specific gene modification in this transgenic model. The Dagla^{fl/fl} mouse allow the Cre dependent cell type specific ablation of the DAGLα enzyme. The CreERT2 recombinase is tamoxifen dependent, tamoxifen treatment is necessary to induce recombination in the DAGLα locus of the double transgenic mice. The tamoxifen-treated Rax-CreERT2 animals were used as control, while the tamoxifen-treated Rax-CreERT2//Dagla^{fl/fl} mice were used as tanycyte-specific DAGLα ablated (T-DAGLα KO) mice. 45-55 day old adult male mice from both strains (N=19-22) were treated with tamoxifen (Sigma-Aldrich) dissolved in corn oil and administered in 175µg/bwg dose daily for 4 days via oral gavage. The dose of the tamoxifen was tested previously in other mouse lines to induce Cre-mediated recombination. One week after the last treatment, metabolic measurements and body composition analysis using EchoMRI 700 whole body magnetic resonance analyser (Zinsser Analytic, Germany) were performed on a cohort of animals (N=7-8). All of the tamoxifen-treated mice were sacrificed 1 week after the last treatment for further examinations as described later. CD1 male mice were used for previous morphological studies to detect the components of the endocannabinoid system in the tanycytes and the hypophysiotropic TRH neurons, therefore we used this mouse line to determine the glutamate and TRH receptor content of tanycytes isolated by laser capture microdissection (LCM) as described later.
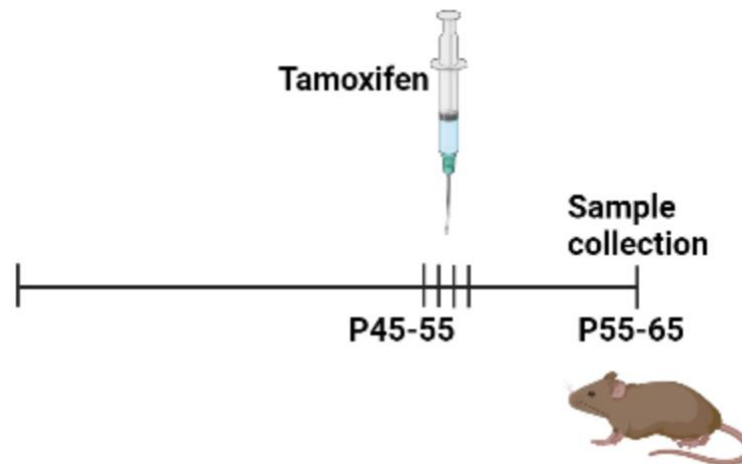
Figure 4: Experimental design of tanycyte-specific deletion of DAGLα

Rax-CreERT2 (control) and Rax-CreERT2//Dagla^{fl/fl} mice were treated with 175µg/bwg

tamoxifen via oral gavage for 4 consecutive days starting at P45-55. 1 week after the last

tamoxifen administration, the animals were sacrificed between age of P55-65 for sample

collection.

Abbreviation: P – postnatal day

Created with BioRender.com

3.1.2. Determination of the development of the HPT axis negative feedback regulation in FVB/Ant and TRH-IRES-tdTomato mouse pups (Experiment 2)

1, 2, 3, 4, 5, 6, 7 and 10 day old TRH-IRES-tdTomato (132) mouse pups were injected (N=4-6) subcutaneously with 200 ng/bwg thyroxine (L-Thyroxine sodium salt pentahydrate, Sigma) or vehicle (0.36 mM NaOH) and were decapitated 8 hours later. The TRH-IRES-tdTomato line was created by inserting an IRES-tdTomato cassette into the mouse TRH locus using CRISPR/Cas9 on FVB/Ant background to allow detection of TRH-expressing cells based on the red fluorescence of tdTomato (132).

 FVB/Ant 1, 3, 4 and 7 day old pups (N=4-7) were treated with 200 ng/bwg thyroxine or vehicle and were decapitated 8 hours later.

3.1.3. Determination of the effect of early hyperthyroidism on physilogical parameters of adult TRH-IRES-tdTomato and THAI mice (Experiment 3)

Male TRH-IRES-tdTomato (N=14) and THAI (Thyroid Hormone Action Indicator (133), N=8) mouse pups were injected subcutaneously daily with 1 µg/bwg thyroxine or vehicle (1.8 mM NaOH) between postnatal day (P) 2-6 and sacrificed as adults at the age of P 55-70. The THAI mouse model was used to study tissue-specific TH action. In these mice, the expression of the firefly luciferase (luc) reporter is driven by a minimal viral promoter that was made TH sensitive by the insertion of three copies of the TH response element of the human dio1 gene (133).

Figure 5: Experimental design of the examination of the effect of early, postnatal hyperthyroidism on the physiological parameters of adult mice

TRH-IRES-TdTomato and THAI mouse pups were treated with 1 µg/bwg T4 or vehicle subcutaneously for 5 consecutive days between P2-6. At the age of P55-70, adult animals were sacrificed for sample collection.

Abbreviation: T4 – thyroxine, P – postnatal day
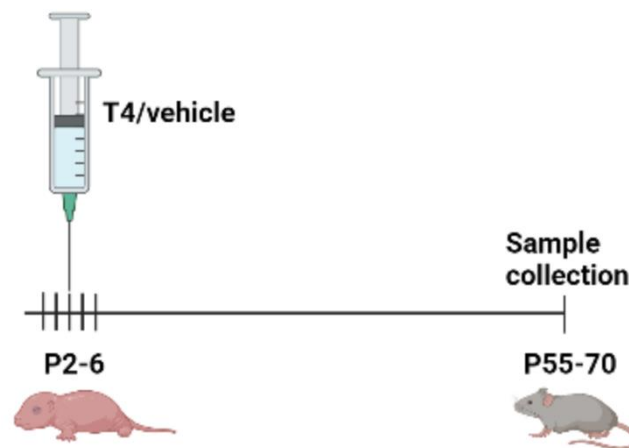
Created with BioRender.com

3.2. Tissue preparation

3.2.1. Preparation of tissues for gene expression analysis

Adult Rax-CreERT2 and Rax-CreERT2//Dagla^{fl/fl} mice (Experiment 1) were decapitated 1 week after the last tamoxifen treatment for collection of blood to measure free TH levels, and pituitary samples for qPCR analysis. Whole brain samples for TRH *in situ* hybridization (ISH) were rapidly removed and frozen in powdered dry ice. All samples were kept at -80 °C until used. Serial, 12 μm coronal sections through the PVN were cut on a cryostat (Leica Microsystems, Wetzlar, Germany) and the sections were saw mounted on gelatin-coated glass slides. Each set of slides contained every fourth section. The sections were air-dried at 56 °C overnight and then stored at -80 °C.

FVB/Ant and TRH-IRES-tdTomato mouse pups (Experiment 2) were decapitated for collecting whole brain samples for TRH ISH, and liver and pituitary samples for qPCR analysis. All of the tissues were removed rapidly, immediately frozen in powdered dry ice, and stored at -80 °C until used. 12 μm coronal sections through the PVN were cut on a cryostat and every third section was collected for a slide. The slides were prepared as described above air-dried at 56 °C overnight and then stored at -80 °C.

Postnatally treated, adult THAI mice (Experiment 3) were decapitated and liver, BAT, small intestine, hippocampus and hypothalamus samples were collected for qPCR measurements. Tissues were frozen in powdered dry ice then stored at -80 °C until used.

3.2.2. Tissue preparation for immunohistochemistry

One week after the last tamoxifen treatment, Rax-CreERT2 and Rax-CreERT2//Dagla [fl/fl] mice (Experiment 1) were deeply anesthetized with ketamine and xylazine (ketamine 50 mg/kg, xylazine 10 mg/kg body weight, i.p.). The animals were transcardially perfused with 10 ml 0.01 M phosphate-buffered saline pH 7.4 (PBS), followed by 50 ml 4% paraformaldehyde (PFA) in 0.1 M phosphate buffer pH 7.4 (PB). After perfusion, the brains were removed and transferred into the fixative solution for 2 hours. For cryoprotection, brains were incubated in 30% sucrose in 0.01 M PBS overnight at 4 °C, then frozen in powdered dry ice. Series of 25 μm coronal sections were cut using Leica SM2000 R freezing microtome (Leica Microsystems, Wetzlar, Germany) and were

placed in antifreeze solution (30% ethylene glycol; 25% glycerol; 0.05 mM PB), then stored at -20 °C until their use for immunohistochemistry.

3.2.3. Tissue preparation of postnatally treated, adult TRH-IRES-tdTomato mice for ISH, hormone and qPCR analysis

Postnatally treated, adult TRH-IRES-tdTomato mice (Experiment 3) were anaesthetized with a mixture of ketamine and xylazine (ketamine 50 mg/kg, xylazine 10 mg/kg body weight, i.p.). Liver samples for qPCR analysis were collected and frozen immediately brefore fixation. Blood was drawn for free TH level measurements from caudal vena cava. For ISH, anaesthetized mice were perfused transcardially with 10 ml RNAse-free 0.01 M PBS, pH 7.4, followed by 50 ml 4% PFA in RNAse-free PBS. After perfusion, the brains were removed and transferred into the fixative solution for 2 hours. For cryoprotection, brains were incubated in 20% sucrose in RNAse-free 0.01 M PBS overnight at 4 °C, then frozen in powdered dry ice and stored at -80 °C until used. Serial 18-µm-thick coronal sections through the PVN were cut on a cryostat. The sections were mounted on Superfrost Plus slides (Fisher, Hampton, NH) to obtain three sets of slides, each set containing every third section through the PVN. The mounted sections were air-dried at 56 °C overnight and stored at -80 °C.

3.2.4. Tissue preparation for laser capture microdissection

Postnatally treated, adult TRH-IRES-tdTomato (Experiment 3), CD1, Rax-CreERT2 and Rax-CreERT2//Dagla$^{fl/fl}$ mice (Experiment 1) were deeply anaesthetized as described above. For isolation of tanycytes with PALM Laser Capture Microdissection (LCM) system (Zeiss), mice were transcardially perfused with 30 ml ice cold 10% RNAlater (Sigma) dissolved in 0.01M RNase-free PBS to preserve the integrity of RNA for further gene expression investigations. The brains were rapidly removed from the skull, frozen in -40 °C isopentane, then stored at -80 °C until used. 12 µm thick coronal sections were cut on a cryostat through the rostrocaudal extent of the ME. The sections were collected on PEN membrane covered slides (Zeiss), fixed in 50% and 70% ethanol, stained with 0.6% cresyl violet dissolved in 70% ethanol, then dehydrated in graded solution of ethanol and dried on a 42 °C hotplate. The stained sections were stored at -80 °C.

Table 2: Summary of tissue preparation and sectioning. Abbreviations: DAGLα – diacylglycerol lipase α, PFA – paraformaldehyde, ME – median eminence, PVN – paraventricular nucleus

Experiment	Strain	Fixative	Sectioning
DAGLα immunohistochemistry (Exp. 1)	Rax-CreERT2 Rax-CreERT2//Dagla fl/fl	4% PFA 30% sucrose	freezing microtome ME 25 μm
In situ hybridization (Exp. 1,2,3)	postnatally treated, adult TRH-IRES-tdTomato	4% RNase-free PFA 20% RNase-free sucrose	cryostat PVN 18 μm Superfrost Plus slide
	Rax-CreERT2 Rax-CreERT2//Dagla fl/fl FVB/Ant pups	-	cryostat PVN 12 μm gelatine-coated slide
Laser capture microdissection (Exp. 1,3)	CD1 Rax-CreERT2 Rax-CreERT2//Dagla fl/fl postnatally treated, adult TRH-IRES-tdTomato	10% RNAlater	cryostat ME 12 μm PenSlide

3.3. Immunohistochemistry for DAGLα in the ME

Every fourth sections of the ME of tamoxifen-treated Rax-CreERT2 and Rax-CreERT2//Dagla^{fl/fl} mice (Experiment 1) were placed into 0.5% Triton X-100 and 0.5% H_2O_2 in 0.01 M PBS for 20 min to improve penetration and block the endogenous peroxidase activity, then incubated in 2% normal horse serum (NHS) in PBS for 10 min to reduce non-specific antibody binding. The sections were incubated in guinea-pig anti-DAGLα antibody (gift from Dr. Ken Mackie, Indiana University, Bloomington, IN, USA) (134) at 1:4000 dilution in 2% NHS for 2 days at 4°C. After washing in 0.01 M PBS, the sections were incubated in biotinylated donkey anti-guinea pig IgG (1:500, Jackson) in 2% NHS for 2 hours, then treated with avidin-biotin-peroxidase complex (1:1000, Vector lab, Vectastain ABC Elite kit). The DAGLα immunoreactivity was visualized with Ni-

DAB developer (0.05% DAB/0.15% Ni-ammonium sulfate/0.005% H_2O_2 in 0.05 M Tris buffer, pH 7.6) and the sections were mounted onto glass slides, dehydrated in ascending series of ethanol followed by xylenes and coverslipped with DPX mountant (Sigma-Aldrich).

3.4. Measurement of blood glucose and serum free TH levels

Blood glucose levels of Rax-CreERT2 and Rax-CreERT2//Dagla^{fl/fl} mice (Experiment 1) were determined from one drop of blood collected from a small tail incision using Accu-Check® Performa blood glucose meter (Roche) before the anesthesia for RNAlater perfusion.

Blood drawn from caudal vena cava of anaesthetized TRH-IRES-tdTomato mice before the perfusion and trunk blood of Rax-CreERT2 and Rax-CreERT2//Dagla^{fl/fl} mice was collected and placed on ice for 1 hour. The blood samples were centrifuged at 4 °C at 3000 rcf for 15 minutes twice, then the sera was collected in new Eppendorf tubes and was stored at -80 °C until used.

The free TH levels were measured from tamoxifen-treated Rax-CreERT2 and Rax-CreERT2//Dagla^{fl/fl} mice by AccuBind™ ELISA fT3 and fT4 kits (Monobind, Lake Forest, CA) according to the manufacturer's protocol using iMARK™ Microplate Absorbance Reader (BIO-RAD). The intraassay coefficients of variation for free triiodothyronine (fT3) assay was 3.1 to 4.9 percent and for fT4 assay it was 3.25 to 10,98 percent, respectively. The interassay coefficients of variation for fT3 assay was 7.9 to 13.1 percent and for fT4 assay it was 6.01 to 10.81, respectively.

FT4 and fT3 levels of postnatally treated, adult TRH-IRES-tdTomato mice (Experiment 3) were measured by AccuLite™ CLIA fT3 and fT4 kits (Monobind, Lake Forest, CA) according to the manufacturer's protocol using a luminometer (Luminoskan Ascent, Thermo Scientific). The intraassay coefficients of variation for fT3 assay was 5.9 to 9 percent and for fT4 assay it was 5.32 to 9.34 percent, respectively. The interassay coefficients of variation for fT3 assay was 8.2 to 10.4 percent and for fT4 assay it was 5.26 to 9.76, respectively.

3.5. Radioactive ISH for determination of proTRH mRNA levels in the PVN

Every third section of the PVN of T4-treated and control 1, 3, 4 and 7 day old FVB/Ant mouse pups (Experiment 2) and postnatally treated, adult TRH-IRES-tdTomato animals (Experiment 3) or every fourth section of the PVN of Rax-CreERT2//Dagla^{fl/fl} and their control Rax-CreERT2 mice (Experiment 1) were processed for ISH with single stranded 741-base long (corresponding to the 106–846 nucleotides of the mouse proTRH (mTRH) mRNA; BC053493) [35S]UTP-labeled cRNA probe for mTRH (38). The mTRH riboprobe was synthetized in the presence of Sp6 enzyme (Roche) and [35S]UTP (Perkin Elmer). The labelled riboprobe was purified with Mini Quick Spin RNA columns (Roche) and counts per million (cpm) of the radiolabelled mTRH was measured by liquid scintillation analyzer (Tri-Carb 2900TR).

The sections of FVB/Ant mouse pups and Rax-CreERT2//Dagla^{fl/fl} mice with their control groups were fixed with 4% PFA in 0.01 M PBS (pH 7.4) for 1 h. Since the samples of TRH-IRES-tdTomato mice were already perfusion fixed with 4% PFA, instead of the 4% PFA treatment, the sections of these animals were treated with 1 μg/ml proteinase K (Sigma-Aldrich) in 0.1 M Tris buffer, pH 8.0, containing 0.05 M EDTA for 30 minutes at 37°C, and the proteinase K digestion was stopped with fixation in 4% PFA for 5 min. After these initial steps, all the sections were treated similarly. The sections were washed in 0.01 M PBS, acetylated with 0.25% acetic anhydride in 0.9% triethanolamine for 20 min, and then treated in graded solutions of ethanol (70, 80, 96, and 100%), chloroform, and a descending series of ethanol (100 and 96%) for 5 min each. The sections were hybridized with the radiolabeled mTRH probe containing hybridization buffer (50% formamide, a 2-fold concentration of standard sodium citrate (2 × SSC), 10% dextran sulfate, 0.5% SDS, 250 μg/ml denatured salmon sperm DNA) under glass coverslips overnight at 56 °C. The concentration of radiolabeled probe used for the different experiments are described in **Table 3**.

After the overnight incubation, the slides were washed in 1× SSC (3X 5 min) and treated with RNaseA (25 μg/ml, Sigma-Aldrich) for 1 h at 37 °C, followed by additional washes in 1X SSC (15 minutes), 0.5X SSC (15 minutes), and 0.1X SSC (2X 30 minutes) at 65°C. After dehydration in graded dilutions of ethanol, the slides were dipped into Kodak NTB autoradiography emulsion (Carestream Health) diluted 1:1 in MQ water and stored at 4

°C. The exposition times are found in **Table 3**. The autoradiograms were developed using EMS Developer D-19 Replacement Kit (Electron Microscopy Sciences).

The slides were dehydrated in ascending series of ethanol followed by xylenes and coverslipped with DPX mountant (Sigma-Aldrich). Darkfield images were captured by Zeiss Axiomager.M1 microscope equipped with AxioCam MRc5 (Carl Zeiss) using 10X objective and AxioVision Se64 Rel.4.9.1 software. Three sections were selected in every group from the mid-level of PVN and integrated density was measured in both sides of the selected sections by using ImageJ software. Background density points were removed by thresholding the image.

Table 3: Concentration of mTRH probe and exposition times used for the ISH experiments. Abbreviations: P – postnatal day, cpm – counts per million

Experiment	Strain	probe (cpm/µl)	Exposition time
Experiment 1	Rax-CreERT2 Rax-CreERT2//Dagla fl/fl	30000	7 days
Experiment 3	Adult TRH-IRES-tdTomato	60000	20 days
Experiment 2	P1 FVB/Ant	50000	18 days
	P3 FVB/Ant		15 days
	P4 FVB/Ant		15 days
	P7 FVB/Ant		11 days

3.6. Examination of DAGLα, Dio2, PPII, glutamate transporter and receptor gene expression in tanycytes isolated with LCM

3.6.1. Isolation of tanycytes using LCM

The RNAlater perfused and preconditioned brain sections of CD1, Rax-CreERT2, Rax-CreERT2//Dagla$^{fl/fl}$ mice (Experiment 1) and postnatally treated, adult TRH-IRES-tdTomato animals (Experiment 3) were thawed at room temperature and kept under vacuum until used. The cell bodies of β2-tanycytes from CD1, Rax-CreERT2 and Rax-CreERT2//Dagla$^{fl/fl}$ mice and α- and β-tanycytes from adult TRH-IRES-tdTomato mice were microdissected separately with PALM Microbeam Laser Capture Microdissection

System (ZEISS) and pressure-catapulted with a single laser pulse into 0.5 ml Adhesive cap, opaque tubes (Carl Zeiss Microimaging) using a 20X objective lens.

3.6.2. RNA isolation and determination of RNA quality

The microdissected samples were kept in Extraction Buffer of the RNA isolation kit at -80°C, then RNA isolation was performed using the Arcturus PicoPure RNA Isolation Kit (Applied Biosystems) according to the manufacturer's protocol. To digest the potential DNA contamination of the samples, DNase treatment was carried out using RNase-free DNase Set (Qiagen). The RNA integrity number (RIN) - which defines the quality of RNA - and the concentration of the isolated RNA samples were measured with Agilent 2100 Bioanalyzer using Agilent RNA 6000 Pico Kit (Agilent Technologies). Samples with RIN below 4 were excluded from further studies.

3.6.3. Reverse transcription and amplification

The RNA samples were transcribed using ViLO Superscript III cDNA Reverse Transcription Kit (Invitrogen) according to the manufacturer's protocol.
Concentration of single-stranded complementary DNA (cDNA) was determined with Qubit Fluorometer using Qubit ssDNA Assay Kit (Invitrogen). The cDNA was preamplified for every studied and housekeeping genes using Preamp Master Mix Kit (Applied Biosystems).

3.6.4. Custom TaqMan Gene Expression Array Card

384-well Custom TaqMan Gene Expression Array Cards (Applied Biosystems) were used to examine the presence of glutamate transporters and glutamate receptor subunits in β2-tanycytes of CD1 mice (Experiment 1). The microfluidic card was preloaded by the manufacturer with selected gene expression assays for our target receptors, transporters and housekeeping genes listed in **Table 5**. ViiA 7 real-time PCR platform with Array Card Block and comparative CT method (Life Technologies) was used for thermal cycles of the qPCR.

The glyceraldehyde-3-phosphate dehydrogenase (Gapdh), the actin beta (Actb) and the hypoxanthine-guanine phosphoribosyltransferase (Hprt) were used as housekeeping genes, the CT values of genes of our interests were normalized to the geometric mean of the CT value of housekeeping genes. The diacylglycerol lipase alpha (Dagla) and type 2 deiodinase (Dio2) served as positive controls, since we have already proved that DAGLα is expressed in tanycytes (95) and Dio2 is known to be expressed by tanycytes (78). The metabotropic glutamate receptor 1 (Grm1) and the metabotropic glutamate receptor 5 (Grm5) were used as negative controls as our *in situ* hybridization analysis revealed that these genes are not expressed in tanycytes (95).

3.6.5. TaqMan quantitative PCR analysis

Equal amount (10 ng) cDNA was applied in each TaqMan reaction using Taqman Fast Universal PCR Mastermix (Thermo Fisher Scientific). The examined genes are listed in **Table 4**. For the qPCR analysis, ViiA 7 real-time PCR platform (Life Technologies) was used for thermal cycles with Fast-96 well block and comparative CT method. The CT values of the genes of interest in β-tanycytes of postnatally treated, adult TRH-IRES-tdTomato mice (Experiment 3) were normalized to the CT value of the geometric mean of three housekeeping genes (Gapdh, Actb, Hprt) since the T4 treatment influenced the gene expression of Gapdh. Gene expressions in α-tanycytes of postnatally treated, adult TRH-IRES-tdTomato (Experiment 3) and β2-tanycytes of Rax-CreERT2 and Rax-CreERT2//Dagla$^{fl/fl}$ mice (Experiment 1) were normalized only to the CT value of Gapdh, since the gene expression of Gapdh was not influenced by our treatments in these cells.

3.7. Determination of the expression of TH sensitive genes in different tissues

The RNA was isolated from pituitary samples by Arcturus PicoPure RNA Isolation Kit (Applied Biosystems) according to the manufacturer's protocol and DNase treatement was performed by RNase-free DNase Set (Qiagen).

From MBH samples, the RNA isolation was performed by RNeasy lipid tissue mini kit (Qiagen).

NucleoSpin RNA (Macherey-Nagel) kit with DNase treatment was used to isolate total RNA from liver, BAT, small intestine, hypothalamus and hippocampus samples. The homogenization of hypothalamus and hippocampus was performed by sonication in RA1 buffer from the NucleoSpin RNA kit, while all other tissues were homogenized in TRIzol Reagent (Invitrogen) with tissue tearor. RNA concentration was determined with Qubit Fluorometer using a Qubit hs-RNA assay kit (Invitrogen) or with Smart Spec Plus Spectrophotometer (BIORAD). Reverse transcription was carried out with High-capacity cDNA reverse transcription kit (Applied Biosystems), then cDNA concentration was measured with Qubit Fluorometer using Qubit ss-DNA assay kit (Invitrogen). MBH, liver, BAT, hypothalamus and hippocampus samples of THAI mice were premaplified for luc gene expression, marker of TH action in the THAI mice, with Hprt which served as housekeeping gene. The TaqMan qPCR analysis was performed as described in **3.6.5.** The examined genes are listed in **Table 4**.

Table 4: List of genes examined by TaqMan qPCR

Tissue	Gene	Gene name	Accession
Rax-CreERT2 and Rax-CreERT2//Dagla^{fl/fl} (Experiment 1)			
Pituitary	tshβ	thyroid stimulating hormone beta	Mm03990915_g1
	gapdh	glyceraldehyde-3-phosphate dehydrogenase	Mm99999915_g1
β2-tanycytes	dagla	diacylglycerol lipase alpha	Mm00813830_m1
	dio2	type 2 deiodinase	Mm00515664_m1
	trhde	pyroglutamyl-peptidase II	Mm00455443_m1
	gapdh	glyceraldehyde-3-phosphate dehydrogenase	Mm99999915_g1
TRH-IRES-tdTomato pups (Experiment 2)			
Pituitary	tshβ	thyroid stimulating hormone beta	Mm03990915_g1
	gapdh	glyceraldehyde-3-phosphate dehydrogenase	Mm99999915_g1
Liver	dio1	type 1 deiodinase	Mm00839358_m1
	dnmt1	DNA (cytosine-5)-methyltransferase 1	Mm01151054_m1

	dnmt3a	DNA (cytosine-5)-methyltransferase 3a	Mm00432881_m1
	dnmt3b	DNA (cytosine-5)-methyltransferase 3b	Mm01240113_m1
	gapdh	glyceraldehyde-3-phosphate dehydrogenase	Mm99999915_g1
Adult TRH-IRES-tdTomato (Experiment 3)			
Liver	dio1	type 1 deiodinase	Mm00839358_m1
	gapdh	glyceraldehyde-3-phosphate dehydrogenase	Mm99999915_g1
	thra	TH receptor alpha	Mm00579691_m1
	thrb	TH receptor beta	Mm00437044_m1
	fasn	fatty acid synthase	Mm00662319_m1
	me1	malic enzyme 1	Mm01731412_m1
	g6pc	glucose-6-phosphatase	Mm00839363_m1
	spot14	TH responsive gene	Mm01273967_m1
Tanycytes	dio2	type 2 deiodinase	Mm00515664_m1
	trhde	pyroglutamyl-peptidase II	Mm00455443_m1
	gapdh	glyceraldehyde-3-phosphate dehydrogenase	Mm99999915_g1
	hprt	hypoxanthine-guanine phosphoribosyltransferase	Mm01545399_m1
	actb	actin beta	Mm02619580_g1
THAI (Experiment 3)			
Liver BAT MBH Hippocampus Hypothalamus	luc	luciferase	DCPGLUC
	hprt	hypoxanthine-guanine phosphoribosyltransferase	Mm01545399_m1
Small intestine	luc	luciferase	DCPGLUC
	gapdh	glyceraldehyde-3-phosphate dehydrogenase	Mm99999915_g1

3.8. Body composition analysis and indirect calorimetry

Male TRH-IRES-tdTomato mouse pups were injected with thyroxine or vehicle as described above and two months later, body composition analysis and indirect calorimetry measurements were performed. One week after the last tamoxifen treatment, the same measurements were performed on Rax-CreERT2 and Rax-CreERT2//Dagla$^{fl/fl}$ mice. Before the measurements, mice were trained to use the special drinking nipples and

feeders in training cages similar to the metabolic cages. The training session lasted for 3 days. Before and after the metabolic measurements, the body composition (total and free water, fat and lean body mass) of the animals was determined by EchoMRI whole body magnetic resonance analyser (Zinsser Analytic, Germany). The food intake, the locomotor activity and the calorimetric parameters of the animals were continuously monitored for 72 hours by TSE PhenoMaster System (TSE Systems GmbH, Bad Homburg, Germany). The metabolic data was analyzed with the TSE PhenoMaster software. The energy expenditure and resting energy expenditure of the animals was normalized to the lean body mass of each mouse. The resting energy expenditure was calculated from the energy expenditure of the time points when the animal ate less than 0.1 g and moves less than 1% of the maximum ambulatory value in the preceding 30 minutes. The respiratory exchange ratio (RER) was calculated from the volume of the produced CO_2 and the consumed O_2 by the animals, which determines the substrate utilization.

3.9. Statistical analysis

Statistical analysis was performed by GraphPad Prism 8.0.1 Software and outliers were excluded by using Grubb's test. All data are represented as mean ± SEM. Two-tailed Student's t-test was used for comparison of two groups, Welch's correction was used if the variances were significantly different. Two-way ANOVA followed by Bonferroni post hoc test and one-way ANOVA followed by Tukey post hoc test was used in the examination of more than two groups. $p < 0.05$ was considered significant (*$p < 0.05$; **$p < 0.01$, ***$p < 0.001$, ****$p < 0.0001$).

4. Results

4.1. Determination of the importance of the endocannabinoid production of tanycytes in the regulation of the HPT axis

4.1.1. β2-tanycytes express glutamate receptors and glutamate transporters in mice

Glutamate is known to regulate the endocannabinoid synthesis (98) and release and it has already proved that hypophysiotropic TRH neurons release glutamate (99). Therefore, gene expression assay of β2-tanycytes from CD1 mice was performed to determine whether the tanycytes might be sensitive for the glutamate and TRH released from the hypophysiotopic TRH neurons. The β2-tanycytes were isolated by LCM and gene expression of DAGLα, Dio2, glutamate receptor subunits, glutamate transporters and TRH receptors **(Table 5)** was measured by using TaqMan gene expression array cards. High level of glutamate transporter SLC1A3 expression was detected in β2-tanycytes, whereas SLC1A1 and SLC1A2 was present in lower levels. However, the SLC1A6 and SLC1A7 glutamate transporter subunit expression was not observed in β2-tanycytes. Measurements of AMPA receptor subunit mRNA levels showed expression of GRIA1 and GRIA2, but not GRIA3 and GRIA4 in the β2-tanycytes. Kainite receptor subunits also expressed in β2-tanycytes. The GRIK3 showed the highest expression, whereas lower level of GRIK2, GRIK4 and GRIK5 expression and no expression of GRIK1 was detected. The NMDA receptor subunit GRIN3A and metabotropic glutamate receptor GRM4 were also present in β2-tanycytes, but the other subunits of these receptor types were absent. Both TRH receptor, TRHR1 and TRHR2, were absent in β2-tanycytes. These results indicating that glutamate can act primarily on the β2-tanycytes via kainite and AMPA receptors and glutamate transporter SLC1A3.

Table 5: Expression of glutamate receptors and transporters in β2-tanycytes. Genes were considered to be expressed if the ΔCT value was under the ΔCT value of negative control GRM5 and considered to be absent if the ΔCT value was above the ΔCT value of negative control GRM5. N=4.

Expression in β2-Tanycytes (CTgene - CTgeomean housekeeping genes ± SEM)	Gene	Gene name
Genes Expressed in Tanycytes		
5.46 ± 0.31	Dagla	Diacylglycerol lipase alpha
1.57 ± 0.25	Dio2	Deiodinase, iodothyronine, type II
5.52 ± 0.92	SLC1A1	Solute carrier family 1, member 1
4.50 ± 0.34	SLC1A2	Solute carrier family 1, member 2
-0.15 ± 0.26	SLC1A3	Solute carrier family 1, member 3
2.89 ± 0.17	GRIA1	Glutamate receptor, ionotropic, AMPA1 (alpha 1)
4.37 ± 0.51	GRIA2	Glutamate receptor, ionotropic, AMPA2 (alpha 2)
5.97 ± 0.68	GRIK2	Glutamate receptor, ionotropic, kainate 2 (beta 2)
-0.59 ± 0.10	GRIK3	Glutamate receptor, ionotropic, kainate 3
5.81 ± 0.27	GRIK4	Glutamate receptor, ionotropic, kainate 4
2.57 ± 0.35	GRIK5	Glutamate receptor, ionotropic, kainate 5 (gamma 2)
3.15 ± 0.09	GRIN3A	Glutamate receptor ionotropic, NMDA3A
5.29 ± 0.16	GRM4	Glutamate receptor, metabotropic 4
Genes Not Expressed in Tanycytes		
8.07 ± 0.61	SLC1A6	Solute carrier family 1, member 6
UD	SLC1A7	Solute carrier family 1, member 7
6.83 ± 1.68	GRIA3	Glutamate receptor, ionotropic, AMPA3 (alpha 3)
6.85 ± 0.58	GRIA4	Glutamate receptor, ionotropic, AMPA4 (alpha 4)

10.24 ± 0.33	GRIK1	Glutamate receptor, ionotropic, kainate 1
6.80 ± 0.75	GRIN1	Glutamate receptor, ionotropic, NMDA1 (zeta 1)
6.88 ± 0.30	GRIN2A	Glutamate receptor, ionotropic, NMDA2A (epsilon 1)
6.54 ± 0.21	GRIN2B	Glutamate receptor, ionotropic, NMDA2B (epsilon 2)
UD	GRIN2C	Glutamate receptor, ionotropic, NMDA2C (epsilon 3)
8.26 ± 0.62	GRIN2D	Glutamate receptor, ionotropic, NMDA2D (epsilon 4)
UD	GRIN3B	Glutamate receptor, ionotropic, NMDA3B
11.77 ± 1.98	GRM1	Glutamate receptor, metabotropic 1
UD	GRM2	Glutamate receptor, metabotropic 2
6.88 ± 1.21	GRM3	Glutamate receptor, metabotropic 3
6.38 ± 0.73	GRM5	Glutamate receptor, metabotropic 5
UD	GRM6	Glutamate receptor, metabotropic 6
9.20 ± 0.27	GRM7	Glutamate receptor, metabotropic 7
UD	GRM8	Glutamate receptor, metabotropic 8
8.08 ± 0.41	TRHR1	Thyrotropin-releasing hormone receptor 1
6.86 ± 1.59	TRHR2	Thyrotropin-releasing hormone receptor 2

4.1.2. Validation of the tanycyte-specific ablation of DAGLα in the Rax-CreERT2//Dagla^{fl/fl}

To determine whether the genetic manipulation decreased the DAGLα expression in β2-tanycytes, first, immunocytochemistry was performed to detect the DAGLα protein in the ME. While immunocytochemistry demonstrated DAGLα-immunoreactivity in the cell bodies and basal processes of β2-tanycytes in the ME of Rax-CreERT2 mice **(Figure 6A)**, it significantly decreased in Rax-CreERT2//Dagla^{fl/fl} mice **(Figure 6B)**. The genetic manipulation did not influence DAGLα-immunoreactivity in other brain regions, like in the ARC. To quantify the change of the DAGLα expression specifically in the β2-tanycytes, the expression of this gene was studied by TaqMan qPCR in the cell bodies of β2-tanycytes isolated by LCM. The expression of DAGLα mRNA **(Figure 6C)** was significantly decreased in β2-tanycytes of T-DAGLα KO mice compared to the controls (Control *vs.* T-DAGLα KO (RQ): 1.00 ± 0.19 *vs.* 0.44 ± 0.09, p=0.02, t=2.796, df=13, N=7-8), supporting the results of the immunohistochemistry study and demonstrating that the Rax-CreERT2//Dagla^{fl/fl} mice can be used to study the role of the DAGLα expression of tanycytes.
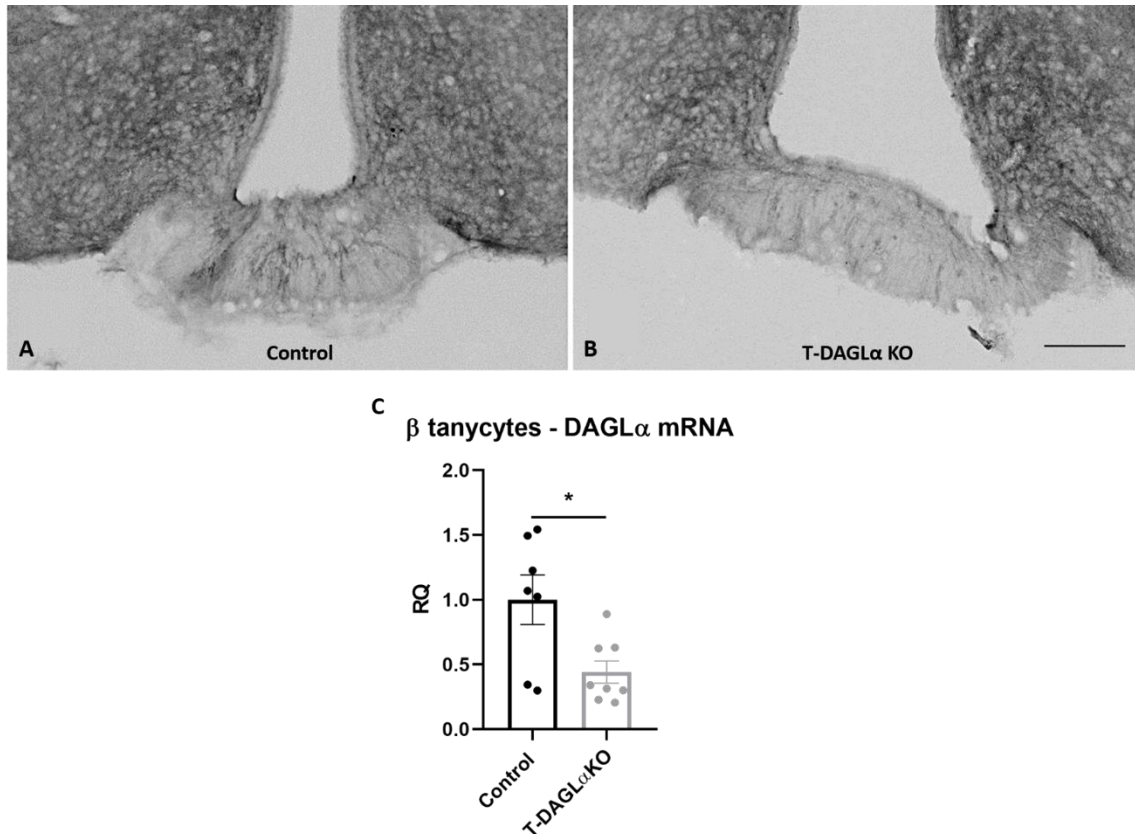
Figure 6: Tamoxifen-induced recombination causes marked decrease of DAGLα immunoreactivity and mRNA level in the tanycytes of Rax-CreERT2//Dagla$^{fl/fl}$ mice.

DAGLα-immunoreactivity in the ME and ARC of the Rax-CreERT2 (control) mice (A). The DAGLα-immunoreactivity is markedly decreased in tanycyte-specific DAGLα ablated (T-DAGLα KO, B) mice compared to the controls. DAGLα-immunoreactivity was not influenced by the genetic manipulation in the ARC. Scale bar is 50 μm. Significantly lower mRNA expression of DAGLα (C, N=7-8) was observed in LCM isolated β2-tanycytes of T-DAGLα KO mice compared to the controls. Data are presented as mean ± SEM and compared with Student's t test. Abbreviations: DAGLα – diacylglycerol lipase alpha.

4.1.3. Tanycyte-specific ablation of DAGLα influences the HPT axis

Since the endocannabinoid production of tanycytes influences the TRH release of the hypophysiotropic neurons, we examined how tanycyte-specific ablation of DAGLα influences the HPT axis. Neurons containing proTRH mRNA were readily visualized by *in situ* hybridization histochemistry, symmetrically distributed in the PVN on either side

of the third ventricle in both genotypes. Expression of proTRH mRNA did not change in the T-DAGLα KO mice compared to the control group (**Figure 7A-F**). Densitometric analysis of autoradiograms revealed no significant differences between the integrated density unit of proTRH mRNA of T-DAGLα KO mice compared to the control group (**Figure 7G**, Control *vs.* T-DAGLα KO (Int. dens. sum): 43.99±3.40 *vs.* 29.58±9.54, p=0.2. t=1.422, df=6.254, N=6).
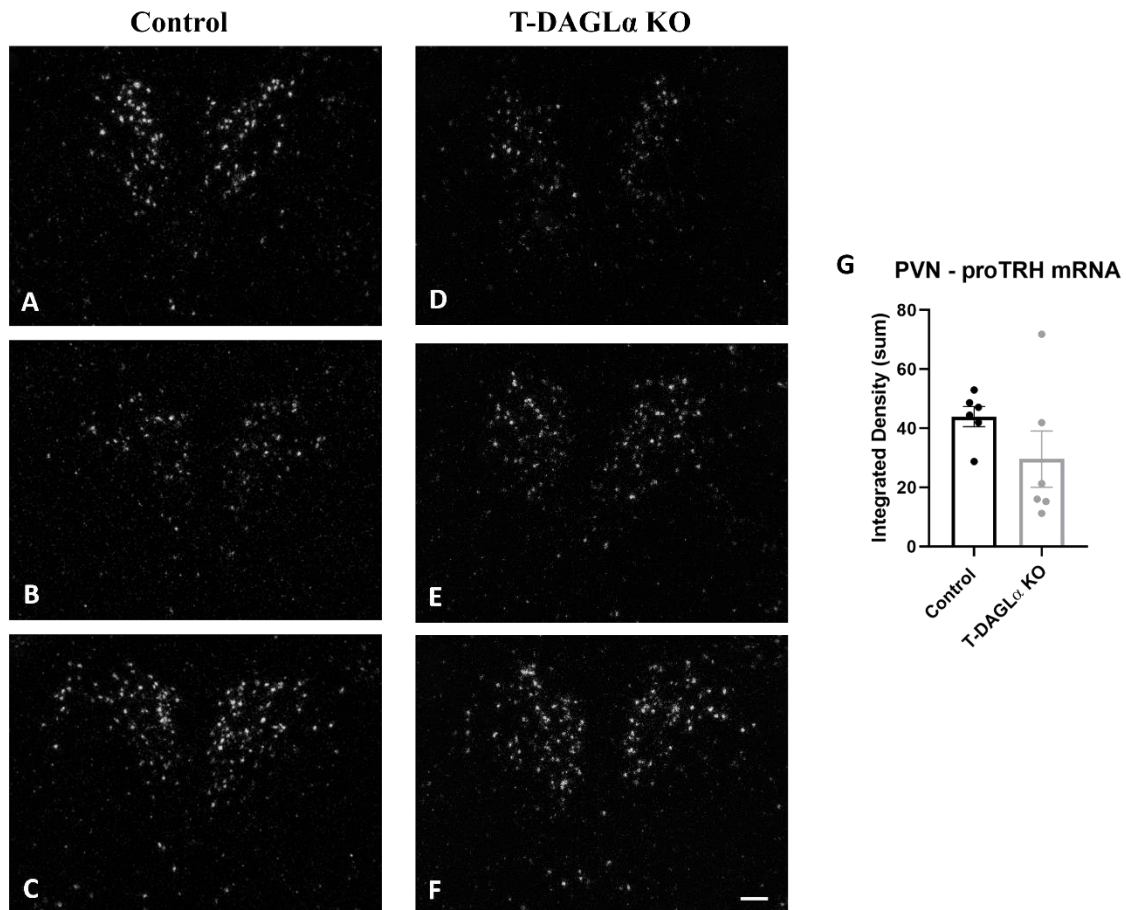
Figure 7: *Effect of tanycyte-specific DAGLα ablation on the proTRH mRNA expression in the PVN.*

Darkfield images (A-F) illustrate the proTRH mRNA expression in three coronal plans of the mid-level of PVN in control and in tanycyte-specific DAGLα ablated (T-DAGLα KO) mice. Densitometric analysis (G) of the selected images showed no significant differences between the proTRH mRNA hybridization signal of hypophysiotropic TRH neurons of the PVN between the two groups (N=6). Data are presented as mean ± SEM and compared

with Student's t test. Scale bar=100μm. Abbreviations: PVN – hypothalamic paraventricular nucleus, proTRH – pro-thyrotropin releasing hormone.

However, the TRH expression of PVN did not change significantly, the TSHβ mRNA level **(Figure 8A)**, showed a two-fold increase in the T-DAGLα KO mice compared to the controls (Control *vs.* T-DAGLα KO (RQ): 1.00 ± 0.07 *vs.* 2.05 ± 0.16, p<0.0001, t=5.889, df=29.06, N=19-22), indicating that TRH release to the portal circulation of the pituitary increased as a result of tanycyte-specific ablation of DAGLα in accordance with our in vitro observation (95).

In accordance with the increased TSH production of the pituitary, the circulating fT4 level **(Figure 8B)** showed ~20% increase in the T-DAGLα KO mice compared to the control animals (Control *vs.* T-DAGLα KO (ng/dl): 2.02 ± 0.15 *vs.* 2.44 ± 0.14; p=0.05, t=2.026, df=35, N=18-19). However, the fT3 level **(Figure 8C)** was not influenced by the genotype (Control *vs.* T-DAGLα KO (ng/dl): 4.15 ± 0.21 *vs.* 4.23 ± 0.22, p=0.8, t=0.255, df=35, N=18-19).

In accordance with the inhibitory effect of THs on the Dio2 expression (135), gene expression of Dio2 from isolated β2-tanycytes **(Figure 8D)** showed significant decrease in T-DAGLα KO mice (Control *vs.* T-DAGLα KO (RQ): 1.00 ± 0.06 *vs.* 0.66 ± 0.09, p=0.009, t=3.053, df=13, N=7-8), indicating that tanycytes reduced the local T3 production as a result of elevated TSHβ and fT4 levels. However, the expression of TRH degrading enzyme PPII **(Figure 8E)** was not changed significantly (Control *vs.* T-DAGLα KO (RQ): 1.00 ± 0.19 *vs.* 0.73 ± 0.15, p=0.28, t=1.138, df=13, N=7-8).
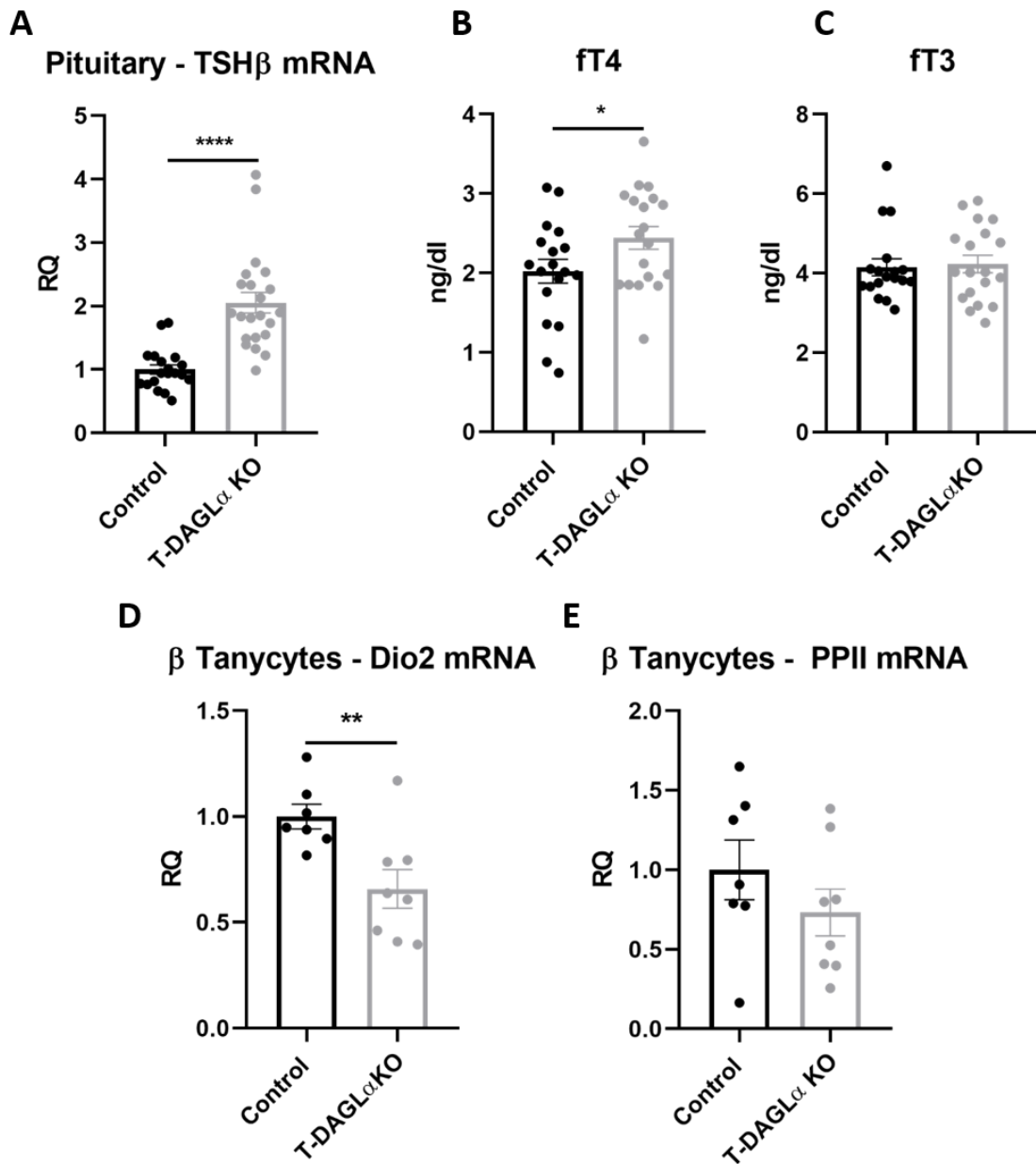
Figure 8: Effect of tanycyte-specific ablation of DAGLα on the HPT axis.

The TSHβ mRNA expression in the pituitary (A, N=19-22) and the fT4 levels in the sera (B, N=18-19) were significantly increased in the T-DAGLα KO mice, however, the fT3 levels (C, N=18-19) were not different between the genotypes. Dio2 gene expression (D, N=7-8) was significantly lower in T-DAGLα KO mice, but PPII expression (E, N=7-8) did not differ significantly between the groups in isolated β2-tanycytes. Data are presented as mean ± SEM and compared with Student's t test. *, p < 0.05; **, p < 0.01;

****, p < 0.0001. Abbreviations: fT4: free thyroxine, fT3: free triiodothyronine, TSHβ: thyroid stimulating hormone beta subunit, Dio2 – type 2 deiodinase, PPII – pyroglutamyl-peptidase II.

4.1.4. Effect of tanycyte-specific ablation of DAGLα on body composition and metabolism

THs play critical role in the regulation of development and energy homeostasis, therefore the effect of genetic manipulation on the body weight was studied by comparing the weight of the animals before and after the 72-hour-long indirect calorimetry measurements. Interestingly, during this 3-day-long period, the T-DAGLα KO animals gained significantly more weight than the controls (**Figure 9A,** Control *vs.* T-DAGLα KO (g): -0.40 ± 0.18 *vs.* 0.29 ± 0.22, p=0.03, t=2.393, df=18, N=9-11). Furthermore, the fat mass normalized by lean body mass (LBM, **Figure 9B**) significantly increased in T-DAGLα KO mice, however, the LBM normalized by the total body weight (TBW, **Figure 9C**) and the hydration ratio **(Figure 9D)** of the animals did not show significant changes (Control *vs.* T-DAGLα KO (%), N=9-11: Fat/LBM: 9.57 ± 0.29 *vs.* 10.85 ± 0.44, p=0.03, t=2.310, df=18; LBM/TBW: 88.81 ± 0.29 *vs.* 87.83 ± 0.48, p=0.13, t=1.586, df=17; Hydration ratio: 83.55 ± 0.22 *vs.* 83.14 ± 0.14, p=0.12, t=1.634, df=18).
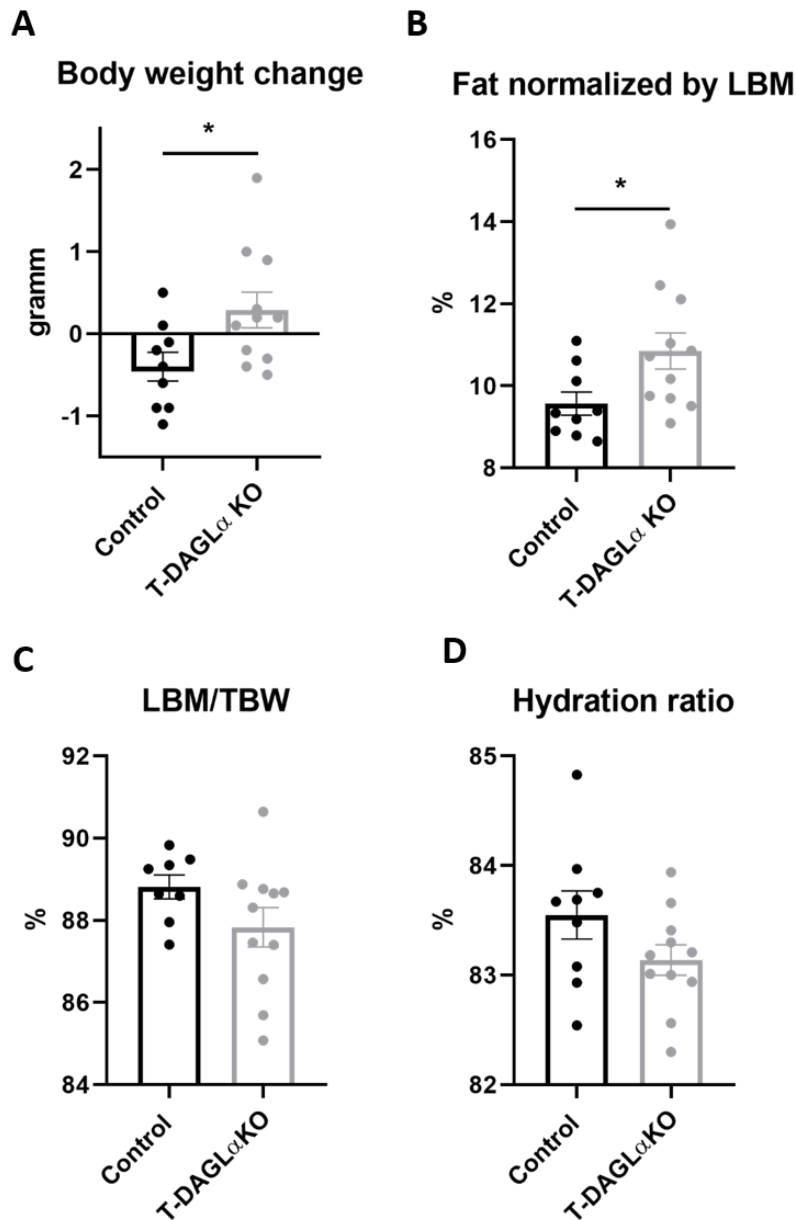
Figure 9: Effect of tanycyte-specific ablation of DAGLα on body composition

The body composition of control and T-DAGLα KO mice was determined by using EchoMRI whole body magnetic resonance after 72 hours indirect calorimetry measurements. Body weight was measured before and after the indirect calorimetry measurements. The body weight change during this period (A) and the LBM normalized fat mass ratio (B) was significantly higher in the T-DAGLα KO mice. However, the TBW normalized LBM (C) and the hydration ratio (D) of the mice did not show significant changes. Data are compared with Student's t test and shown as mean ± SEM, N=9-11, *p < 0.05. Abbreviation: LBM – lean body mass, TBW – total body weight.

Interestingly, the blood glucose level of the T-DAGLα KO group was significantly lower compared to the controls (**Figure 10A**, Control *vs.* T-DAGLα KO (mmol/l): 9.20 ± 0.23 *vs.* 8.20 ± 0.21, p=0.005, t=3.255, df=17, N=9-10). In accordance with that higher blood glucose level inhibits food intake, the T-DAGLα KO showed tendency for increased LBM normalized food intake compared to control animals (**Figure 10B**, Control *vs.* T-DAGLα KO (g/h/kg lbm): 6.90 ± 0.24 *vs.* 7.70 ± 0.30, p=0.06, t=2.097, df=12, N=7-8). The horizontal, XY activity **(Figure 10C)** of the T-DAGLα KO mice (Control *vs.* T-DAGLα KO (cnts/h): 4517.00 ± 442.20 *vs.* 5786.00 ± 359.40, p=0.04, t=2.249, df=13, N=7-8) was significantly increased in their home cages.

The energy expenditure (**Figure 10D**, Control *vs.* T-DAGLα KO (Kcal/h/kg lbm): 22.70 ± 0.49 *vs.* 22.27 ± 0.23, p=0.43, t=0.819, df=13, N=7-8), the resting energy expenditure (**Figure 10E**, Control *vs.* T-DAGLα KO (Kcal/h/kg lbm): 19.77 ± 0.50 *vs.* 19.73 ± 0.22, p=0.94, t=0.082, df=13, N=7-8) and RER (**Figure 10F**, Control *vs.* T-DAGLα KO (RER/h): 0.85 ± 0.006 *vs.* 0.85 ± 0.005, p=0.91, t=0.101, df=13, N=7-8) of the animals did not show significant changes.
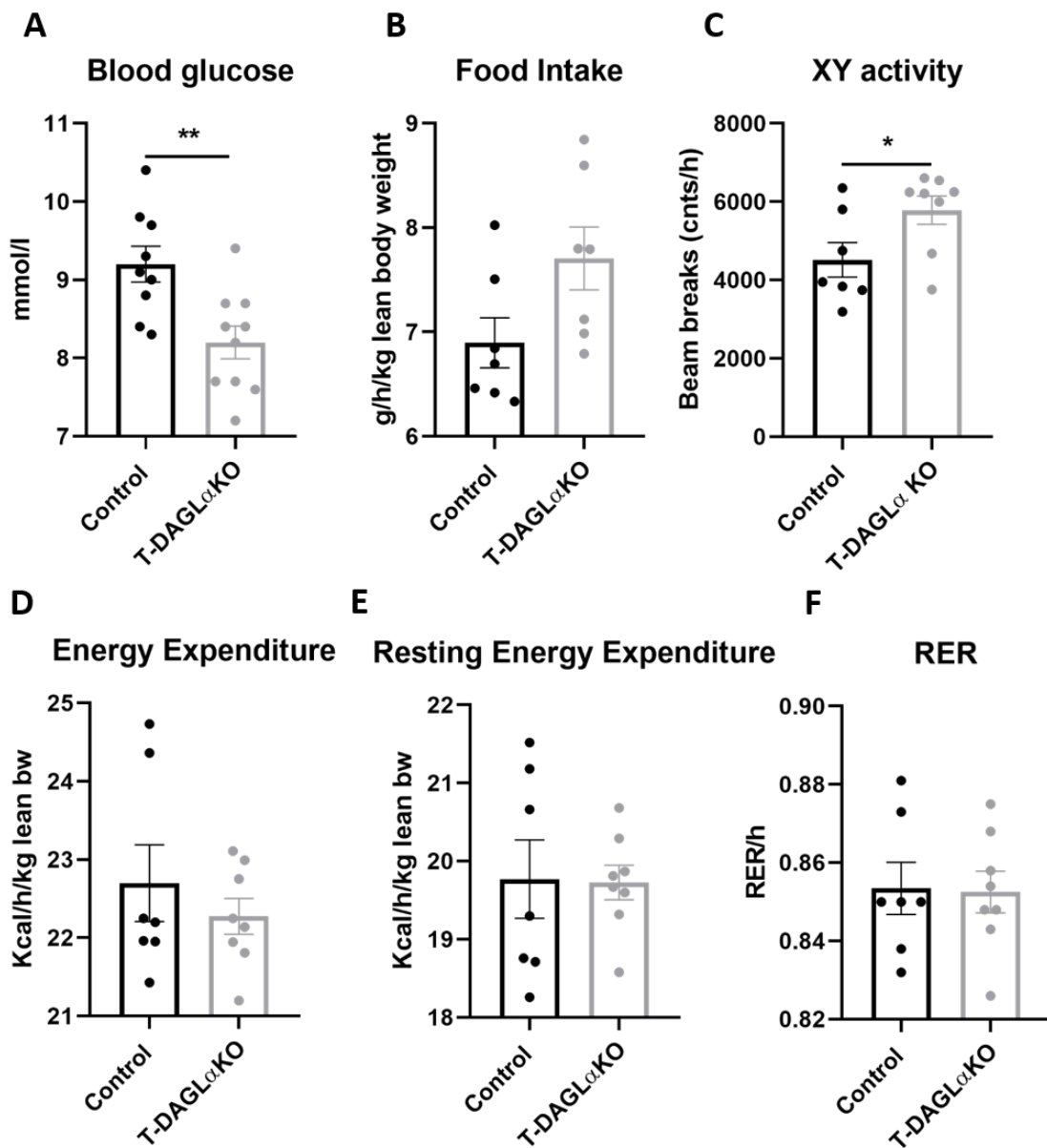
Figure 10: Effect of tanycyte-specific ablation of DAGLα on metabolic parameters.

The energy homeostasis of control and T-DAGLα KO adult mice was determined by using TSE PhenoMaster System. T-DAGLα KO mice had significantly decreased blood glucose level (A, N=9-10) and showed tendency for increased food intake (B) and significantly increased XY activity (C). The LBM normalized energy expenditure (D), resting energy expenditure (E) and the RER (F) did not changed significantly. Data are compared with Student's t test and shown as mean ± SEM. B-F: N=7-8, *p < 0.05, **p < 0.01. Abbreviation: RER – Respiratory Exchange Ratio.

4.2. Development of the HPT axis negative feedback regulation in mice

The set point of the HPT axis develops around birth, but the exact timing is unknown in mice, therefore, we examined the development of the feedback regulation of the HPT axis in newborn mouse pups. 200ng/bwg thyroxine was administered to 1-7 and 10 day old pups and the animals were sacrificed 8h later.

4.2.1. THs already regulate the TRH expression in the PVN and the TSHβ expression in the pituitary in newborn mice

The TSHβ mRNA expression of the pituitary in the T4-treated TRH-IRES-TdTomato mouse pups decreased significantly in all age groups (**Figure 11**, p<0.0001, N=4-6) compared to the respective controls, indicating that the feedback regulation at the pituitary level is already developed after birth in mice. Therefore, we examined if the feedback regulation is also developed at the hypothalamic level after birth. We repeated the treatments in a new cohort of 1, 3, 4 and 7 day old FVB/Ant pups and proTRH mRNA level was determined by ISH in the mid-level of PVN. Representative images of all age groups showed that proTRH mRNA level was decreased in the T4-treated pups compared to the control animals **(Figure 12)**. Densitometric analysis of the selected images revealed significant decrease of the proTRH mRNA level of P3 (**Figure 12D**, Control *vs.* T4 (Int. dens. sum): 86.68±7.96 *vs.* 63.98±2.98, p=0.02, t=2.839, df=11, N=6-7), P4 (**Figure 12F**, Control *vs.* T4 (Int. dens. sum): 183.20±39.58 *vs.* 63.96±8.95, p=0.03, t=2.680, df= 9, N=5-6) and P7 (**Figure 12H**, Control *vs.* T4 (Int. dens. sum): 222.40±24.67 *vs.* 150.10±13.41, p=0.03, t=2.573, df=10, N=6) T4-treated mouse pups. However, P1 age group **(Figure 12B)** showed only a strong tendency (p=0.06) for decrease of proTRH expression in T4 group compared to the control (Control *vs.* T4 (Int. dens. sum): 183.00±51.41 *vs.* 74.41±23.58, t=2.142, df=8, N=4-6) which can be due to the low sample size.

Pituitary - TSHβ mRNA
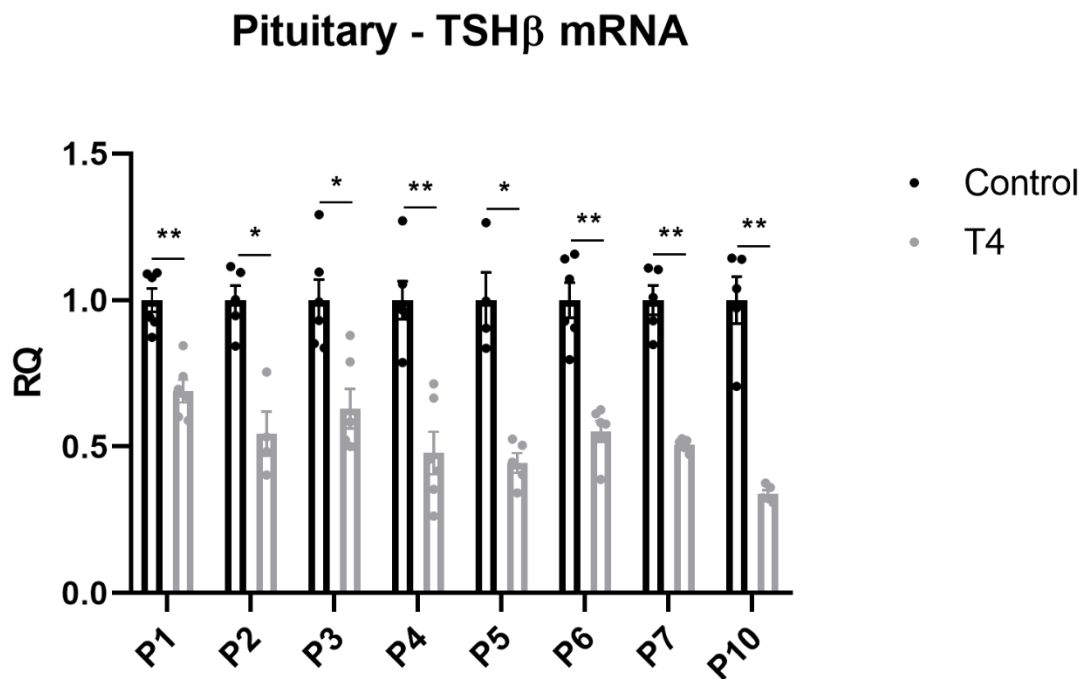
Figure 11: Changes of TSHβ expression after T4 treatment in P1-10 mouse pups.

TaqMan qPCR analysis of TSHβ mRNA expression in pituitary 8 hours after injection of 200 ng/bwg T4 or vehicle in P1-7 and 10 day old TRH-IRES-TdTomato mouse pups. Pituitary TSHβ mRNA levels were significantly decreased in all age groups compared to the controls. Data are compared with Two-way ANOVA followed by Bonferroni post hoc test. Data are shown as mean ± SEM. N=4-6, *p < 0.05; **p < 0.01. Abbreviations: TSHβ - thyroid stimulating hormone beta, P - postnatal day, T4 – thyroxine.

A P1 - Control   P1 – T4

B

PVN - proTRH mRNA
P1

C P3 - Control   P3 – T4

D

PVN - proTRH mRNA
P3
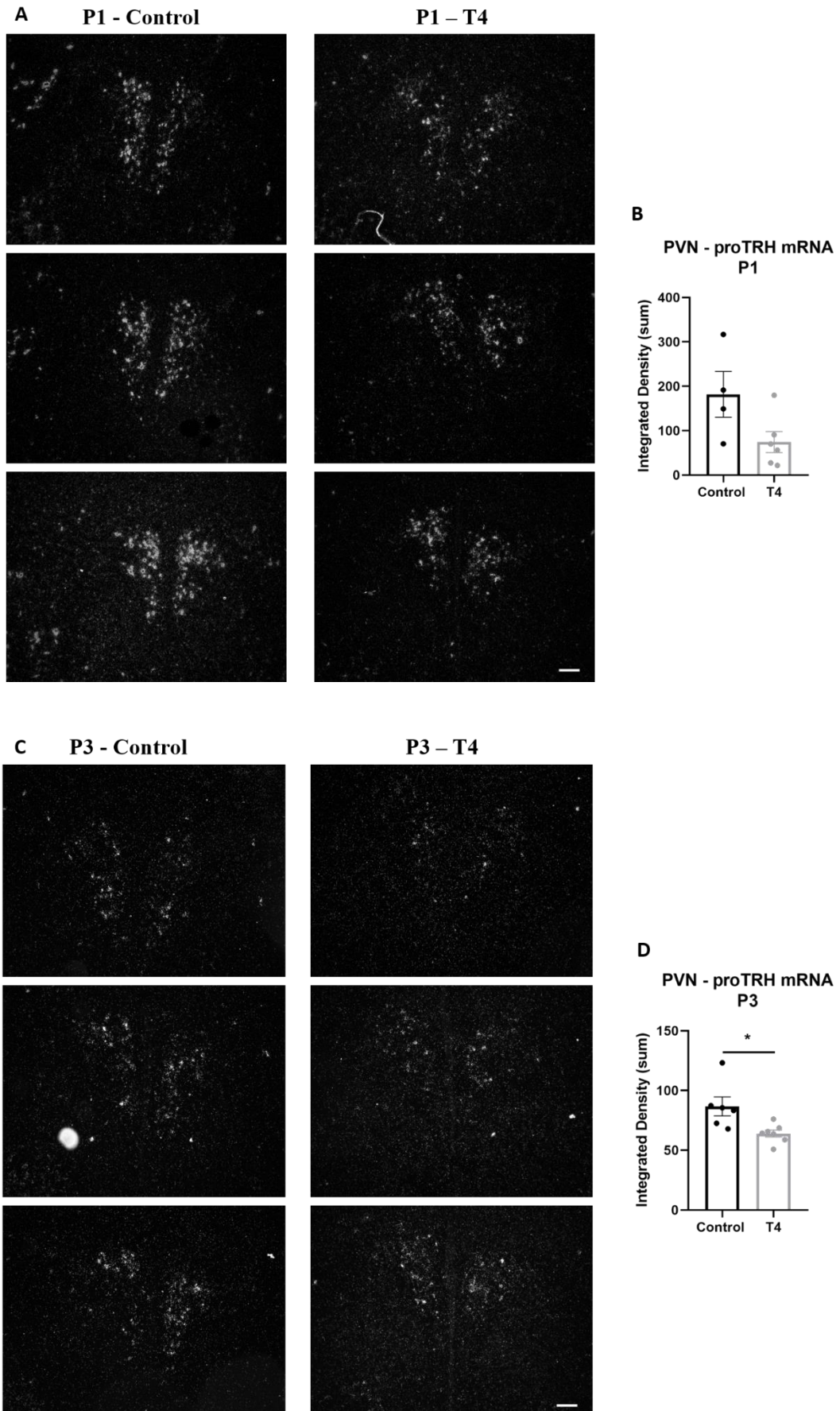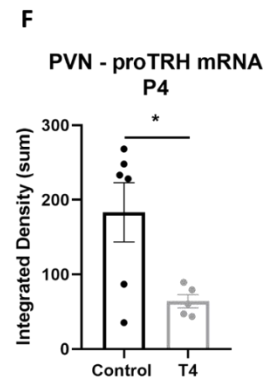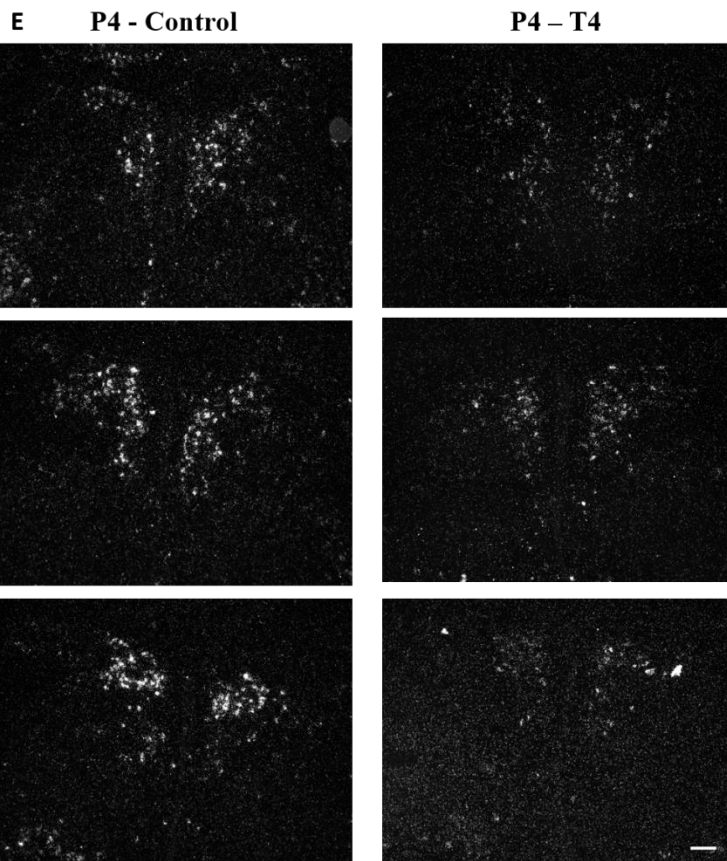
Figure 12: Response of proTRH expression in the PVN to peripheral T4 treatment in mouse pups.

1, 3, 4 and 7 day old FVB/Ant mouse pups were treated with 200 ng/bwg T4 or vehicle and sacrificed 8 hours later to determine TRH expression in PVN. Representative images of proTRH mRNA ISH autoradiograms in 1 (A), 3 (C), 4 (E), 7 (G) day old FVB/Ant mouse pups. Densitometric analysis of the selected images of proTRH mRNA hybridization signal in the PVN showed significant decrease in 3 (D), 4 (F) and 7 (H) day old (N=5-7) T4-treated groups compared to the controls and tendency for decrease in P1 (B, N=4-6) age group. Data are compared with Student's t test. Data are shown as mean ± SEM. *p < 0.05. Abbreviations: P - postnatal day, T4 – thyroxine, ISH – in situ hybridization, PVN - hypothalamic paraventricular nucleus, proTRH – pro-thyrotropin releasing hormone.

4.2.2. Effect of early postnatal hyperthyroidism on the expression of Dio1 in the liver

Liver expression of the highly TH sensitive Dio1 was examined as a marker of circulating TH levels in 1-7 and 10 day old TRH-IRES-TdTomato mouse pups. Dio1 mRNA expression **(Figure 13)** was significantly increased in the liver ($p<0.0001$, N=4-8) in all T4-treated animals compared to the respective controls, indicating the hyperthyroid state of the treated animals.
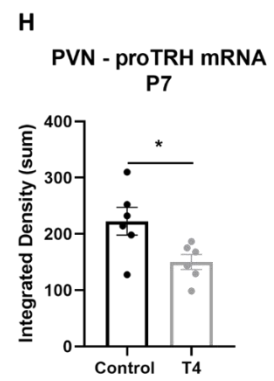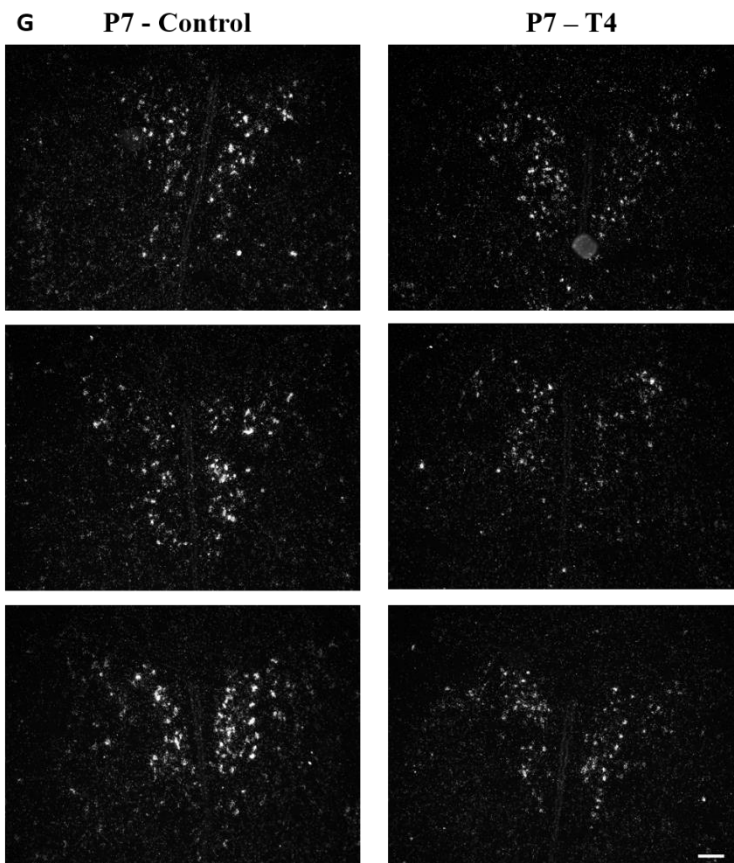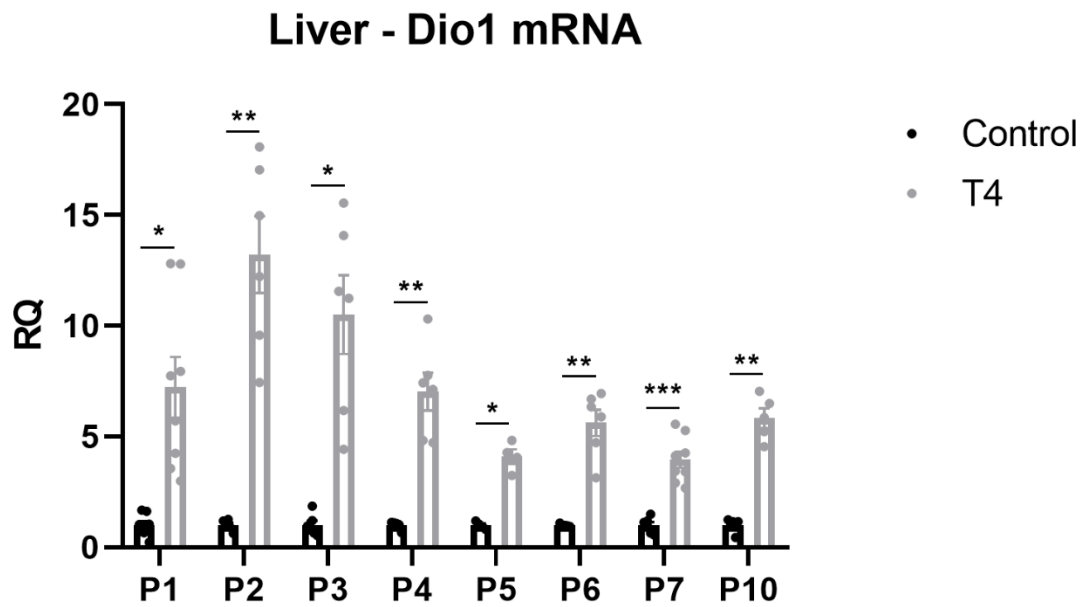
Liver - Dio1 mRNA

Figure 13: Expression of Dio1 in liver of P1-7, 10 mouse pups.

TaqMan qPCR analysis of Dio1 mRNA expression (N=4-8) in liver 8 hours after injection of 200 ng/bwg T4 or vehicle in P1-7 and P10 mouse pups. Liver Dio1 mRNA levels were significantly increased in all age groups compared to the controls by two-way ANOVA followed by Bonferroni post hoc test and shown as mean ± SEM. *p < 0.05; **p < 0.01, ***p < 0.001. Abbreviations: Dio1 − type 1 deiodinase, P - postnatal day, T4 − thyroxine.

4.3. Characterization of the effects of early postnatal hyperthyroidism on the HPT axis, metabolism and tissue-specific TH action of adult mice

To determine the effect of early postnatal hyperthyroidism in adult mice, male TRH-IRES-TdTomato and THAI mouse pups were injected subcutaneously daily with 1µg/bwg T4 between P2-P6 and sacrificed 2 months later.

4.3.1. Early postnatal hyperthyroidism induced lifelong changes of the HPT axis

Early postnatal T4 administration resulted in a marked decrease of the proTRH mRNA hybridization signal in the PVN of adult TRH-IRES-TdTomato mice compared to the

control group **(Figure 14A-F)**. By image analysis **(Figure 14G)**, postnatal T4 treatment induced an approximately 30% reduction in the density values of proTRH mRNA hybridization signal in the PVN of adult mice (Control *vs.* T4 (Int. dens.): 296.00±23.91 *vs.* 212.80±20.27, p=0.02, t=2.654, df=16, N=9).

Figure 14: Effect of early postnatal hyperthyroidism on the TRH expression in the PVN of adult mice.

TRH-IRES-TdTomato male mouse pups were treated with 1μg/bwg T4 or vehicle between P2-6 days and sacrificed at adulthood to determine the TRH expression in PVN by ISH. Darkfield images (A-F) and densitometric analysis (G, N=9) of proTRH mRNA expression of the PVN showed that the early postnatal T4 treatment resulted in marked decrease of TRH synthesis in adult mice. Data are compared with Student's t test and shown as mean ± SEM. *, p < 0.05. Abbreviations: T4: thyroxine, PVN – hypothalamic paravnetricular nucleus, proTRH – pro-thyrotropin releasing hormone.

However, the TSHβ mRNA expression of the pituitary **(Figure 15A)** did not change significantly despite of the reduced hypothalamic TRH expression (Control *vs.* T4 (RQ): 1.00±0.07 *vs.* 0.92±0.09, p=0.46, t=0.759, df=19, N=10-11), but the circulating fT4 level **(Figure 15B)** decreased significantly in the group treated with T4 in the postnatal period compared to the control group (Control *vs.* T4 (ng/dl): (0.82±0.03 *vs.* 0.68±0.04, p=0.02, t=2.527, df=26, N=14). The presence of decreased TRH expression and decreased fT4 level supports the existence of central hypothyroidism in this mouse model. The fT3 level, however, **(Figure 15C)** was not altered by the treatment (Control *vs.* T4 (ng/dl): 3.10±0.39 *vs.* 2.78±0.30; p=0.52, t=0.656, df=25, N=13-14), suggesting that changes of peripheral TH metabolism can normalize the fT3 level despite of the lower fT4 level.
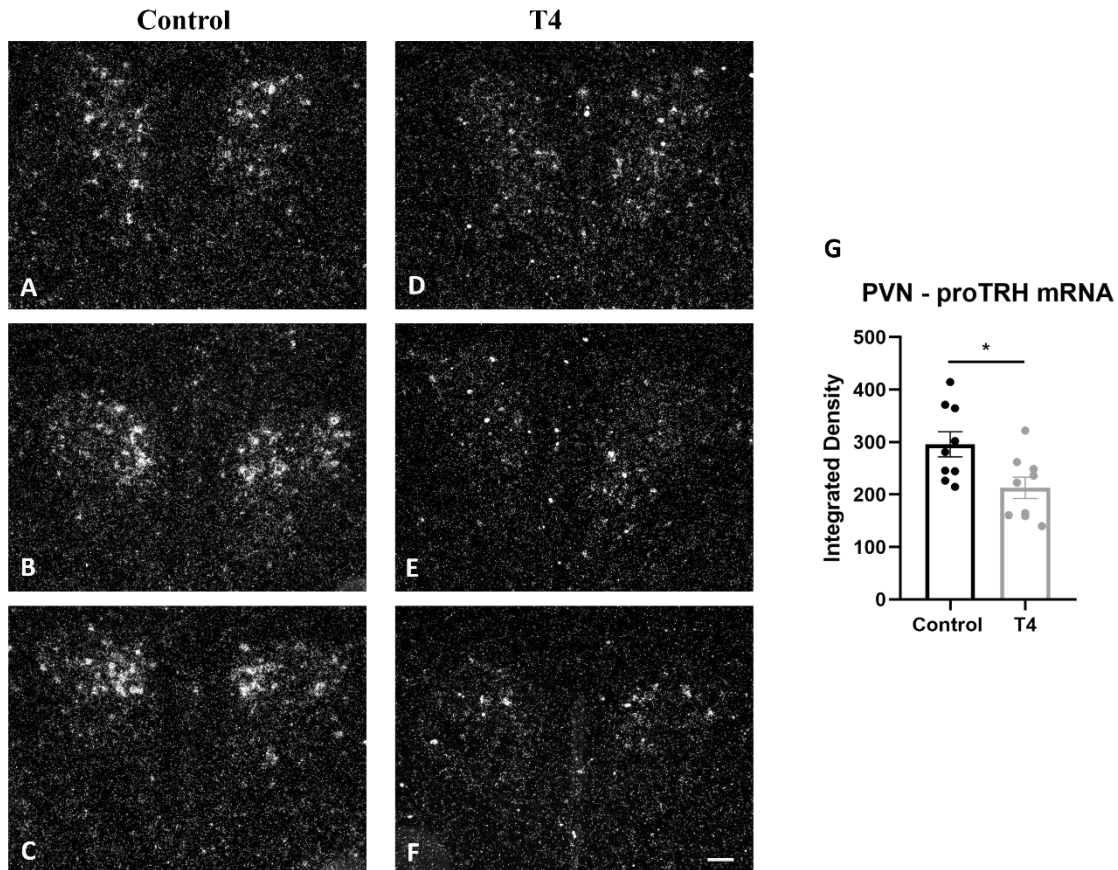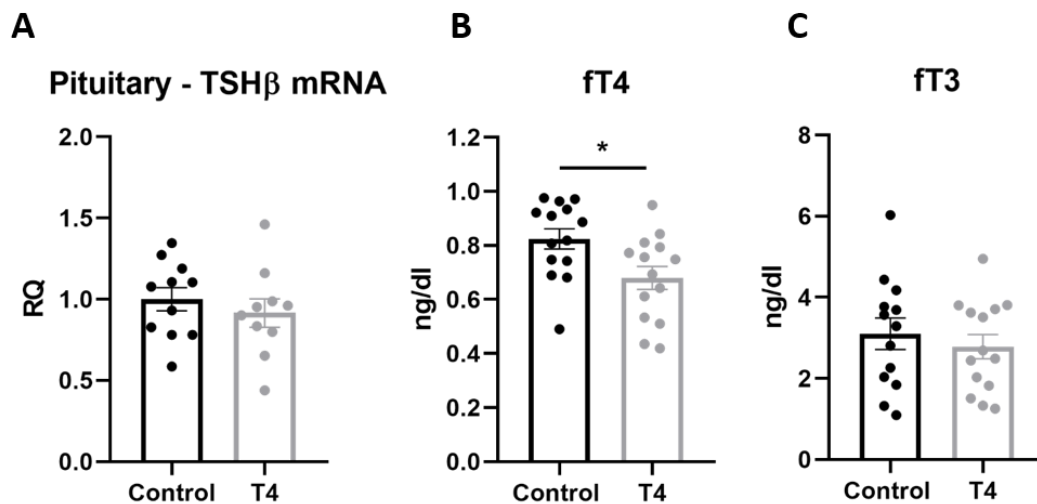

Figure 15: Effect of early postnatal hyperthyroidism on the TSHβ expression and TH levels in adult mice.

TRH-IRES-tdTomato male mouse pups were treated with 1µg/bwg T4 or vehicle between P2-6 days and sacrificed at adulthood to measure TSHβ expression in the pituitary by TaqMan qPCR analysis and TH levels from sera. The pituitary TSHβ mRNA (A, N=10-11) level was not change significantly in the groups. Serum fT4 (B, N=14) level was significantly lower in the adult, postnatally T4-treated mice. However, the serum fT3 (C, N=13-14) was not influenced by the treatment. Data are compared with Student's t test and shown as mean ± SEM. *, p < 0.05. Abbreviations: T4: thyroxine, TSHβ - thyroid stimulating hormone beta subunit, fT4 – free thyroxine, fT3 – free triiodothyronine.

4.3.2. Tanycytes are not involved in the regulation of the HPT axis set point by postnatal hyperthyroidism

The TH activating capability of tanycytes can influence the feedback regulation of the TRH neurons (78). Therefore, the expression of Dio2 gene coding the TH activating enzyme D2 was studied in the MBH of adult, postnatally T4-treated THAI mice to investigate whether the central hypothyroidism resulted by the postnatal T4 treatment is due to altered TH activating capacity of tanycytes. Since the Dio2 in the MBH is only expressed by the tanycytes, we isolated α- and β-tanycyte subgroups separately by LCM of postnatally treated TRH-IRES-TdTomato adult mice. The Dio2 mRNA expression did not change significantly neither in α- (**Figure 16A,** Control *vs.* T4 (RQ): 1.00±0.10 *vs.* 0.96±0.20, p=0.88, t=0.159, df=10, N=6), nor in β-tanycytes (**Figure 16B,** Control *vs.* T4 (RQ): 1.00±0.29 *vs.* 0.85±0.26, p=0.71, t=0.385, df=7, N=4-5).

Tanycytes can also influence the activity of the HPT axis by degrading TRH in the ME by PPII enzyme. Neither α- (**Figure 16C,** Control *vs.* T4 (RQ): 1.00±0.06 *vs.* 1.01±0.10, p=0.93, t=0.932, df=10, N=6), nor β-tanycytes (**Figure 16D,** Control *vs.* T4 (RQ): 1.00±0.23 *vs.* 0.50±0.13, p=0.09, t=1.965, df=7, N=4-5) showed significant change in the expression of PPII between the control and postnatally T4-treated, adult TRH-IRES-tdTomato mice,

As D2 activity is highly regulated posttranslationally, we also studied whether the TH action is influenced by the postnatal T4 treatment in the MBH of adult mice. For this experiment, we used THAI mice in which the expression of luc is highly regulated by THs (133). In the MBH of postnatally T4-treated adult THAI mice, luc expression - the indicator of TH action - was not influenced by the early postnatal treatment (**Figure 16E,** Control *vs.* T4 (RQ): 1.00±0.13 *vs.* 0.81±0.11, p=0.31, t=1.056, df=11, N=6-7) excluding the possibility that in this model, the effect of postnatal T4 treatment on the HPT axis of adult mice is mediated by tanycyte induced alteration of the feedback regulation of TRH neurons.

These results demonstrate that the tanycytes are not involved in the regulation of the HPT axis set point by postnatal hyperthyroidism.
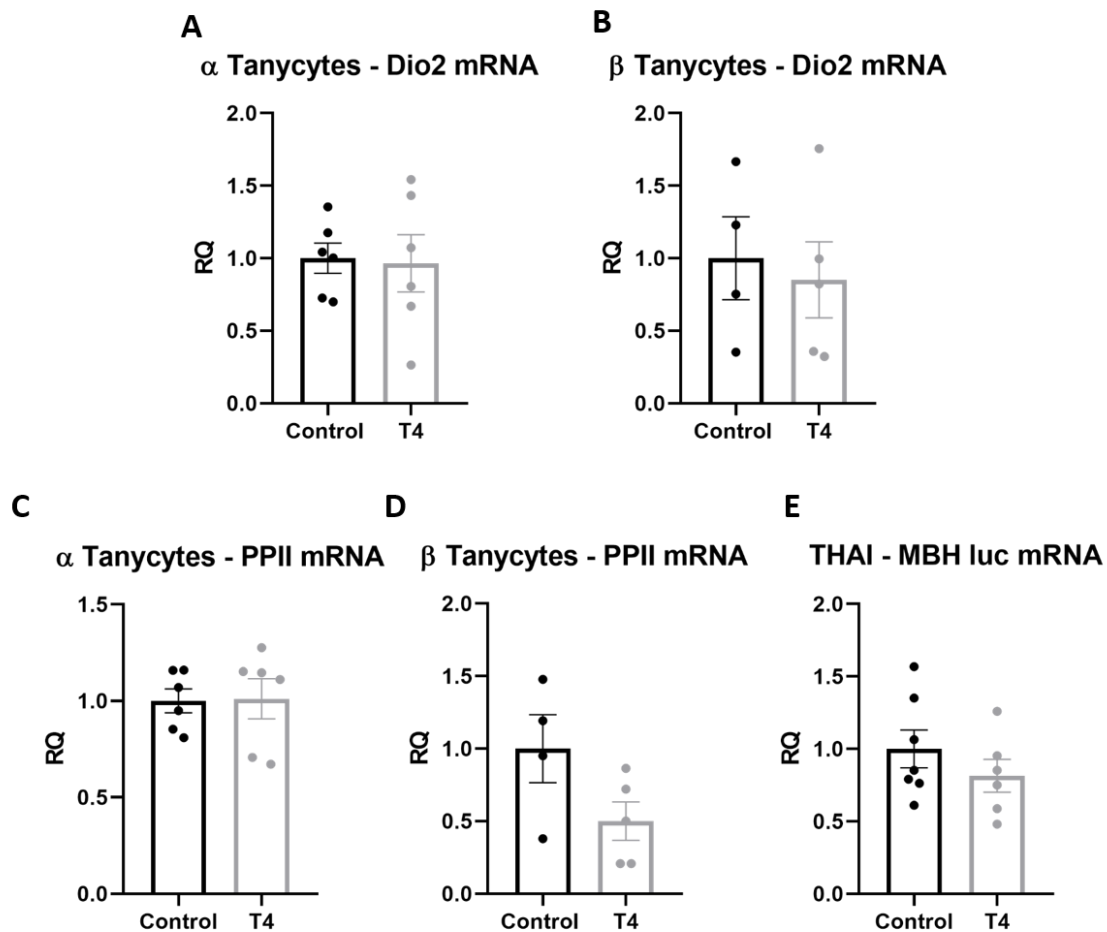
Figure 16: Early postnatal hyperthyroidism did not influence the TH activating and TRH degrading capacity of tanycytes.

Male THAI and TRH-IRES-TdTomato mouse pups were treated with 1μg/bwg T4 or vehicle between P2-6 days and sacrificed at adulthood. The Dio2 expression in α- (A) and β-tanycytes (B) did not change significantly between control and T4-treated mice. The treatment also did not influence the PPII mRNA level in α- (C) or β-tanycytes (D) and luc expression of MBH of THAI mice (E). Data are compared with Student's t test and shown as mean ± SEM. Abbreviations: THAI – thyroid hormone action indicator mouse, MBH – mediobasal hypothalamus, Dio2 – type 2 deioidinase, luc – luciferase, PPII – pyroglutamyl-peptidase II.

4.3.3. Early postnatal hyperthyroidism influences the body composition of adult mice

THs play critical role in the regulation of development and energy homeostasis, therefore the effect of early postnatal hyperthyroidism was studied on the body composition and energy homeostasis of adult TRH-IRES-tdTomato mice.

The adult, postnatally T4-treated animals showed significantly decreased body weight compared to the controls (**Figure 17A,** Control *vs.* T4 (g): 22.84±0.63 *vs.* 19.18±0.50, p=0.001, t=4.637, df=22, N=11-13). Furthermore, the body length of the T4 group was significantly decreased compared to the control animals (**Figure 17B,** Control *vs.* T4 (cm): 9.54±0.19 *vs.* 8.79±0.16, p<0.0001, t=9.657, df=19, N=10-11). The body composition of mice was mesaured by EchoMRI whole body magnetic resonance analyser. Neither the fat mass / LBM ratio (**Figure 17C**, Control *vs.* T4 (%): 14.09±1.08 *vs.* 13.63±0.74, p=0.72, t=0.357, df=22, N=11-13), nor the LBM / body weight ratio (**Figure 17D**, Control *vs.* T4 (%): 84.05±0.79 *vs.* 84.44±0.62, p=0.7, t=0.397, df=22, N=11-13) were different between the control and T4-treated groups. The LBM normalized food intake was not different between the groups (**Figure 17E,** Control *vs.* T4 (g/h/kg lbw): 7.68±0.72 *vs.* 8.13±0.35, p=0.55, t=0.616, df=10, N=5-7). Thus, the marked decrease of body weight is not due to altered body composition, but rather gross retardation, since the thyroid status influences the bone growing.
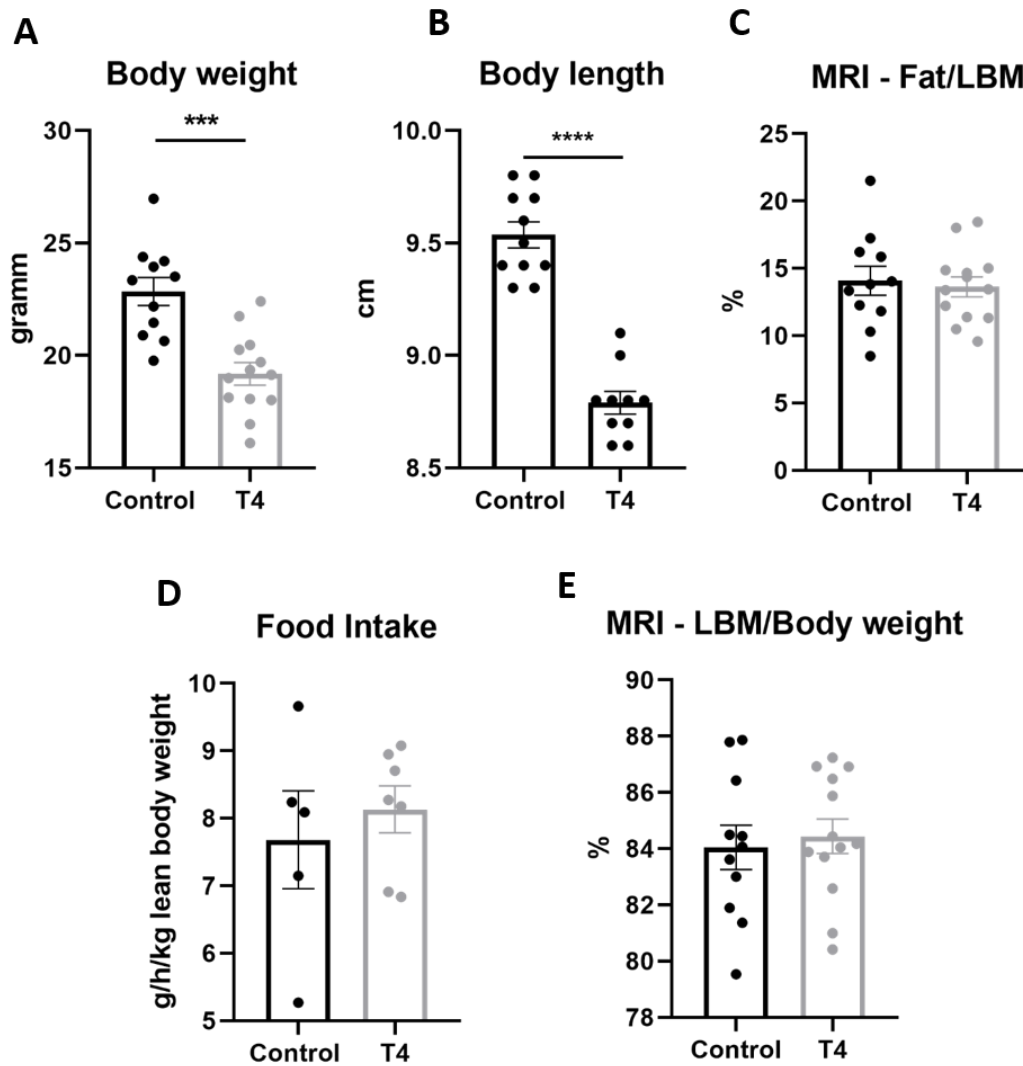
Figure 17: The effect of early postnatal T4 treatment on body weight and body composition.

Early postnatal T4 treatment resulted in significantly decreased body weight (A, N=11-13) and body length (B, N=10-11) at adulthood. Body composition analysis did not show significant differences in fat and LBM (C, N=11-13) and in LBM and body weight (D, N=11-13) ratios between the groups. The LBM normalized food intake was not significantly different between the groups (E, N=5-7). Data are compared with Student's t test and shown as mean ± SEM. ***p < 0.001. Abbreviation: LBM – lean body mass.

4.3.4. Early postnatal hyperthyroidism influences the activity and energy homeostasis of adult mice

The locomotor activity and energy homeostasis of adult TRH-IRES-TdTomato mice was determined by using TSE PhenoMaster System. Despite the decreased fT4 levels, the postnatally T4-treated mice showed significantly increased locomotor activity in the metabolic cages, including XY activity (**Figure 18A**, Control *vs.* T4 (cnts/h): 3433±392.60 *vs.* 4691±349.40, p=0.04, t=2.371, df=10, N=5-7), travelled distance (**Figure 18B**, Control *vs.* T4 (cm/h): 11383±554.10 *vs.* 22240±3648.00, p=0.03, t=2.466, df=10, N=5-7) and speed (**Figure 18C**, Control *vs.* T4 (cm/sec): 3.14±0.16 *vs.* 6.17±1.02, p=0.03, t=2.471, df=10, N=5-7). The higher activity was accompanied by significantly higher energy expenditure (**Figure 18D**, Control *vs.* T4 (Kcal/h/kg lbw): 24.64±0.73 *vs.* 27.39±0.54, p=0.01, t=3.098, df=10, N=5-7). Furthermore, the resting energy expenditure of the postnatally T4-treated mice was also significantly higher (**Figure 18E**, Control *vs.* T4 (Kcal/h/kg lbw): 22.61±0.67 *vs.* 24.91±0.60, p=0.03, t=2.516, df=10, N=5-7), suggesting that the central hypothyroidism is compensated at the level of tissues. The RER was not different between the two groups (**Figure 18F**, Control *vs.* T4 (RER/h): 0.84±0.02 *vs.* 0.84±0.01, p=0.98, t=0.026, df=10, N=5-7).
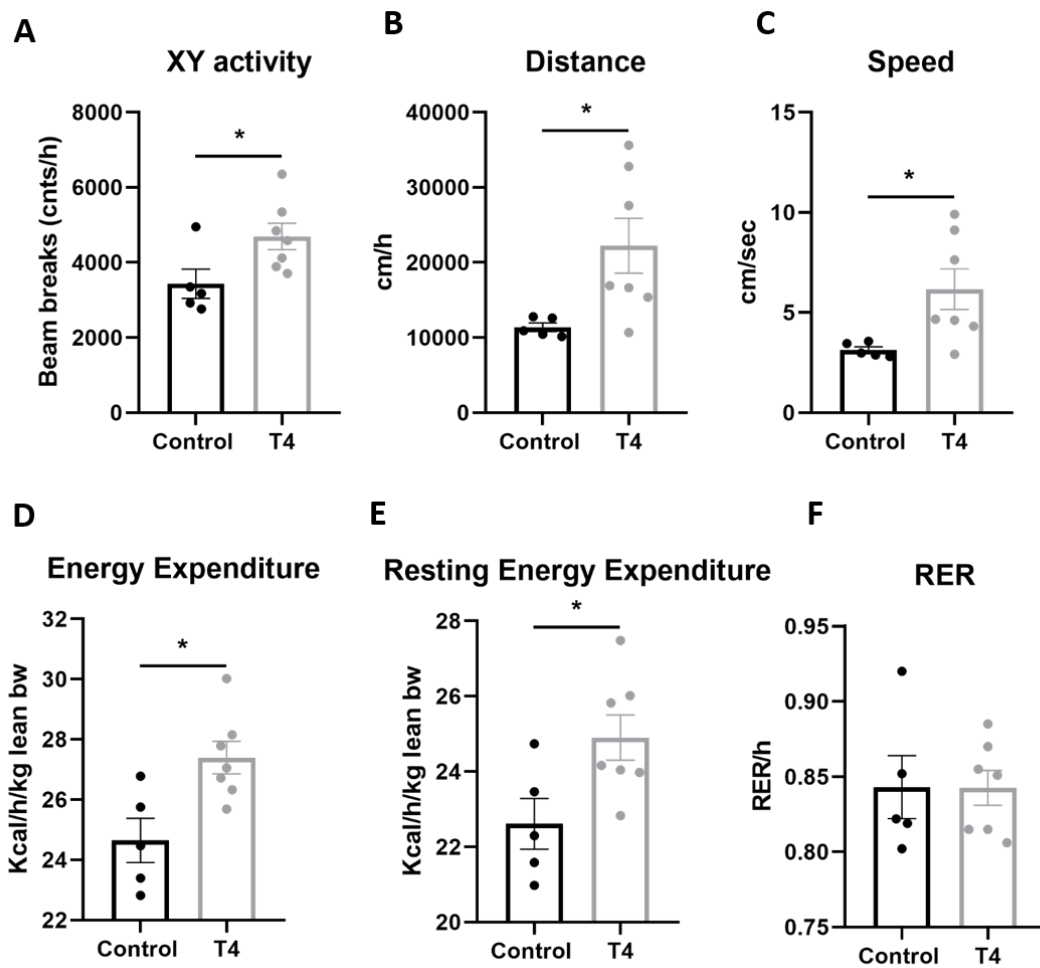
Figure 18: The effect of early postnatal hyperthyroidism on the activity and metabolism of adult TRH-IRES-TdTomato mice.

The postnatally T4-treated group showed significant increase in the XY activity (A), travelled distance (B) and speed (C) parameters compared to the control group. The LBM normalized energy expenditure (D) and resting energy expenditure was significantly increased in T4-treated mice compared to the controls. The RER (F) was not significantly different between the groups. Data are compared with Student's t test and shown as mean ± SEM. N=5-7; *p < 0.05. Abbreviation: RER – respiratory exchange ratio.

4.3.5. Effects of early postnatal hyperthyroidism on the TH action in tissues of adult mice

THAI mice were treated with 1µg/bwg T4 or vehicle between P2-6 and were sacrificed at adulthood. To determine the tissue-specific TH action, luc expression (marker of TH action in the THAI mice) was studied in different tissues. Neither the hypothalamus **(Figure 19A)**, nor the hippocampus **(Figure 19B)** showed significant changes in the luc expression in T4-treated mice compared to the controls (Control *vs.* T4 (RQ): hypothalamus: 1.00 ± 0.21 *vs.* 0.85 ± 0.19, p=0.6, t=0.533, df=13, N=7-8; hippocampus: 1.00 ± 0.13 *vs.* 0.76 ± 0.28, p=0.42, t=0.853, df=8, N4-6). We also examined the luc expression in TH sensitive peripheral tissues. The luc expression decreased only in the small intestine **(Figure 19C)** in the postnatally T4-treated adult mice, but in BAT **(Figure 19D)**, the luc mRNA level was unchanged (Control *vs.* T4 (RQ): small intestine: 1.00 ± 0.12 *vs.* 0.72 ± 0.05, p=0.04, t=2.202, df=14, N=8; BAT: 1.00 ± 0.31 *vs.* 0.62 ± 0.16, p=0.28, t=1.129, df=13, N=7-8).
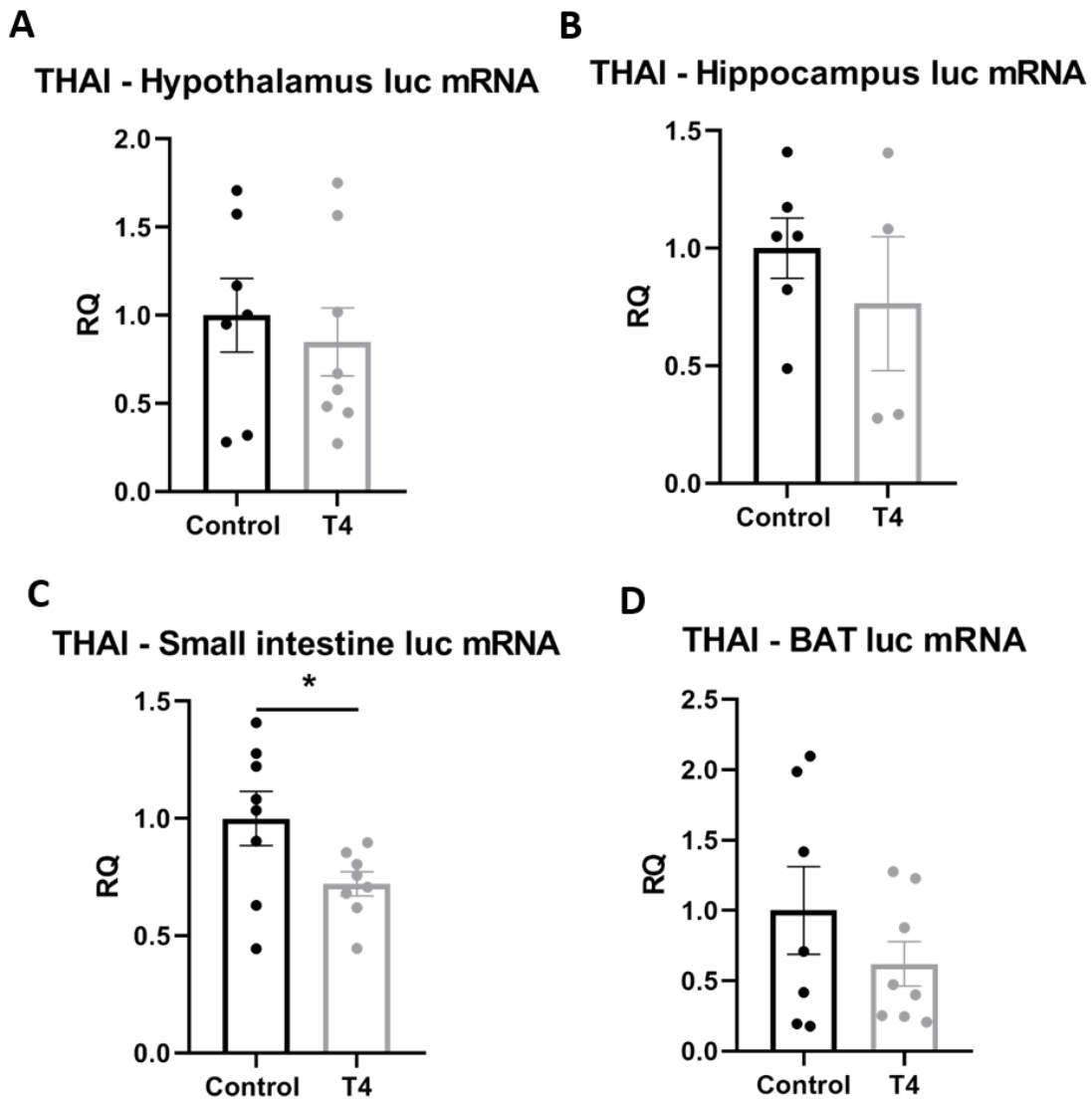
Figure 19: Tissue-specific TH action.

*THAI mice were treated with 1μg/bwg T4 or vehicle between P2-6 and were sacrificed at adulthood and tissues were collected to determine tissue-specific TH action. TaqMan qPCR analysis revealed no significant differences in luc expression of hypothalamus (A), hippocampus (B) and BAT (D), but in the small intestine (C), the early postnatal T4 treatment resulted in decreased luc expression. Data are compared with Student's t test and shown as mean ± SEM. N=6-8; *p < 0.05.. Abbreviation: THAI – thyroid hormone action indicator mouse, luc – luciferase, BAT – brown adipose tissue.*

4.3.6. Early postnatal hyperthyroidism induced changes in TH-releated genes of adult mouse liver

Since the liver is one of the main target tissues of THs, expression of TH-related genes was examined by TaqMan qPCR analysis in the liver of postnatally T4-treated adult TRH-IRES-TdTomato mice. First, we determined the Dio1 expression of liver that is considered to be the most sensitive marker of TH action in this tissue (**4.2.2., Figure 13**). Early postnatal T4 treatment resulted in marked, approximately 90% decrease of Dio1 expression in the liver (**Figure 20A**, Control *vs.* T4 (RQ): 1.00±0.16 *vs.* 0.09±0.02, p=0.0007, t=4.340, df=14, N=6-10). To determine the tissue-specific TH action, luc expression was also studied in the liver of postnatally T4-treated THAI mice. However, the luc expression as a marker of thyroid hormone action did not change significantly in the liver (**Figure 20B**, 1.00±0.16 *vs.* 1.14±0.15, p=0.55, t=0.619, df=11, N=6-7) indicating euthyroid status in this tissue. To better understand the thyroid status of liver in this animal model, the expression of other TH sensitive genes was also determined. The TH receptor α and β (THRA, THRB) expression did not change significantly in this tissue (**Figure 20C,D**, Control *vs.* T4 (RQ): THRA: 1.00±0.10 *vs.* 0.98±0.09, p=0.90, t=0.131, df=18, N=10; THRB: 1.00±0.13 *vs.* 0.84±0.06, p=0.27, t=1.136, df=18, N=10). The TH responsive (Spot14) gene is known to respond rapidly to TH and is responsible for the tissue-specific regulation of lipid metabolism as a lipogenic gene in the liver (136). Interestingly, the lower fT4 level of the animals did not change the gene expression of Spot14 in the postnatally T4-treated mice (**Figure 20E**, Control *vs.* T4 (RQ): 1.00±0.13 *vs.* 0.85±0.23, p=0.59, t=0.555, df=17, N=9-10). The expression of other genes involved in the fatty acid metabolism and regulated positively by TH (137, 138) were also studied. Both the malic enzyme 1 (ME1, **Figure 20F**) and fatty acid synthase (FASN, **Figure 20G**) showed significant decrease in the T4-treated group compared to the control animals (Control *vs.* T4: ME1 (RQ): 1.00±0.10 *vs.* 0.58±0.07, p=0.003, t=3.441, df=16, N=9; FASN: 1.00±0.15 *vs.* 0.54±0.03, p=0.01, t=2.898, df=15, N=8-9). The expression of the catalytic subunit of glucose-6-phosphatase (G6PC) - which is essential for endogenous glucose production (139) - did not change significantly (**Figure 20H**, Control *vs.* T4 (RQ): 1.00±0.11 *vs.* 0.92±0.10, p=0.62, t=0.511, df=18, N=10).

A Liver - Dio1 mRNA

B THAI - Liver luc mRNA

C Liver - THRA mRNA

D Liver - THRB mRNA

E Liver - Spot14 mRNA

F Liver - ME1 mRNA

G Liver - FASN mRNA

H Liver - G6PC mRNA
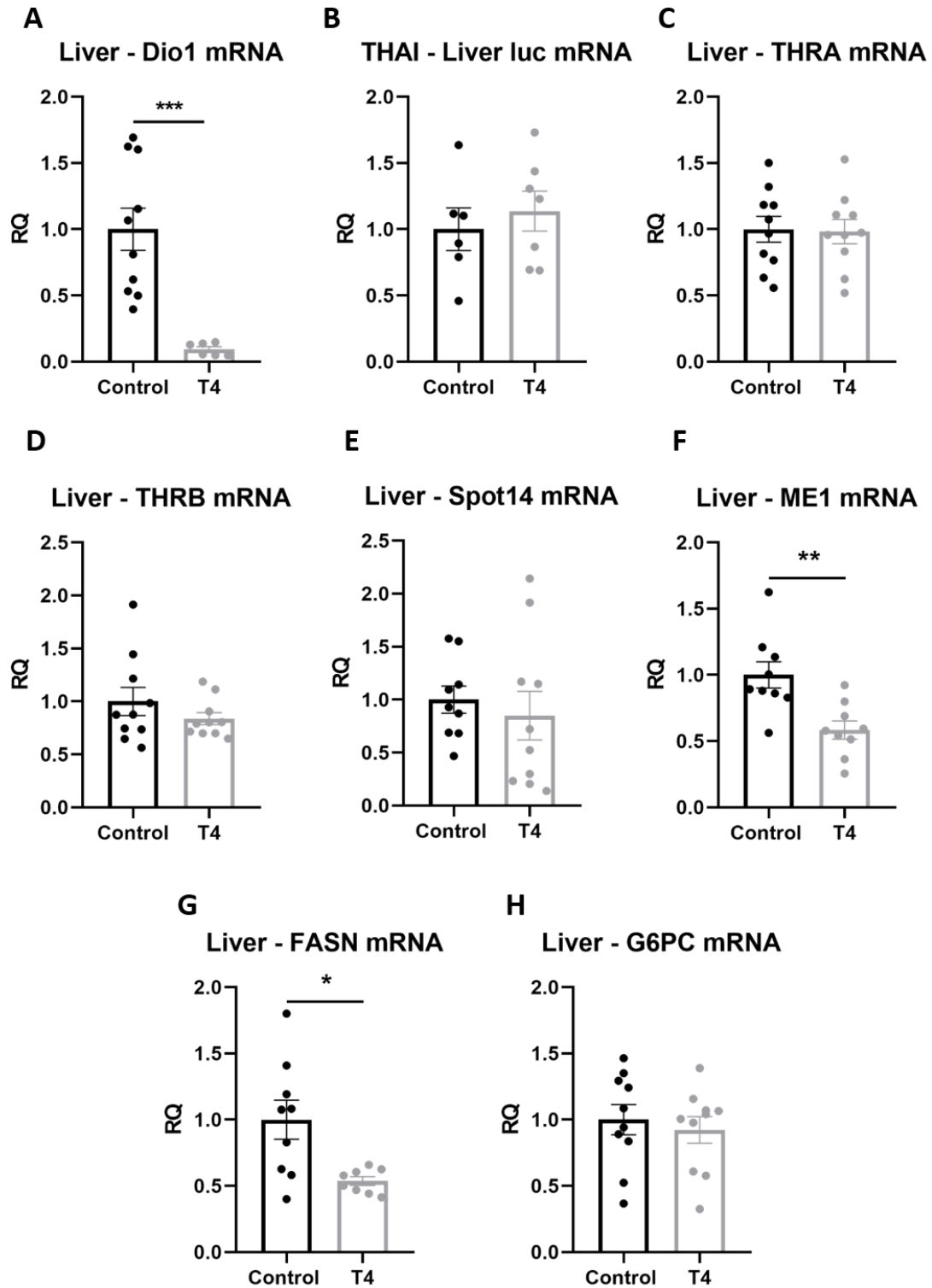
Figure 20: Effect of early postnatal hyperthyroidism on TH-releated genes of adult mouse liver

TaqMan qPCR analysis in liver of adult TRH-IRES-TdTomato male mice treated with 1μg/bwg T4 or vehicle between P2-6 days. Liver Dio1 expression (A, N=6-10) decreased significantly in T4-treated group. The liver luc expression of THAI mice did not change significantly (B, N=6-8). The gene expression of TH receptors THRA (C), THRB (D) and Spot14 (E) did not change significantly in this group. The postnatal T4 treatment resulted in decreased mRNA level of ME1 (F) and FASN (G) compared to the control. The expression of G6PC (H) did not change significantly. C-H: N=8-10. Data are compared with Student's t test and shown as mean ± SEM. *p < 0.05; **p < 0.01. Abbreviations: Dio1 – type 1 deiodinase, THAI – thyroid hormone action indicator mouse, luc – luciferase, THRA - TH receptor α, THRB - TH receptor β, Spot14 - TH responsive, ME1 – malic enzyme 1, FASN - fatty acid synthase, G6PC - glucose-6-phosphatase.

4.3.7. Effect of early postnatal hyperthyroidism on the expression of DNA methyltransferase enzymes in the liver

To determine whether the changes in the expression profile of certain TH-dependent genes in the liver could be due to epigenetic regulation, the expression of genes involved in DNA methylation were measured in liver of T4-treated and control 2 and 6 day old mouse pups. Dnmt1 level (**Figure 21A,** Control *vs.* T4 (RQ): 1.00±0.06 *vs.* 1.28±0.14, p=0.13, t=1.667, df=9, N=5-6) showed a tendency to increase in the T4 group, but the change was not significant, while Dnmt3a (**Figure 21B,** Control *vs.* T4 (RQ): 1.00±0.05 *vs.* 1.37±0.10, p=0.009, t=3.337, df=9, N=5-6) and Dnmt3b (**Figure 21C,** Control *vs.* T4 (RQ): 1.00±0.03 *vs.* 1.37±0.08, p=0.004, t=3.855, df=9, N=5-6) expression was significantly increased in the T4 group compared to the controls at P2. The level of these genes did not show significant changes at P6 (**Figure 21D-F,** Control *vs.* T4 (RQ): Dnmt1: 1.00±0.05 *vs.* 1.04±0.10, p=0.76, t=0.316, df=10, N=6); Dnmt3a: 1.00±0.05 *vs.* 1.10±0.08, p=0.35, t=0.984, df=10, N=6; Dnmt3b: 1.00±0.04 *vs.* 1.02±0.14, p=0.1,

t=0.207, df=10, N=6), indicating that the P2 but not the P6 mice are in the sensitive period, when the thyroid status may influence the set point of TH dependent genes in the liver and induce epigenetic changes by DNA methylation.

A

P2 Liver - Dnmt1 mRNA

B

P2 Liver - Dnmt3a mRNA

C

P2 Liver - Dnmt3b mRNA

D

P6 Liver - Dnmt1 mRNA

E

P6 Liver - Dnmt3a mRNA

F

P6 Liver - Dnmt3b mRNA
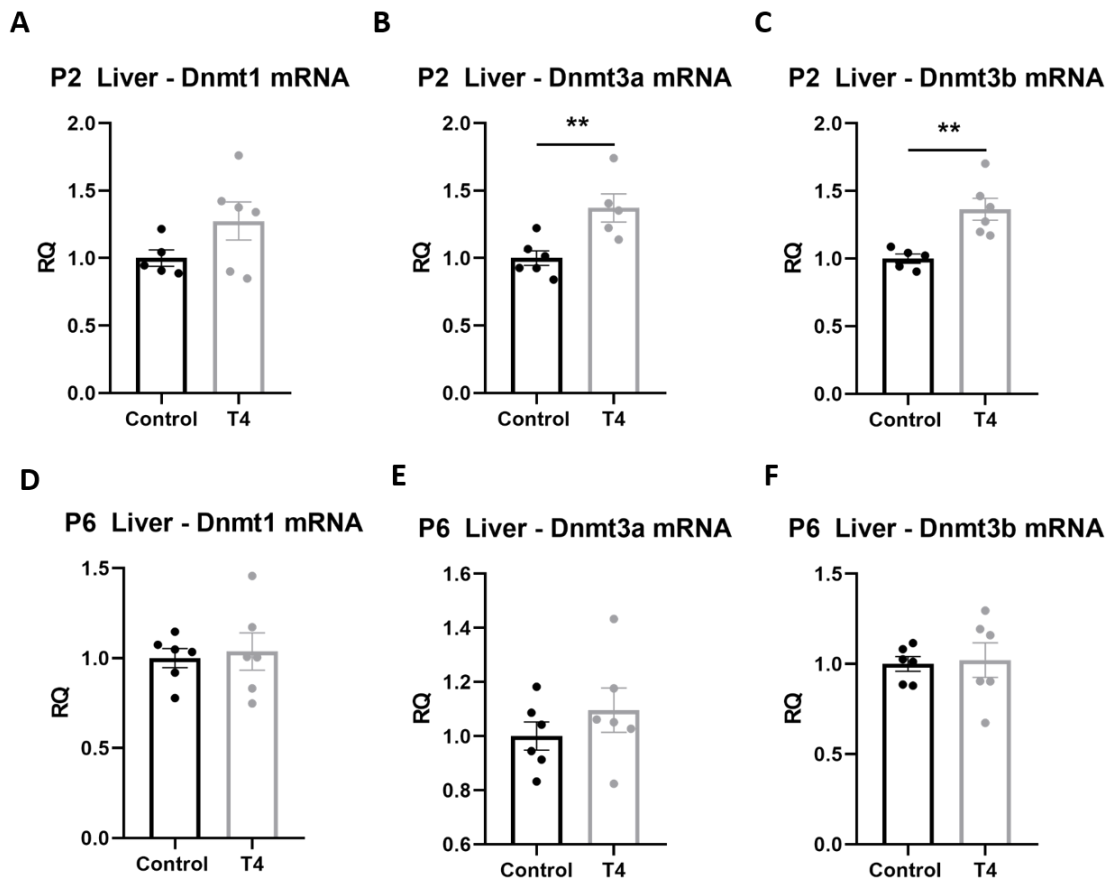
Figure 21: Expression of DNA methylation-related genes in the liver of T4-treated P2 and P6 mouse pups.

TaqMan qPCR analysis of Dnmt1, Dnmt3a and Dnmt3b mRNA expression in liver 8 hours after injection of 200 ng/bwg T4 or vehicle in P2 (A-C, N=5-6) and P6 (D-F, N=6) pups. Liver Dnmt1 (A) expression was not changed significantly in P2, while Dnmt3a (B) and Dnmt3b (C) expression was significantly increased in P2 animals. The Dnmt1 (D), Dnmt3a (E) and Dnmt3b (F) levels of P6 animals did not change signifcantly. Data are compared with Student's t test and shown as mean ± SEM. *p < 0.05; **p < 0.01, ***p < 0.001. Abbreviations: P - postnatal day, T4 – thyroxine, dnmt1 - DNA (cytosine-5)-

methyltransferase 1, dnmt3a - DNA (cytosine-5)-methyltransferase 3a, dnmt3b - DNA (cytosine-5)-methyltransferase 3b.

5. Discussion

5.1. The effect of the tanycytic endocannabinoid system on the HPT axis and metabolism

The HPT axis regulates the relatively steady level of circulating THs (122) and this mechanism is tightly controlled by the interaction of tanycytes and the axons of the hypophysiotropic TRH neurons in the external zone of the ME (76). In this brain region, the endfeet processes of tanycytes are in contact with the axon terminals of the hypophysiotropic TRH neurons in the vicinity of the fenestrated capillaries of the hypophysial portal capillary circulation (31). This close anatomical relationship allows that the tanycytes can control the access of TRH axons to the capillaries. Therefore, the tanycytes can regulate the amount of TRH released into the portal capillaries by mechanically separating the TRH axons from the capillaries (76). In addition, the tanycytes can modulate the T3 availability of TRH neurons by D2 catalyzed conversion of T4 toT3, thus these cells can influence the feedback regulation of TRH neurons (48). Furthermore, tanycytes synthetize the TRH-degrading enzyme PPII (86). Therefore, tanycytes can regulate the amount of TRH that can enter to the portal circulation. Recently, we have described a novel regulatory microcircuit between TRH neurons and tanycytes (95). The majority of TRH axons in the PVN contain CB1 receptor, and our study using ME explants revealed that inhibition of CB1 receptor results in marked increase of TRH release (95). We showed that the source of the endocannabinoids that act on the CB1 of TRH axons is the tanycytes (95). Tanycytes express DAGLα and DAGLα-immunoreactive tanycytes are in contact with CB1-containing TRH axons (95). Glutamate is an important neurotransmitter in the regulation of endocannabinoid production in neuronal systems (91), it stimulates DAGLα activity (98) and TRH neurons known to release glutamate in the external zone of ME (99). To understand whether the endocannabinoid production of tanycytes may be regulated by the glutamate or TRH release of TRH axons, we studied the glutamate and TRH receptor and the glutamate transporter expression of β2-tanycytes isolated by LCM. Our study revealed that β2-tanycytes express glutamate transporters and receptors, but TRHR1 and TRHR2 receptor were absent, indicating that TRH neurons influence the tanycytes primarily via glutamate

release. The most abundant glutamate receptor subunits of the tanycytes are the GRIA1 and GRIA2 AMPA receptors and the GRIK3 kainate receptor, whereas GRIK2, GRIK4, and GRIK5 kainate receptor subunits are expressed in lower levels. The NMDA and the other metabotropic glutamate receptor subunits were almost absent, only GRIN3A and GRM4 subunits were detectable in β2-tanycytes, indicating that the glutamate released by TRH neurons primarily act on kainite and AMPA receptors. Indeed, electrophysiological studies of our laboratory proved that glutamate depolarize the β-tanycytes and this effect can be blocked by the simultaneous inhibition of the AMPA and kainite receptors and the TBOA sensitive glutamate transporters. In contrast, TRH administration did not influence the electrophysological properties and the intracellular Ca^{2+} level of tanycytes. Furthermore, it was shown that simultaneous inhibition of the AMPA and kainite receptors and the glutamate transporters decreases the endocannabinoid content of ME explants further demonstrating the functional role of the AMPA and kainite receptors and glutamate transporters in the regulation of the endocannabinoid synthesis of tanycytes (95).

As our previous studies demonstrated, that the endocannabinoids produced by the tanycytes serve as the ligand of the CB1 of hypophysiotropic TRH axons and induce tonic inhibition of TRH release (95), we hypothesized that tanycytes regulate the activity of the HPT axis by endocannabinoids. To test this hypothesis, we generated a tanycyte-specific DAGLα ablated (T-DAGLα KO) mouse line by crossing DAGLα$^{fl/fl}$ mice with RAX-CreERT2 mice. This later mouse line provides tanycyte-specific Cre recombinase expression in adult mice (129). The Cre mediated recombination was induced by tamoxifen treatment. The characterization of the DAGLα expression in these animals showed that the genetic manipulation decreased the amount of DAGLα protein only in the ME. The DAGLα content of other brain regions was not influenced. Analysis of the DAGLα mRNA content of the cell bodies of β2-tanycytes further demonstrated the marked decrease of DAGLα expression in the tanycytes of T-DAGLα KO mice. To avoid the potential effect of tamoxifen on the studied parameters, the RAX-CreERT2 that were used as control, were also treated with tamoxifen.

Our group has previously showed that TRH release is tonically inhibited by the endocannabinoids in EM explants (95). In this experiment, CB1 antagonist or inhibition of DAGLα stimulated, while CB1 agonist had no effect on the TRH release (95). Despite

of the unchanged TRH expression in the PVN, the TSHβ expression was markedly increased in the pituitary of T-DAGLα KO mice that was accompanied by increased fT4 level in the circulation. These data together indicate that the marked decrease of endocannabinoid production of tanycytes in the T-DAGLα KO caused disinhibition of TRH release resulting in increased TSH production in the pituitary and concomitant increase of fT4 level in the blood of these animals. Interestingly, the fT3 level of the T-DAGLα KO group was similar than that of the control group indicating that alteration of the peripheral TH metabolism can compensate the elevated fT4 level.

Tanycytes are located outside of the BBB (70), therefore, circulating signals can easily access these cells and may regulate their endocannabinoid production. Thus, the regulation of the TRH release provides a mechanism that allows very fast regulation of the HPT axis activity by peripheral signals.

We also studied whether other regulatory mechanisms of tanycytes were also influenced by the decreased endocannabinoid producing capacity of these cells. We observed that the genetic manipulation did not influence the PPII production of the tanycytes. However, the Dio2 expression of β2-tanycytes markedly decreased in the T-DAGLα KO. We hypothesize that the change of Dio2 expression is a compensatory mechanism to decrease the effect of the elevated circulating fT4 level.

As both THs and the endocannabinoid system are critical in regulation of food intake and metabolism (3, 140), we studied the body composition, energy homeostasis and blood glucose level to understand the consequences of the tanycyte-specific decrease of DAGLα expression. The T-DAGLα KO mice had significantly lower blood glucose level and increased fat mass ratio with increased body weight gain compared to the controls. The increased fat accumulation and the decreased blood glucose level suggest that the insulin action is increased in the tissues of these animals. Further studies are needed to understand whether this is due to increased insulin production or due to increased insulin sensitivity of tissues and how the tanycytes can influence these parameters of glucose homeostasis. However, the energy expenditure of the animals was not influenced by the genetic manipulation. In hyperthyroid state, increased energy expenditure, body weight loss (19, 20) and elevated blood glucose level (141) are typical. Therefore, we suggest that the effect of the tanycyte-specific ablation of the DAGLα on the body composition and blood glucose level are independent from the effect of the genetic manipulation on HPT axis.

5.2. Development of the HPT axis feedback regulation in mice

The negative feedback mechanism of the HPT axis is essential to maintain stable TH concentrations (39, 142). The set point of the feedback system of the HPT axis is set for lifetime during the development indicating that the set point is a fixed entity (122). However, during a critical developmental period, genetic and environmental factors or alterations of maternal thyroid status may induce lifelong changes of the set point of HPT axis feedback regulation (117, 118, 122). Studies in humans revealed that infants born from hyperthyroid mothers show hyperthyroidism, but later this state turns to central hypothyroidism due to the changes of set point (117, 118). Environmental factors like endocrine disruptors can influence the development of the offspring's HPT axis in the sensitive period (123). Twin studies revealed that, however, the fT4 and TSH have a very stable log negative relationship during the life (102), heritability accounts for only 60% of the interindividual HPT axis variability suggesting that internal and environmental factors like hormonal status, feeding status and acute or chronic inflammations have also large impact on the development of set point (122). The feedback regulation of the HPT axis of different species develops in distinct periods around birth: in the third trimester in humans (29), between embryonic day 19 and posthatching day 2 in chickens (103) and during the first postnatal week in rats (104). In perinatal or newborn rats, perturbation of TH levels by pharmacologic manipulation or changes in maternal thyroid status induced long lasting alteration in circulating TH levels (101, 119). To better understand the development of the negative feedback regulation of the hypophysiotropic TRH neurons, we examined the timing of this development in mice. P1-10 day old mice were administered of T4 and sacrificed 8 hours later to study the response of pituitary TSHβ expression and the PVN TRH expression. The Dio1 mRNA expression of the liver was used as a marker of the thyroid status of the animals as the very small blood volume of the mouse pus did not allow the measurement of blood TH levels.

Administration of T4-induced a marked decrease in TSHβ mRNA expression in all age groups of mouse pups, indicating that the TSH response for elevated TH level is already functional from birth in mice. TRH expression in the PVN of 1, 3, 4 and 7 day old mice also decreased after T4 administration, suggesting that the HPT axis negative feedback regulation is already developed in newborn mice. In mammals, the critical period of the

evaluation of HPT axis set point is around birth and disturbances in this sensitive period can result in lifelong changes in the individual (101, 143).

5.3. Early disturbance in TH status induces lifelong changes in the HPT axis and metabolism

Based on the results that disturbance of thyroid status in perinatal mice may induce epigenetic changes, we treated mice with T4 between P2-P6 and examined the activity of HPT axis, metabolism and expression of TH sensitive genes in tissues. The early postnatal hyperthyroidism resulted in central hypothyroidism at adulthood. TRH expression in the PVN and serum fT4 level decreased in the postnatally hyperthyroid adult mice without significant changes of serum fT3 and TSHβ expression of the pituitary. The lower fT4 and normal TSH level is typical in central hypothyroidism (144, 145). Due to the high impact of the glycosylation of TSH on its biological activity, the effect of TSH on the thyroid gland can not be always assumed based on the rate of TSH production or the amount of circulating TSH (146, 147). TRH regulates the TSH synthesis, but it also has critical role in the regulation of TSH glycosylation (147). Thus, it is likely that the lower TRH release results in decreased TSH bioactivity despite of the similar rate of TSH transcription. Despite of the lower fT4 level, the early postnatal T4 treatment had no effect on the fT3 level of the adult animals. It is likely that this discrepancy is due to adaptation of peripheral TH metabolism that can compensate the decreased fT4 levels. This could include increased peripheral TH activation or decreased T3 degradation that can help to maintain the normal concentration of the active form of TH, the T3. The normal regulatory mechanism of HPT axis is that in response to the decline of T3 or T4 levels, the TRH expression of hypophysiotropic neurons in the PVN is increased (40), however in our study, the animals have decreased TRH expression despite of the lower fT4 level, indicating that the short postnatal hyperthyroidism induced long term changes of the set point of the TH negative feedback regulation.

In addition to the hypophysiotropic TRH neurons, the tanycytes of the ME are also involved in the regulation of negative feedback mechanism of the HPT axis via regulating the T3 availability for the TRH neurons (31). For instance, the inhibitory effect of

infections on the hypophysiotropic TRH neurons is induced by the local hyperthyroidism in the MBH, which is mediated by the D2 activity of tanycytes (84). The other regulatory mechanism of tanycytes in hyperthyroid state is the increased PPII activity to reduce the released amount of TRH (86). Thus, we hypothesized that the early disturbance in thyroid status may induce changes in the HPT axis by acting on the tanycytes. The early postnatal hyperthyroidism did not change the D2 and PPII expressions in neither the α-, nor in the β-tanycytes. As D2 activity has very complex posttranslational regulation, we also determined whether the tanycytes may inhibit the hypophysiotropic TRH neurons in this model by increased TH activation, but the TH action, determined by the examination of the luc expression in the THAI mice, was not increased in the MBH. These results indicate that the tanycytes are not involved in the early postnatal hyperthyroidism induced changes of the HPT axis development.

As THs has critical role in the regulation of food intake, metabolism and development (1, 3), we studied the changes of body composition and energy homeostasis to understand the consequences of the central hypothyroidism of the postnatally T4-treated mice. The early postnatal hyperthyroidism resulted in decreased body weight at adulthood without changes in LBM/body weight and fat mass/LBM ratios compared to the control animals. Moreover, the food intake did not differ between the groups. The unchanged body compositions and the shorter length of the postnatally T4-treated adult mice indicates that the lower bodyweight of these animals is due to growth retardation and not due to altered energy homeostasis. The growth retardation is probably a direct consequence of the early hyperthyroidism and was not caused by the central hypothyroidism at adulthood, as thyrotoxicosis in childhood is known to induce premature closure of growth plates in long bones resulting in growth retardation (148).

Interestingly, in our experiment, both the energy homeostasis and activity of the early postnatal T4-treated mice increased significantly. Studies in rats revealed that hypothyroidism decreases (149), whereas hyperthyroidism increases (150) the resting metabolic rate, however the T4-treated mice showed elevated energy- and resting energy expenditure despite of the central hypothyroidism. These changes in the energy homeostasis suggest that the peripheral tissues of adult mice may compensate the effect of the central hypothyroidism caused by the early postnatal hyperthyroidism and the tissues are euthyroid despite of the lower circulating fT4 level. Therefore, we examined

the tissue-specific TH action by measuring luc expression of tissues in early postnatal hyperthyroid THAI mice. The lower circulating fT4 level indicates lower TH action in tissues, however, most of the examined tissues did not show decreased TH action. Interestingly, the luc expression decreased significantly only in the small intestine, suggesting lower TH action of this tissue. The intestines are among the most TH sensitive tissues (151). Altered TH levels result in intestinal diseases and abnormal morphology (152). Either hypo- or hyperthyroidism results in gastrointestinal abnormalities, such as altered motility, autoimmune gastritis, or esophageal compression (153). While hyperthyroidism induces frequent bowel movements, diarrhea, nausea, and vomiting, hypothyroidism causes overall decreased metabolic functions accompanied by slow intestinal motility and constipation (154).

BAT is known to be an important target tissue of TH with high D2 activity to regulate the adaptive thermogenesis (18). The postnatally T4-treated mice did not show significant changes in luc expression of BAT, indicating the euthyroid state of this tissue.

Based on the luc expression in THAI mice, the TH action was also unchanged in the liver of postnatally T4-treated mice. However, the expression of the highly TH sensitive Dio1 gene was markedly decreased in the liver of postnatally T4-treated adult mice. This large fall of Dio1 level could indicate a serious tissue hypothyroidism as Dio1 expression of liver is considered a good marker of the TH status (14), but in contrast to the luc expression of THAI mice, the liver Dio1 expression is regulated by many other factors beside the TH (155, 156). As our results in T4-treated mouse pups showed that epigenetic changes occur in the liver at the first postnatal days, it is possible that the early postnatal hyperthyroidism in the liver induces a long term compensatory inhibition of Dio1 expression. Because of the highly different regulation of the TH action marker luc and the highly TH sensitive Dio1 in the liver of our animal model, we also studied a set of TH sensitive liver genes involved in the lipid and glucose homeostasis and the expression of TH receptors. The expression of ME1 and FASN genes decreased significantly, however, the change of the expression of these genes was far less profound than the decrease of Dio1 expression. In contrast to the genes involved in fatty acid metabolism, the expressions of the glucose producing G6PC, the TH sensitive SPOT14 and the two TH receptor genes were not altered in the postnatally T4-treated adult mice. The highly different regulation of TH sensitive genes together with the unchanged luc expression in

the perinatally T4-treated adult THAI mice suggests that the liver of these animals is euthyroid and the expression of Dio1, ME1 and FASN are either regulated epigenetically or by factors other than TH. This observation also highlights the point that even the highly TH sensitive endogenous genes are regulated by many other factors and therefore, the examination of the expression of these genes may give misleading information about the TH status of the animals.

It has been demonstrated that perinatal effect of environmental factors or perturbation of the humoral system in the critical period can cause lifelong epigenetic regulation of certain genes (157). One of the most common epigenetic modifications is DNA methylation catalyzed by DNA methyltransferase enzymes (158). DNA methylation of promoters can modify the transcriptional initiation, alternative splicing and modulates the activity of regulatory elements, which is essential for adaptation for environmental changes (125). Previous data revealed that prenatal stress or glucocorticoid treatment changes the methylation status of genes, including the glucocorticoid receptor and induce lifelong changes in the activity of hypothalamic-pituitary-adrenal axis (159, 160). Thus, we examined the gene expression of DNA methyltransferase genes in liver of hyperthyroid P2 and P6 mice. However, the negative feedback regulation of the HPT axis is already developed in these life stages, the expression of DNA methyltransferases was increased in hyperthyroid P2 mice, but did not change in P6 age group. These results suggest that there is an early, sensitive period when the expression of DNMT genes is TH sensitive in the liver and therefore TH can cause life-long changes of liver gene expression. The epigenetic modifications could ensure the adaptation to environmental changes. For instance, the markedly decreased Dio1 levels in the postnatally T4-treated adult mice may help to preserve the organism from the high T4 levels. These results are in agreement with a study demonstrated that D2 is expressed only transiently in the liver of mice before P5, but transgenic ablation of D2 from hepatocytes highly influences the methylation and the expression of numerous genes involved in the lipid metabolism of liver (128).

These results indicate that the early postnatal hyperthyroidism may induces epigenetic changes in certain genes of the liver involved in the metabolism.

6. Conclusions

The present study provides a better understanding of the central regulation of the HPT axis by endocannabinoids and how disturbances in thyroid status induce lifelong changes in this sensitive system.

It has known that tanycytes can influence the HPT axis via several mechanisms. Recently, our group revealed a novel regulatory microcircuit, which involves the tanycytic endocannabinoid production. In the current study, we showed that the tanycyte-specific genetic ablation of DAGLα results in increased TSH synthesis and elevated fT4 level, supporting the view that the TRH release is tonically inhibited by the endocannabinoid production of tanycytes. Despite of the elevated fT4 level, the energy expenditure of the T- DAGLα KO mice was not increased suggesting that the increased TH level is compensated by TH metabolism in tissues. Interestingly, T- DAGLα KO mice had decreased blood glucose level indicating that the 2-AG production of tanycytes is also involved in the regulation of glucose homeostasis, but the mechanism of this effect needs further examination.

Our experiments revealed that the thyroid status has critical effect on the development of the feedback regulation of the HPT axis in the early postnatal period. Hyperthyroidism in this critical period induces lifelong changes of the set point of this regulation, suggesting that epigenetic modifications occur in certain TH-dependent genes of the HPT axis. This hypothesis is supported by the TH regulation of DNMT enzymes in P2 mouse pups.

Despite of the hypothyroidism of adult mice induced by the early postnatal hyperthyroidism, most tissues of these animals are euthyroid and they have normal energy expenditure suggesting that the peripheral tissues can compensate the lower fT4 level of this model. However, tanycytes play critical role in the regulation of the HPT axis, our data indicate that these cells are not involved in the mediation of the effects of early postnatal hyperthyroidism on the HPT axis.

These results support that not only hypothyroidism, but also hyperthyroidism in the developmental period has major lifelong effect.

7. Summary

Thyroid hormones (TH) play critical role in the regulation of most organs and physiological processes. The level of TH is regulated by the negative feedback regulation of the hypothalamic-pituitary-thyroid (HPT) axis to ensure stable circulating TH levels. The set point of the axis determines the individual optimum of TRH-TSH-TH relationship. Perinatal events can have lifelong effect on the set point of the feedback mechanism of the HPT axis, but the development of this process is poorly understood. The tanycytes, a special glial cell type of the hypothalamus are known to influence the activity of HPT axis, but the role of the tanycytic endocannabinoid system in this regulatory mechanism in vivo is unknown.

Therefore, we examined how tanycyte-specific ablation of the endocannabinoid system influences the HPT axis and metabolism of mice.

Our data demonstrated that the genetic inhibition of tanycyte-specific endocannabinoid production disinhibits the TRH release and therefore, increases the TSH synthesis and the circulating fT4 level. The major effect of this genetic manipulation on the activity of the HPT axis demonstrates the key role of tanycytes in the regulation of this neuroendocrine axis. The tanycyte-specific ablation of DAGLα also resulted in decrease of blood glucose level suggesting that the endocannabinoid production of tanycytes is involved in the regulation of glucose homeostasis.

Our studies focusing on the development of the feedback regulation of the HPT axis demonstrated, that the feedback regulation of this axis is already functional in newborn mice. We also showed that early postnatal T4 treatment of mice induces central hypothyroidism in adult mice indicating, that early disturbance of thyroid status induces lifelong changes of the HPT axis. Furthermore, the increased energy expenditure in this animal model suggests that despite of the reduced HPT axis activity, the TH action is normalized at the level of tissues. The lifelong effect of the postnatal treatment suggests that the effect of postnatal hyperthyroidism is mediated by epigenetic regulation of gene expression. This hypothesis is supported by the TH regulation of DNMT genes in P2 pups.

8. Összefoglalás

A pajzsmirigyhormonok (PMH) fontos szerepet játszanak a szerveink és fiziológiai folyamataink szabályozásában. A PMH szint szabályozása a hipotalamusz-hipofízis-pajzsmirigy (HHP) tengely negatív *feedback* regulációja által valósul meg, ami elősegíti az állandó keringő PMH szint fenntartását. A tengely *set point*-ja határozza meg a TRH-TSH-PMH egyéni optimumát. A perinatális időszak eseményeinek élethosszig tartó hatása lehet a HHP tengely *feedback* szabályozásának *set point*-jára, de e hatás mechanizmusa jelenleg még kevéssé ismert.

A taniciták - a hipotalamusz speciális glia sejtjei - befolyásolják a HHP tengely működését, de *in vivo* a taniciták által termelt endokannabinoidok szerepe ebben a szabályozó mechanizmusban még nem ismert.

Ezért vizsgáltuk, hogy az endokannabinoid termelés tanicita specifikus hiánya hogyan befolyásolja a HHP tengely működését és a metabolizmust egerekben.

Az eredményeink alátámasztják, hogy az endokannabinoid termelés tanicita specifikus genetikai gátlása feloldja a TRH felszabadulás gátlását, ezért növekszik a TSH termelés és a keringő T4 szint. E genetikai manipulációnak a hatása a HHP tengely aktivitására igazolja, hogy a taniciták fontos szerepet játszanak e neuroendokrin tengely szabályozásában. A DAGLα tanicita specifikus hiánya csökkent vércukor szintet is eredményezett, ami felveti, hogy a taniciták endokannabinoid termelése szerepet játszik a glükóz homeosztázis szabályozásában is.

A HHP tengely negatív *feedback* regulációjának fejlődését vizsgáló kutatásaink azt mutatják, hogy a tengely *feedback* szabályozása már működik újszülött egerekben is. Továbbá kimutattuk, hogy a korai posztnatális T4 kezelés eredményeként centrális hipotiroidizmus jön létre felnőtt egerekben igazolva, hogy a PMH státusz újszülöttkori megváltozása élethosszig tartó változásokat eredményezhet a HHP tengely működésében. Ezen állatok megnövekedett energiafelhasználása azt mutatja, hogy a csökkent HHP tengely aktivitás ellenére a PMH hatás nem csökken a szövetekben. A posztnatális PMH kezelés által kiváltott élethosszig tartó változások felvetik, hogy korai hipertiroidizmus a gének expressziójának epigenetikai változását indukálják. E feltételezést alátámasztja az eredményünk, mely szerint a PMH szabályozza a DNMT géneket P2 korú egerekben.

9. References

1. Bloise FF, Cordeiro A, Ortiga-Carvalho TM (2018) Role of thyroid hormone in skeletal muscle physiology. J Endocrinol **236**:R57-R68.

2. Zhang J, Lazar MA (2000) The mechanism of action of thyroid hormones. Annu Rev Physiol **62**:439-466.

3. Sinha RA, Singh BK, Yen PM (2018) Direct effects of thyroid hormones on hepatic lipid metabolism. Nat Rev Endocrinol **14**:259-269.

4. Ortiga-Carvalho TM, Sidhaye AR, Wondisford FE (2014) Thyroid hormone receptors and resistance to thyroid hormone disorders. Nat Rev Endocrinol **10**:582-591.

5. Oetting A, Yen PM (2007) New insights into thyroid hormone action. Best Pract Res Clin Endocrinol Metab **21**:193-208.

6. Cheng SY, Leonard JL, Davis PJ (2010) Molecular aspects of thyroid hormone actions. Endocr Rev **31**:139-170.

7. Brent GA, Larsen PR, Harney JW, Koenig RJ, Moore DD (1989) Functional characterization of the rat growth hormone promoter elements required for induction by thyroid hormone with and without a co-transfected beta type thyroid hormone receptor. J Biol Chem **264**:178-182.

8. Chatonnet F, Guyot R, Benoit G, Flamant F (2013) Genome-wide analysis of thyroid hormone receptors shared and specific functions in neural cells. Proc Natl Acad Sci U S A **110**:E766-775.

9. Gereben B, Zavacki AM, Ribich S, Kim BW, Huang SA, Simonides WS, Zeold A, Bianco AC (2008) Cellular and molecular basis of deiodinase-regulated thyroid hormone signaling. Endocr Rev **29**:898-938.

10. Bianco AC, Salvatore D, Gereben B, Berry MJ, Larsen PR (2002) Biochemistry, cellular and molecular biology, and physiological roles of the iodothyronine selenodeiodinases. Endocr Rev **23**:38-89.

11. Bianco AC, Kim BW (2006) Deiodinases: implications of the local control of thyroid hormone action. J Clin Invest **116**:2571-2579.

12. Kuiper GG, Kester MH, Peeters RP, Visser TJ (2005) Biochemical mechanisms of thyroid hormone deiodination. Thyroid **15**:787-798.

13. St Germain DL, Galton VA (1997) The deiodinase family of selenoproteins. Thyroid **7**:655-668.

14. Zavacki AM, Ying H, Christoffolete MA, Aerts G, So E, Harney JW, Cheng SY, Larsen PR, Bianco AC (2005) Type 1 iodothyronine deiodinase is a sensitive marker of peripheral thyroid status in the mouse. Endocrinology **146**:1568-1575.

15. Silva JE, Larsen PR (1985) Potential of brown adipose tissue type II thyroxine 5'-deiodinase as a local and systemic source of triiodothyronine in rats. J Clin Invest **76**:2296-2305.

16. Lowell BB, Spiegelman BM (2000) Towards a molecular understanding of adaptive thermogenesis. Nature **404**:652-660.

17. Iwen KA, Schroder E, Brabant G (2013) Thyroid hormones and the metabolic syndrome. Eur Thyroid J **2**:83-92.

18. Mullur R, Liu YY, Brent GA (2014) Thyroid hormone regulation of metabolism. Physiol Rev **94**:355-382.

19. Motomura K, Brent GA (1998) Mechanisms of thyroid hormone action. Implications for the clinical manifestation of thyrotoxicosis. Endocrinol Metab Clin North Am **27**:1-23.

20. Brent GA (2008) Clinical practice. Graves' disease. N Engl J Med **358**:2594-2605.

21. Jabbar A, Pingitore A, Pearce SH, Zaman A, Iervasi G, Razvi S (2017) Thyroid hormones and cardiovascular disease. Nat Rev Cardiol **14**:39-55.

22. Biondi B, Kahaly GJ, Robertson RP (2019) Thyroid Dysfunction and Diabetes Mellitus: Two Closely Associated Disorders. Endocr Rev **40**:789-824.

23. Srinivasan S, Misra M (2015) Hyperthyroidism in children. Pediatr Rev **36**:239-248.

24. Biondi B, Klein I (2004) Hypothyroidism as a risk factor for cardiovascular disease. Endocrine **24**:1-13.

25. Maushart CI, Loeliger R, Gashi G, Christ-Crain M, Betz MJ (2019) Resolution of Hypothyroidism Restores Cold-Induced Thermogenesis in Humans. Thyroid **29**:493-501.

26. Williams GR (2008) Neurodevelopmental and neurophysiological actions of thyroid hormone. J Neuroendocrinol **20**:784-794.

27. Maraka S, Ospina NM, O'Keeffe DT, Espinosa De Ycaza AE, Gionfriddo MR, Erwin PJ, Coddington CC, 3rd, Stan MN, Murad MH, Montori VM (2016) Subclinical Hypothyroidism in Pregnancy: A Systematic Review and Meta-Analysis. Thyroid **26**:580-590.

28. Amano I, Takatsuru Y, Khairinisa MA, Kokubo M, Haijima A, Koibuchi N (2018) Effects of Mild Perinatal Hypothyroidism on Cognitive Function of Adult Male Offspring. Endocrinology **159**:1910-1921.

29. Moog NK, Entringer S, Heim C, Wadhwa PD, Kathmann N, Buss C (2017) Influence of maternal thyroid hormones during gestation on fetal brain development. Neuroscience **342**:68-100.

30. Brent GA (2012) Mechanisms of thyroid hormone action. J Clin Invest **122**:3035-3043.

31. Fekete C, Lechan RM (2014) Central regulation of hypothalamic-pituitary-thyroid axis under physiological and pathophysiological conditions. Endocr Rev **35**:159-194.

32. Fekete C, Lechan RM (2007) Negative feedback regulation of hypophysiotropic thyrotropin-releasing hormone (TRH) synthesizing neurons: role of neuronal afferents and type 2 deiodinase. Front Neuroendocrinol **28**:97-114.

33. Biag J, Huang Y, Gou L, Hintiryan H, Askarinam A, Hahn JD, Toga AW, Dong HW (2012) Cyto- and chemoarchitecture of the hypothalamic paraventricular nucleus in the C57BL/6J male mouse: a study of immunostaining and multiple fluorescent tract tracing. J Comp Neurol **520**:6-33.

34. Mariotti S, Beck-Peccoz P 2000 Physiology of the Hypothalamic-Pituitary-Thyroid Axis. In: Feingold KR, Anawalt B, Boyce A, Chrousos G, Dungan K, Grossman A, Hershman JM, Kaltsas G, Koch C, Kopp P, Korbonits M, McLachlan R, Morley JE, New M, Perreault L, Purnell J, Rebar R, Singer F, Trence DL, Vinik A, Wilson DP, (eds) Endotext. Vol., South Dartmouth (MA).

35. Weintraub BD, Gesundheit N, Taylor T, Gyves PW (1989) Effect of TRH on TSH glycosylation and biological action. Ann N Y Acad Sci **553**:205-213.

36. Lechan RM, Fekete C (2006) The TRH neuron: a hypothalamic integrator of energy metabolism. Prog Brain Res **153**:209-235.

37. Ishikawa K, Taniguchi Y, Inoue K, Kurosumi K, Suzuki M (1988) Immunocytochemical delineation of thyrotrophic area: origin of thyrotropin-releasing hormone in the median eminence. Neuroendocrinology **47**:384-388.

38. Kadar A, Sanchez E, Wittmann G, Singru PS, Fuzesi T, Marsili A, Larsen PR, Liposits Z, Lechan RM, Fekete C (2010) Distribution of hypophysiotropic thyrotropin-releasing hormone (TRH)-synthesizing neurons in the hypothalamic paraventricular nucleus of the mouse. J Comp Neurol **518**:3948-3961.

39. Segerson TP, Kauer J, Wolfe HC, Mobtaker H, Wu P, Jackson IM, Lechan RM (1987) Thyroid hormone regulates TRH biosynthesis in the paraventricular nucleus of the rat hypothalamus. Science **238**:78-80.

40. Fonseca TL, Correa-Medina M, Campos MP, Wittmann G, Werneck-de-Castro JP, Arrojo e Drigo R, Mora-Garzon M, Ueta CB, Caicedo A, Fekete C, Gereben B, Lechan RM, Bianco AC (2013) Coordination of hypothalamic and pituitary T3 production regulates TSH expression. J Clin Invest **123**:1492-1500.

41. Perello M, Friedman T, Paez-Espinosa V, Shen X, Stuart RC, Nillni EA (2006) Thyroid hormones selectively regulate the posttranslational processing of prothyrotropin-releasing hormone in the paraventricular nucleus of the hypothalamus. Endocrinology **147**:2705-2716.

42. Lechan RM, Qi Y, Jackson IM, Mahdavi V (1994) Identification of thyroid hormone receptor isoforms in thyrotropin-releasing hormone neurons of the hypothalamic paraventricular nucleus. Endocrinology **135**:92-100.

43. Dyess EM, Segerson TP, Liposits Z, Paull WK, Kaplan MM, Wu P, Jackson IM, Lechan RM (1988) Triiodothyronine exerts direct cell-specific regulation of thyrotropin-releasing hormone gene expression in the hypothalamic paraventricular nucleus. Endocrinology **123**:2291-2297.

44. Abel ED, Ahima RS, Boers ME, Elmquist JK, Wondisford FE (2001) Critical role for thyroid hormone receptor beta2 in the regulation of paraventricular thyrotropin-releasing hormone neurons. J Clin Invest **107**:1017-1023.

45. Refetoff S, Dumitrescu AM (2007) Syndromes of reduced sensitivity to thyroid hormone: genetic defects in hormone receptors, cell transporters and deiodination. Best Pract Res Clin Endocrinol Metab **21**:277-305.

46. Sugrue ML, Vella KR, Morales C, Lopez ME, Hollenberg AN (2010) The thyrotropin-releasing hormone gene is regulated by thyroid hormone at the level of transcription in vivo. Endocrinology **151**:793-801.

47. Kakucska I, Rand W, Lechan RM (1992) Thyrotropin-releasing hormone gene expression in the hypothalamic paraventricular nucleus is dependent upon feedback regulation by both triiodothyronine and thyroxine. Endocrinology **130**:2845-2850.

48. Fekete C, Mihaly E, Herscovici S, Salas J, Tu H, Larsen PR, Lechan RM (2000) DARPP-32 and CREB are present in type 2 iodothyronine deiodinase-producing tanycytes: implications for the regulation of type 2 deiodinase activity. Brain Res **862**:154-161.

49. Ortiga-Carvalho TM, Chiamolera MI, Pazos-Moura CC, Wondisford FE (2016) Hypothalamus-Pituitary-Thyroid Axis. Compr Physiol **6**:1387-1428.

50. Shupnik MA, Chin WW, Habener JF, Ridgway EC (1985) Transcriptional regulation of the thyrotropin subunit genes by thyroid hormone. J Biol Chem **260**:2900-2903.

51. Schomburg L, Bauer K (1997) Regulation of the adenohypophyseal thyrotropin-releasing hormone-degrading ectoenzyme by estradiol. Endocrinology **138**:3587-3593.

52. Fuzesi T, Wittmann G, Lechan RM, Liposits Z, Fekete C (2009) Noradrenergic innervation of hypophysiotropic thyrotropin-releasing hormone-synthesizing neurons in rats. Brain Res **1294**:38-44.

53. Schwartz MW, Woods SC, Porte D, Jr., Seeley RJ, Baskin DG (2000) Central nervous system control of food intake. Nature **404**:661-671.

54. Toni R, Jackson IM, Lechan RM (1990) Neuropeptide-Y-immunoreactive innervation of thyrotropin-releasing hormone-synthesizing neurons in the rat hypothalamic paraventricular nucleus. Endocrinology **126**:2444-2453.

55. Legradi G, Lechan RM (1999) Agouti-related protein containing nerve terminals innervate thyrotropin-releasing hormone neurons in the hypothalamic paraventricular nucleus. Endocrinology **140**:3643-3652.

56. Fekete C, Legradi G, Mihaly E, Huang QH, Tatro JB, Rand WM, Emerson CH, Lechan RM (2000) alpha-Melanocyte-stimulating hormone is contained in nerve terminals innervating thyrotropin-releasing hormone-synthesizing neurons in the hypothalamic paraventricular nucleus and prevents fasting-induced suppression of prothyrotropin-releasing hormone gene expression. J Neurosci **20**:1550-1558.

57. Kim MS, Small CJ, Stanley SA, Morgan DG, Seal LJ, Kong WM, Edwards CM, Abusnana S, Sunter D, Ghatei MA, Bloom SR (2000) The central melanocortin system affects the hypothalamo-pituitary thyroid axis and may mediate the effect of leptin. J Clin Invest **105**:1005-1011.

58. Takahashi KA, Cone RD (2005) Fasting induces a large, leptin-dependent increase in the intrinsic action potential frequency of orexigenic arcuate nucleus neuropeptide Y/Agouti-related protein neurons. Endocrinology **146**:1043-1047.

59. Mizuno TM, Kleopoulos SP, Bergen HT, Roberts JL, Priest CA, Mobbs CV (1998) Hypothalamic pro-opiomelanocortin mRNA is reduced by fasting and [corrected] in ob/ob and db/db mice, but is stimulated by leptin. Diabetes **47**:294-297.

60. Legradi G, Emerson CH, Ahima RS, Flier JS, Lechan RM (1997) Leptin prevents fasting-induced suppression of prothyrotropin-releasing hormone messenger ribonucleic acid in neurons of the hypothalamic paraventricular nucleus. Endocrinology **138**:2569-2576.

61. Wittmann G, Liposits Z, Lechan RM, Fekete C (2002) Medullary adrenergic neurons contribute to the neuropeptide Y-ergic innervation of hypophysiotropic thyrotropin-releasing hormone-synthesizing neurons in the rat. Neurosci Lett **324**:69-73.

62. Wittmann G, Liposits Z, Lechan RM, Fekete C (2004) Medullary adrenergic neurons contribute to the cocaine- and amphetamine-regulated transcript-immunoreactive innervation of thyrotropin-releasing hormone synthesizing neurons in the hypothalamic paraventricular nucleus. Brain Res **1006**:1-7.

63. Mihaly E, Fekete C, Legradi G, Lechan RM (2001) Hypothalamic dorsomedial nucleus neurons innervate thyrotropin-releasing hormone-synthesizing neurons in the paraventricular nucleus. Brain Res **891**:20-31.

64. Scott MM, Lachey JL, Sternson SM, Lee CE, Elias CF, Friedman JM, Elmquist JK (2009) Leptin targets in the mouse brain. J Comp Neurol **514**:518-532.

65. Singru PS, Fekete C, Lechan RM (2005) Neuroanatomical evidence for participation of the hypothalamic dorsomedial nucleus (DMN) in regulation of the hypothalamic paraventricular nucleus (PVN) by alpha-melanocyte stimulating hormone. Brain Res **1064**:42-51.

66. Bellinger LL, Bernardis LL, McCusker RH, Campion DR (1985) Plasma hormone levels in growth-retarded rats with dorsomedial hypothalamic lesions. Physiol Behav **34**:783-790.

67. Liposits Z, Paull WK, Wu P, Jackson IM, Lechan RM (1987) Hypophysiotrophic thyrotropin releasing hormone (TRH) synthesizing neurons. Ultrastructure, adrenergic innervation and putative transmitter action. Histochemistry **88**:1-10.

68. Cote-Velez A, Perez-Martinez L, Diaz-Gallardo MY, Perez-Monter C, Carreon-Rodriguez A, Charli JL, Joseph-Bravo P (2005) Dexamethasone represses cAMP rapid upregulation of TRH gene transcription: identification of a composite glucocorticoid response element and a cAMP response element in TRH promoter. J Mol Endocrinol **34**:177-197.

69. Arancibia S, Rage F, Astier H, Tapia-Arancibia L (1996) Neuroendocrine and autonomous mechanisms underlying thermoregulation in cold environment. Neuroendocrinology **64**:257-267.

70. Rodriguez EM, Blazquez JL, Pastor FE, Pelaez B, Pena P, Peruzzo B, Amat P (2005) Hypothalamic tanycytes: a key component of brain-endocrine interaction. Int Rev Cytol **247**:89-164.

71. Rodriguez EM, Gonzalez CB, Delannoy L (1979) Cellular organization of the lateral and postinfundibular regions of the median eminence in the rat. Cell Tissue Res **201**:377-408.

72. Mullier A, Bouret SG, Prevot V, Dehouck B (2010) Differential distribution of tight junction proteins suggests a role for tanycytes in blood-hypothalamus barrier regulation in the adult mouse brain. J Comp Neurol **518**:943-962.

73. Rethelyi M (1984) Diffusional barrier around the hypothalamic arcuate nucleus in the rat. Brain Res **307**:355-358.

74. Rodriguez-Rodriguez A, Lazcano I, Sanchez-Jaramillo E, Uribe RM, Jaimes-Hoy L, Joseph-Bravo P, Charli JL (2019) Tanycytes and the Control of Thyrotropin-Releasing Hormone Flux Into Portal Capillaries. Front Endocrinol (Lausanne) **10**:401.

75. Ebling FJP, Lewis JE (2018) Tanycytes and hypothalamic control of energy metabolism. Glia **66**:1176-1184.

76. Muller-Fielitz H, Stahr M, Bernau M, Richter M, Abele S, Krajka V, Benzin A, Wenzel J, Kalies K, Mittag J, Heuer H, Offermanns S, Schwaninger M (2017) Tanycytes control the hormonal output of the hypothalamic-pituitary-thyroid axis. Nat Commun **8**:484.

77. Riskind PN, Kolodny JM, Larsen PR (1987) The regional hypothalamic distribution of type II 5'-monodeiodinase in euthyroid and hypothyroid rats. Brain Res **420**:194-198.

78. Tu HM, Kim SW, Salvatore D, Bartha T, Legradi G, Larsen PR, Lechan RM (1997) Regional distribution of type 2 thyroxine deiodinase messenger ribonucleic acid in rat hypothalamus and pituitary and its regulation by thyroid hormone. Endocrinology **138**:3359-3368.

79. Mayerl S, Visser TJ, Darras VM, Horn S, Heuer H (2012) Impact of Oatp1c1 deficiency on thyroid hormone metabolism and action in the mouse brain. Endocrinology **153**:1528-1537.

80. Heuer H, Maier MK, Iden S, Mittag J, Friesema EC, Visser TJ, Bauer K (2005) The monocarboxylate transporter 8 linked to human psychomotor retardation is highly expressed in thyroid hormone-sensitive neuron populations. Endocrinology **146**:1701-1706.

81. Kallo I, Mohacsik P, Vida B, Zeold A, Bardoczi Z, Zavacki AM, Farkas E, Kadar A, Hrabovszky E, Arrojo EDR, Dong L, Barna L, Palkovits M, Borsay BA, Herczeg L, Lechan RM, Bianco AC, Liposits Z, Fekete C, Gereben B (2012) A novel pathway regulates thyroid hormone availability in rat and human hypothalamic neurosecretory neurons. PLoS One **7**:e37860.

82. Diano S, Naftolin F, Goglia F, Horvath TL (1998) Fasting-induced increase in type II iodothyronine deiodinase activity and messenger ribonucleic acid levels is not reversed by thyroxine in the rat hypothalamus. Endocrinology **139**:2879-2884.

83. Serrano-Lozano A, Montiel M, Morell M, Morata P (1993) 5' Deiodinase activity in brain regions of adult rats: modifications in different situations of experimental hypothyroidism. Brain Res Bull **30**:611-616.

84. Fekete C, Sarkar S, Christoffolete MA, Emerson CH, Bianco AC, Lechan RM (2005) Bacterial lipopolysaccharide (LPS)-induced type 2 iodothyronine deiodinase (D2) activation in the mediobasal hypothalamus (MBH) is independent of the LPS-induced fall in serum thyroid hormone levels. Brain Res **1056**:97-99.

85. Freitas BC, Gereben B, Castillo M, Kallo I, Zeold A, Egri P, Liposits Z, Zavacki AM, Maciel RM, Jo S, Singru P, Sanchez E, Lechan RM, Bianco AC (2010) Paracrine signaling by glial cell-derived triiodothyronine activates neuronal gene expression in the rodent brain and human cells. J Clin Invest **120**:2206-2217.

86. Sanchez E, Vargas MA, Singru PS, Pascual I, Romero F, Fekete C, Charli JL, Lechan RM (2009) Tanycyte pyroglutamyl peptidase II contributes to regulation of the hypothalamic-pituitary-thyroid axis through glial-axonal associations in the median eminence. Endocrinology **150**:2283-2291.

87. Kano M, Ohno-Shosaku T, Hashimotodani Y, Uchigashima M, Watanabe M (2009) Endocannabinoid-mediated control of synaptic transmission. Physiol Rev **89**:309-380.

88. Katona I, Freund TF (2012) Multiple functions of endocannabinoid signaling in the brain. Annu Rev Neurosci **35**:529-558.

89. Meccariello R, Santoro A, D'Angelo S, Morrone R, Fasano S, Viggiano A, Pierantoni R (2020) The Epigenetics of the Endocannabinoid System. Int J Mol Sci **21**.

90. Freund TF, Katona I, Piomelli D (2003) Role of endogenous cannabinoids in synaptic signaling. Physiol Rev **83**:1017-1066.

91. Piomelli D (2003) The molecular logic of endocannabinoid signalling. Nat Rev Neurosci **4**:873-884.

92. Ohno-Shosaku T, Kano M (2014) Endocannabinoid-mediated retrograde modulation of synaptic transmission. Curr Opin Neurobiol **29**:1-8.

93. Schuele LL, Glasmacher S, Gertsch J, Roggan MD, Transfeld JL, Bindila L, Lutz B, Kolbe CC, Bilkei-Gorzo A, Zimmer A, Leidmaa E (2021) Diacylglycerol lipase alpha in astrocytes is involved in maternal care and affective behaviors. Glia **69**:377-391.

94. Gao Y, Vasilyev DV, Goncalves MB, Howell FV, Hobbs C, Reisenberg M, Shen R, Zhang MY, Strassle BW, Lu P, Mark L, Piesla MJ, Deng K, Kouranova EV, Ring RH, Whiteside GT, Bates B, Walsh FS, Williams G, Pangalos MN, Samad TA, Doherty P (2010) Loss of retrograde endocannabinoid signaling and reduced adult neurogenesis in diacylglycerol lipase knock-out mice. J Neurosci **30**:2017-2024.

95. Farkas E, Varga E, Kovacs B, Szilvasy-Szabo A, Cote-Velez A, Peterfi Z, Matziari M, Toth M, Zelena D, Mezriczky Z, Kadar A, Kovari D, Watanabe M, Kano M, Mackie K, Rozsa B, Ruska Y, Toth B, Mate Z, Erdelyi F, Szabo G, Gereben B, Lechan RM, Charli JL, Joseph-Bravo P, Fekete C (2020) A Glial-Neuronal Circuit in the Median Eminence Regulates Thyrotropin-Releasing Hormone-Release via the Endocannabinoid System. iScience **23**:100921.

96. Wittmann G, Deli L, Kallo I, Hrabovszky E, Watanabe M, Liposits Z, Fekete C (2007) Distribution of type 1 cannabinoid receptor (CB1)-immunoreactive axons in the mouse hypothalamus. J Comp Neurol **503**:270-279.

97. Regehr WG, Carey MR, Best AR (2009) Activity-dependent regulation of synapses by retrograde messengers. Neuron **63**:154-170.

98. Katona I, Urban GM, Wallace M, Ledent C, Jung KM, Piomelli D, Mackie K, Freund TF (2006) Molecular composition of the endocannabinoid system at glutamatergic synapses. J Neurosci **26**:5628-5637.

99. Hrabovszky E, Wittmann G, Turi GF, Liposits Z, Fekete C (2005) Hypophysiotropic thyrotropin-releasing hormone and corticotropin-releasing hormone neurons of the rat contain vesicular glutamate transporter-2. Endocrinology **146**:341-347.

100. Kawakami S (2000) Glial and neuronal localization of ionotropic glutamate receptor subunit-immunoreactivities in the median eminence of female rats:

GluR2/3 and GluR6/7 colocalize with vimentin, not with glial fibrillary acidic protein (GFAP). Brain Res **858**:198-204.

101. Alonso M, Goodwin C, Liao X, Page D, Refetoff S, Weiss RE (2007) Effects of maternal levels of thyroid hormone (TH) on the hypothalamus-pituitary-thyroid set point: studies in TH receptor beta knockout mice. Endocrinology **148**:5305-5312.

102. Leow MK, Goede SL (2014) The homeostatic set point of the hypothalamus-pituitary-thyroid axis--maximum curvature theory for personalized euthyroid targets. Theor Biol Med Model **11**:35.

103. Mohacsik P, Fuzesi T, Doleschall M, Szilvasy-Szabo A, Vancamp P, Hadadi E, Darras VM, Fekete C, Gereben B (2016) Increased Thyroid Hormone Activation Accompanies the Formation of Thyroid Hormone-Dependent Negative Feedback in Developing Chicken Hypothalamus. Endocrinology **157**:1211-1221.

104. Taylor T, Gyves P, Burgunder JM (1990) Thyroid hormone regulation of TRH mRNA levels in rat paraventricular nucleus of the hypothalamus changes during ontogeny. Neuroendocrinology **52**:262-267.

105. Fisher DA, Nelson JC, Carlton EI, Wilcox RB (2000) Maturation of human hypothalamic-pituitary-thyroid function and control. Thyroid **10**:229-234.

106. Koutcherov Y, Mai JK, Ashwell KW, Paxinos G (2002) Organization of human hypothalamus in fetal development. J Comp Neurol **446**:301-324.

107. Hyyppa M (1969) Differentiation of the hypothalamic nuclei during ontogenetic development in the rat. Z Anat Entwicklungsgesch **129**:41-52.

108. Pope C, McNeilly JR, Coutts S, Millar M, Anderson RA, McNeilly AS (2006) Gonadotrope and thyrotrope development in the human and mouse anterior pituitary gland. Dev Biol **297**:172-181.

109. Japon MA, Rubinstein M, Low MJ (1994) In situ hybridization analysis of anterior pituitary hormone gene expression during fetal mouse development. J Histochem Cytochem **42**:1117-1125.

110. Thommes RC, Williams DJ, Woods JE (1984) Hypothalamo-adenohypophyseal-thyroid interrelationships in the chick embryo. VI. Midgestational adenohypophyseal sensitivity to thyrotrophin-releasing hormone. Gen Comp Endocrinol **55**:275-279.

111. Gregory CC, Dean CE, Porter TE (1998) Expression of chicken thyroid-stimulating hormone beta-subunit messenger ribonucleic acid during embryonic and neonatal development. Endocrinology **139**:474-478.

112. Geris KL, Berghman LR, Kuhn ER, Darras VM (1998) Pre- and posthatch developmental changes in hypothalamic thyrotropin-releasing hormone and somatostatin concentrations and in circulating growth hormone and thyrotropin levels in the chicken. J Endocrinol **159**:219-225.

113. Burgunder JM, Taylor T (1989) Ontogeny of thyrotropin-releasing hormone gene expression in the rat diencephalon. Neuroendocrinology **49**:631-640.

114. Chan S, Kachilele S, McCabe CJ, Tannahill LA, Boelaert K, Gittoes NJ, Visser TJ, Franklyn JA, Kilby MD (2002) Early expression of thyroid hormone deiodinases and receptors in human fetal cerebral cortex. Brain Res Dev Brain Res **138**:109-116.

115. Chan SY, Franklyn JA, Pemberton HN, Bulmer JN, Visser TJ, McCabe CJ, Kilby MD (2006) Monocarboxylate transporter 8 expression in the human placenta: the effects of severe intrauterine growth restriction. J Endocrinol **189**:465-471.

116. Glinoer D (2001) Potential consequences of maternal hypothyroidism on the offspring: evidence and implications. Horm Res **55**:109-114.

117. Higuchi R, Miyawaki M, Kumagai T, Okutani T, Shima Y, Yoshiyama M, Ban H, Yoshikawa N (2005) Central hypothyroidism in infants who were born to mothers with thyrotoxicosis before 32 weeks' gestation: 3 cases. Pediatrics **115**:e623-625.

118. Higuchi R, Kumagai T, Kobayashi M, Minami T, Koyama H, Ishii Y (2001) Short-term hyperthyroidism followed by transient pituitary hypothyroidism in a very low birth weight infant born to a mother with uncontrolled Graves' disease. Pediatrics **107**:E57.

119. Pracyk JB, Seidler FJ, McCook EC, Slotkin TA (1992) Pituitary-thyroid axis reactivity to hyper- and hypothyroidism in the perinatal period: ontogeny of regulation of regulation and long-term programming of responses. J Dev Physiol **18**:105-109.

120. Dietrich JW, Landgrafe G, Fotiadou EH (2012) TSH and Thyrotropic Agonists: Key Actors in Thyroid Homeostasis. J Thyroid Res **2012**:351864.

121. Panicker V, Wilson SG, Spector TD, Brown SJ, Kato BS, Reed PW, Falchi M, Richards JB, Surdulescu GL, Lim EM, Fletcher SJ, Walsh JP (2008) Genetic loci linked to pituitary-thyroid axis set points: a genome-wide scan of a large twin cohort. J Clin Endocrinol Metab **93**:3519-3523.

122. Fliers E, Kalsbeek A, Boelen A (2014) Beyond the fixed setpoint of the hypothalamus-pituitary-thyroid axis. Eur J Endocrinol **171**:R197-208.

123. Calsolaro V, Pasqualetti G, Niccolai F, Caraccio N, Monzani F (2017) Thyroid Disrupting Chemicals. Int J Mol Sci **18**.

124. Dupont C, Armant DR, Brenner CA (2009) Epigenetics: definition, mechanisms and clinical perspective. Semin Reprod Med **27**:351-357.

125. Leenen FA, Muller CP, Turner JD (2016) DNA methylation: conducting the orchestra from exposure to phenotype? Clin Epigenetics **8**:92.

126. Okano M, Xie S, Li E (1998) Cloning and characterization of a family of novel mammalian DNA (cytosine-5) methyltransferases. Nat Genet **19**:219-220.

127. Oppenheimer JH, Schwartz HL, Mariash CN, Kinlaw WB, Wong NC, Freake HC (1987) Advances in our understanding of thyroid hormone action at the cellular level. Endocr Rev **8**:288-308.

128. Fonseca TL, Fernandes GW, McAninch EA, Bocco BM, Abdalla SM, Ribeiro MO, Mohacsik P, Fekete C, Li D, Xing X, Wang T, Gereben B, Bianco AC (2015) Perinatal deiodinase 2 expression in hepatocytes defines epigenetic susceptibility to liver steatosis and obesity. Proc Natl Acad Sci U S A **112**:14018-14023.

129. Pak T, Yoo S, Miranda-Angulo AL, Wang H, Blackshaw S (2014) Rax-CreERT2 knock-in mice: a tool for selective and conditional gene deletion in progenitor cells and radial glia of the retina and hypothalamus. PLoS One **9**:e90381.

130. Jenniches I, Ternes S, Albayram O, Otte DM, Bach K, Bindila L, Michel K, Lutz B, Bilkei-Gorzo A, Zimmer A (2016) Anxiety, Stress, and Fear Response in Mice With Reduced Endocannabinoid Levels. Biol Psychiatry **79**:858-868.

131. Lee DA, Bedont JL, Pak T, Wang H, Song J, Miranda-Angulo A, Takiar V, Charubhumi V, Balordi F, Takebayashi H, Aja S, Ford E, Fishell G, Blackshaw S (2012) Tanycytes of the hypothalamic median eminence form a diet-responsive neurogenic niche. Nat Neurosci **15**:700-702.

132. Varga E, Farkas E, Zseli G, Kadar A, Venczel A, Kovari D, Nemeth D, Mate Z, Erdelyi F, Horvath A, Szenci O, Watanabe M, Lechan RM, Gereben B, Fekete C (2019) Thyrotropin-Releasing-Hormone-Synthesizing Neurons of the Hypothalamic Paraventricular Nucleus Are Inhibited by Glycinergic Inputs. Thyroid **29**:1858-1868.

133. Mohacsik P, Erdelyi F, Baranyi M, Botz B, Szabo G, Toth M, Haltrich I, Helyes Z, Sperlagh B, Toth Z, Sinko R, Lechan RM, Bianco AC, Fekete C, Gereben B (2018) A Transgenic Mouse Model for Detection of Tissue-Specific Thyroid Hormone Action. Endocrinology **159**:1159-1171.

134. Keimpema E, Alpar A, Howell F, Malenczyk K, Hobbs C, Hurd YL, Watanabe M, Sakimura K, Kano M, Doherty P, Harkany T (2013) Diacylglycerol lipase alpha manipulation reveals developmental roles for intercellular endocannabinoid signaling. Sci Rep **3**:2093.

135. Bianco AC, Dumitrescu A, Gereben B, Ribeiro MO, Fonseca TL, Fernandes GW, Bocco B (2019) Paradigms of Dynamic Control of Thyroid Hormone Signaling. Endocr Rev **40**:1000-1047.

136. Cunningham BA, Moncur JT, Huntington JT, Kinlaw WB (1998) "Spot 14" protein: a metabolic integrator in normal and neoplastic cells. Thyroid **8**:815-825.

137. Nikodem VM, Magnuson MA, Dozin B, Morioka H (1989) Coding nucleotide sequence of rat malic enzyme mRNA and tissue specific regulation by thyroid hormone. Endocr Res **15**:547-564.

138. Xiong S, Chirala SS, Hsu MH, Wakil SJ (1998) Identification of thyroid hormone response elements in the human fatty acid synthase promoter. Proc Natl Acad Sci U S A **95**:12260-12265.

139. Mutel E, Abdul-Wahed A, Ramamonjisoa N, Stefanutti A, Houberdon I, Cavassila S, Pilleul F, Beuf O, Gautier-Stein A, Penhoat A, Mithieux G, Rajas F (2011) Targeted deletion of liver glucose-6 phosphatase mimics glycogen storage disease type 1a including development of multiple adenomas. J Hepatol **54**:529-537.

140. Pagotto U, Pasquali R (2006) Endocannabinoids and energy metabolism. J Endocrinol Invest **29**:66-76.

141. Laville M, Riou JP, Bougneres PF, Canivet B, Beylot M, Cohen R, Serusclat P, Dumontet C, Berthezene F, Mornex R (1984) Glucose metabolism in experimental hyperthyroidism: intact in vivo sensitivity to insulin with abnormal binding and increased glucose turnover. J Clin Endocrinol Metab **58**:960-965.

142. Costa-e-Sousa RH, Hollenberg AN (2012) Minireview: The neural regulation of the hypothalamic-pituitary-thyroid axis. Endocrinology **153**:4128-4135.

143. Srichomkwun P, Anselmo J, Liao XH, Hones GS, Moeller LC, Alonso-Sampedro M, Weiss RE, Dumitrescu AM, Refetoff S (2017) Fetal Exposure to High Maternal Thyroid Hormone Levels Causes Central Resistance to Thyroid Hormone in Adult Humans and Mice. J Clin Endocrinol Metab **102**:3234-3240.

144. Lania A, Persani L, Beck-Peccoz P (2008) Central hypothyroidism. Pituitary **11**:181-186.

145. Persani L (2012) Clinical review: Central hypothyroidism: pathogenic, diagnostic, and therapeutic challenges. J Clin Endocrinol Metab **97**:3068-3078.

146. Beck-Peccoz P, Persani L (1994) Variable biological activity of thyroid-stimulating hormone. Eur J Endocrinol **131**:331-340.

147. Persani L (1998) Hypothalamic thyrotropin-releasing hormone and thyrotropin biological activity. Thyroid **8**:941-946.

148. Kim HY, Mohan S (2013) Role and Mechanisms of Actions of Thyroid Hormone on the Skeletal Development. Bone Res **1**:146-161.

149. Liverini G, Iossa S, Barletta A (1992) Relationship between resting metabolism and hepatic metabolism: effect of hypothyroidism and 24 hours fasting. Horm Res **38**:154-159.

150. Iossa S, Liverini G, Barletta A (1992) Relationship between the resting metabolic rate and hepatic metabolism in rats: effect of hyperthyroidism and fasting for 24 hours. J Endocrinol **135**:45-51.

151. Brent GA (2000) Tissue-specific actions of thyroid hormone: insights from animal models. Rev Endocr Metab Disord **1**:27-33.

152. Bao L, Roediger J, Park S, Fu L, Shi B, Cheng SY, Shi YB (2019) Thyroid Hormone Receptor Alpha Mutations Lead to Epithelial Defects in the Adult Intestine in a Mouse Model of Resistance to Thyroid Hormone. Thyroid **29**:439-448.

153. Ebert EC (2010) The thyroid and the gut. J Clin Gastroenterol **44**:402-406.

154. Maser C, Toset A, Roman S (2006) Gastrointestinal manifestations of endocrine disease. World J Gastroenterol **12**:3174-3179.

155. Liu J, Hernandez-Ono A, Graham MJ, Galton VA, Ginsberg HN (2016) Type 1 Deiodinase Regulates ApoA-I Gene Expression and ApoA-I Synthesis Independent of Thyroid Hormone Signaling. Arterioscler Thromb Vasc Biol **36**:1356-1366.

156. Kanamoto N, Tagami T, Ueda-Sakane Y, Sone M, Miura M, Yasoda A, Tamura N, Arai H, Nakao K (2012) Forkhead box A1 (FOXA1) and A2 (FOXA2) oppositely regulate human type 1 iodothyronine deiodinase gene in liver. Endocrinology **153**:492-500.

157. Desplats PA (2015) Perinatal programming of neurodevelopment: epigenetic mechanisms and the prenatal shaping of the brain. Adv Neurobiol **10**:335-361.

158. Jin B, Robertson KD (2013) DNA methyltransferases, DNA damage repair, and cancer. Adv Exp Med Biol **754**:3-29.

159. Crudo A, Petropoulos S, Moisiadis VG, Iqbal M, Kostaki A, Machnes Z, Szyf M, Matthews SG (2012) Prenatal synthetic glucocorticoid treatment changes DNA methylation states in male organ systems: multigenerational effects. Endocrinology **153**:3269-3283.

160. Daskalakis NP, Yehuda R (2014) Site-specific methylation changes in the glucocorticoid receptor exon 1F promoter in relation to life adversity: systematic review of contributing factors. Front Neurosci **8**:369.

10. List of publications

10.1. List of publication the thesis based on

Kővári D, Penksza V, Szilvásy-Szabó A, Sinkó R, Gereben B, Mackie K, Fekete C. (2022) Tanycyte specific ablation of diacylglycerol lipase alpha stimulates the hypothalamic-pituitary-thyroid axis by decreasing the endocannabinoid mediated inhibition of TRH release. Journal of Neuroendocrinology, 2022;34:e13079.

Farkas E, Varga E, Kovács B, Szilvásy-Szabó A, Cote-Vélez A, Péterfi Z, Matziari M, Tóth M, Zelena D, Mezriczky Z, Kádár A, Kővári D, Watanabe M, Kano M, Mackie K, Rózsa B, Yvette R, Tóth B, Máté Z, Erdélyi F, Szabó G, Gereben B, Lechan RM, Charli JL, Joseph-Bravo P, Fekete C. (2020) A glial-neuronal circuit in the median eminence regulates thyrotropin-releasing hormone-release via the endocannabinoid system. iScience, 27;23(3):100921

10.2. Other publications

Varga E, Farkas E, Zséli G, Kádár A, Venczel A, Kővári D, Németh D, Máté Z, Erdélyi F, Horváth A, Szenci O, Watanabe M, Lechan RM, Gereben B, Fekete C. (2019) Thyrotropin-releasing-hormone-synthesizing neurons of the hypothalamic paraventricular nucleus are inhibited by glycinergic inputs. Thyroid, 29:12 pp. 1858-1868

Ruska Y, Szilvásy-Szabó A, Kővári D, Kádár A, Mácsai L, Sinkó R, Hrabovszky E, Gereben B, Fekete C. (2021) Expression of glucagon-like peptide 1 receptor in neuropeptide Y neurons of the arcuate nucleus in mice. Brain Structure & Function, 227, pages 77-87(2022)

11. Acknowledgements

First of all I would like to express my sincere thanks to my tutor, Dr. Csaba Fekete, who greatly supported my work and professional improvement, supervised my activity by sharing his wide knowledge and technical skills and he could always be calm, even when I could not.

I am also very grateful to Dr. Balázs Gereben for his help to extend my technical background and sharing his knowledge and ideas to improve the experiments.

I would like to thank my closest colleagues, *Anett, Veronika, Andi* and the past and present members of the Lendület Laboratory of Integrative Neurobiology: *Dr. Edina Varga, Dr. Andrea Kádár, Panna Ágnes Hegedűs, Yvette Ruska, Balázs Kovács, Dr. Zoltán Péterfi, Ágnes Simon*, who provided cooperation and friendly atmosphere.

I would like to thank the past and present members of the Molecular Cell Metabolism Laboratory: *Dr. Petra Mohácsik, Richárd Sinkó, Dr. Lilla Mácsai, Dorottya Németh, Kristóf Rada* and especially *Andrea Juhász* for their help in molecular techniques.

I also wish to thank the members of the Reproductive Neurobiology Laboratory: Balázs Götz, Dr. Erik Hrabovszky, Dr. Miklós Sárvári, Dr. Katalin Skrapits, Dr. Szabolcs Takács.

Most importantly, I would like to thank the patience and supporting to all my friends, my mother and sister and especially to my father who was always the proudest of me and pushed me to not give up.